ANALYSIS OF THE ORIGINS OF DEVIATIONS IN THE PREDICTIONS OF VSASQ1

by

Consultant JSE Inc.

Mars 1991

TABLE OF CONTENTS

RÉSUMÉ

Est-ce que la promesse de réduction des émissions de SO_2 de 50% par les gouvernements nord-américains peut suffire à protéger adéquatement les écosystèmes aquatiques et forestiers boréaux durant la fonte des neiges? En supposant qu'une réduction de 50% se traduit par une réduction correspondante de la déposition sous le couvert forestier et sur le couvert de glace du lac, est-ce suffisant pour réduire le choc acide printanier et maintenir le pH des eaux d'un lac à des valeurs supérieur à 6 (seuil d'impacts biologiques; Jeffries et al, 1990) durant la fonte. Étant donné qu'une bonne partie des eaux de fontes arrivant dans les cours d'eau proviennent de la neige se trouvant sur le sol forestier, nous devons donc connaître les interactions entre l'écosystème forestier et les eaux de fonte, avant de pouvoir répondre à cette question .

Lorsque les interactions sont connues, elles peuvent être incorporées dans un modèle basé sur des processus physiques, qui peut être ensuite utilisé pour prédire les effets des différents scénarios de réduction des émissions de SO_2 sur la qualité de l'eau. Un tel modèle serait un atout car il présenterait l'avantage d'être facilement transférable d'un bassin à l'autre. Ce document présente les résultats d'une analyse des simulations d'un tel modèle(VSASQ1) basée sur les données de fonte printanière de 1988. Les données ont été recueillies au bassin du Lac Laflamme, à 80 km au nord de la ville de Québec.

Le modèle VSASQ1 est constitué de quatre modules: SNOQUAL, VSAS2, SOILEQ et SHORMIX. Suite à l'analyse du premier exercice de simulation, nous pouvons conclure que les résultats sont très prometteurs. Pour améliorer les prédictions, certains processus jusqu'alors jugés non importants devront être ajoutés aux modules Pour SNOQUAL, une fois que la simulation a débuté, on devrait pouvoir tenir compte du phénomène de ségrégation des ions qui se produit lors d'une période de dégel et regel. Pour assurer la transportabilité de VSAS2, l'effet du gel sur les propriétés hydrologiques

du sol et de son effet subséquent sur les voies d'écoulement des eaux de fonte sont à ajouter. Un module complet décrivant les processus physiques et chimiques du lac devra aussi être ajouté à VSAS2 pour simuler adéquatement l'effet des processus de gel et de fonte du couvert de glace ainsi que l'effet de l'écoulement sous la glace sur la qualité des eaux du lac. Pour SOILEQ, il faudra tenir compte de l'écoulement ascendant vertical et latéral à travers les couches de sol . En vue d'améliorer la prédiction de SO_4^{2-} et du pH, l'algorithme d'absorption de SO_4^{2-} devra être modifié et le besoin d'inclure l'effet de l'altération des roches devra être examinée. Une évaluation adéquate des performances de SHORMIX nécessitera une simulation de l'ensemble du bassin versant du lac.

ABSTRACT

Is the North-American governments pledge of reducing there SO_2 emissions by 50% sufficient to protect adequately the boreal forested and aquatic ecosystems during snowmelt? Assuming that a 50% reduction in SO_2 emission is translated in a corresponding reduction in deposition under the forest canopy and on the lake ice cover, is it enough to reduce the Spring acid shock and maintain the pH lake waters above 6 (biological threshold; Jeffries et al, 1990) during snowmelt. Since part of the snowpack is situated under the forest canopy, we need to know the interactions between the forest ecosystem and the snowmelt waters, before we can answer the question above.

Once these interactions are known, they can be incorporated in a physically-based model which can be further used to predict the effect of different scenarios of SO_2 emission reduction on water quality. Such a model would be a valuable asset because it would be easily transportable from one watershed to the other. This paper presents the results of the simulation analysis of such a model (VSASQ1) based on the data collected during the spring of 1988 at the Lac Laflamme watershed, 80 km north of Quebec City.

The model VSASQ1 is made up of four modules: SNOQUAL, VSAS2, SOILEQ and SHORMIX. Following the analysis of the first simulation run, we can conclude that the results are promising. To improve the predictions, certain processes previously judged not important will have to be added to the modules. For SNOQUAL, once the simulation has started it should take into account the segregation of ions occurring during a thawing and freezing period. To ensure the transportability of VSAS2, the effect of freezing on the soil hydrological properties and its subsequent effects on flowpaths need to be added. A complete module simulating the physical and chemical processes occurring to the lake will need to be added to VSAS2. This module would simulate adequately the effect of the freezing and melting processes of the lake ice cover along with the flow occurring under the

ice on the lake water quality.. For SOILEQ, the vertical upward movement of water through the soil layers along with its lateral movement will need to be added. To improve the prediction of SO_4^{2-} and pH, the adsorption model of SO_4^{2-} needs to be modified. The necessity of including the effect of mineral weathering process should be examined. An adequate evaluation of SHORMIX deed will necessitate the simulation of the whole lake watershed.

INTRODUCTION

The recent acidification of precipitation (Likens and Butler, 1981) in North America has given rise to concern on the subsequent acidification of poorly buffered surface waters and on the effects of acid pollutants on forest ecosystems (Morrison, 1984). The greater part of the eastern boreal forest lies on the Canadian Shield where the low mineral content of the surface waters renders it them susceptible to acidification. In addition, the forest soils of this region are generally thin and, under the influence of acidic pollutants, may suffer from accelerated leaching of base cations (Cronan et al., 1978) or the inhibition of biological activity (Stroo and Alexander, 1986).

Much of the precipitation on this region is in the form of snow which covers the ground for 5-8 months of the year. The rapid release during spring time of strong acids accumulated during the mid-winter period by the snowpack can lead to high acidity values in surface waters and concomitant stress conditions for the aquatic biota (Driscoll et al., 1980).

The spring acid stress can compromise the survival of fish populations when it interferes with individuals at different stage of their life cycle and particularly the fries and the young classes of population. Several factors can affect the response of populations to the acid stress. Besides the biotic and abiotic natural variables which affect the initial state of the populations, other factors like the presence of organic matter, acidity, concentration in aluminium, calcium, sodium are considered important in the response of populations to the acid stress.

During their life cycle, fish populations live in two different types of media; the interstitial waters (sediments) and the ambient (lakes, streams, rivers) waters. The critical

conditions in these media should determine the response of entire fish populations to the spring acid stress.

This paper presents the results of the simulation analysis of a physically-based model (VSASQ1) based on the data collected during the spring of 1988 at the Lac Laflamme watershed, 80 km north of Quebec City.

The value of this predictive model will depends on its capacity to correctly predict the water quality evolution of surface waters during springmelt at the sites having a strategic role to the fish population survival.

STUDY SITE

The research site is located on the lac Laflamme basin which is an upland first order watershed (47° N, 71° W) situated 80 km north of Quebec City (Figure 1). It covers 68 ha of which 6 ha are occupied by the lake, and 1 ha by a wet zone at the east end of the lake. The watershed altitudes range from 777 to 864 m(above sea level) and the slopes vary from 0 to 30%. The lac Laflamme watershed which is part of the Forêt Montmorency Experimental Station of Université Laval is characterized by a climate with an average annual mean temperature of 0.2°C. The average annual precipitation is 1424 mm of which one third falls as snow accumulating to a depth of 150 cm. The average monthly mean temperature varies from -15.2°C in January to 14.8°C in July.

The basin is covered by the balsam fir-white birch forest type (Rowe, 1972) growing on an orthic humo-ferric podzol (Jurdant and Bernier, 1965). The forest stand consists of 80% balsam fir (Abies balsamea (L) Mill.), 10% white birch (Betula papyrifera Marsh.) and 10% white spruce (Picea glauca (Moench) Voss) 50-70 years old, averaging

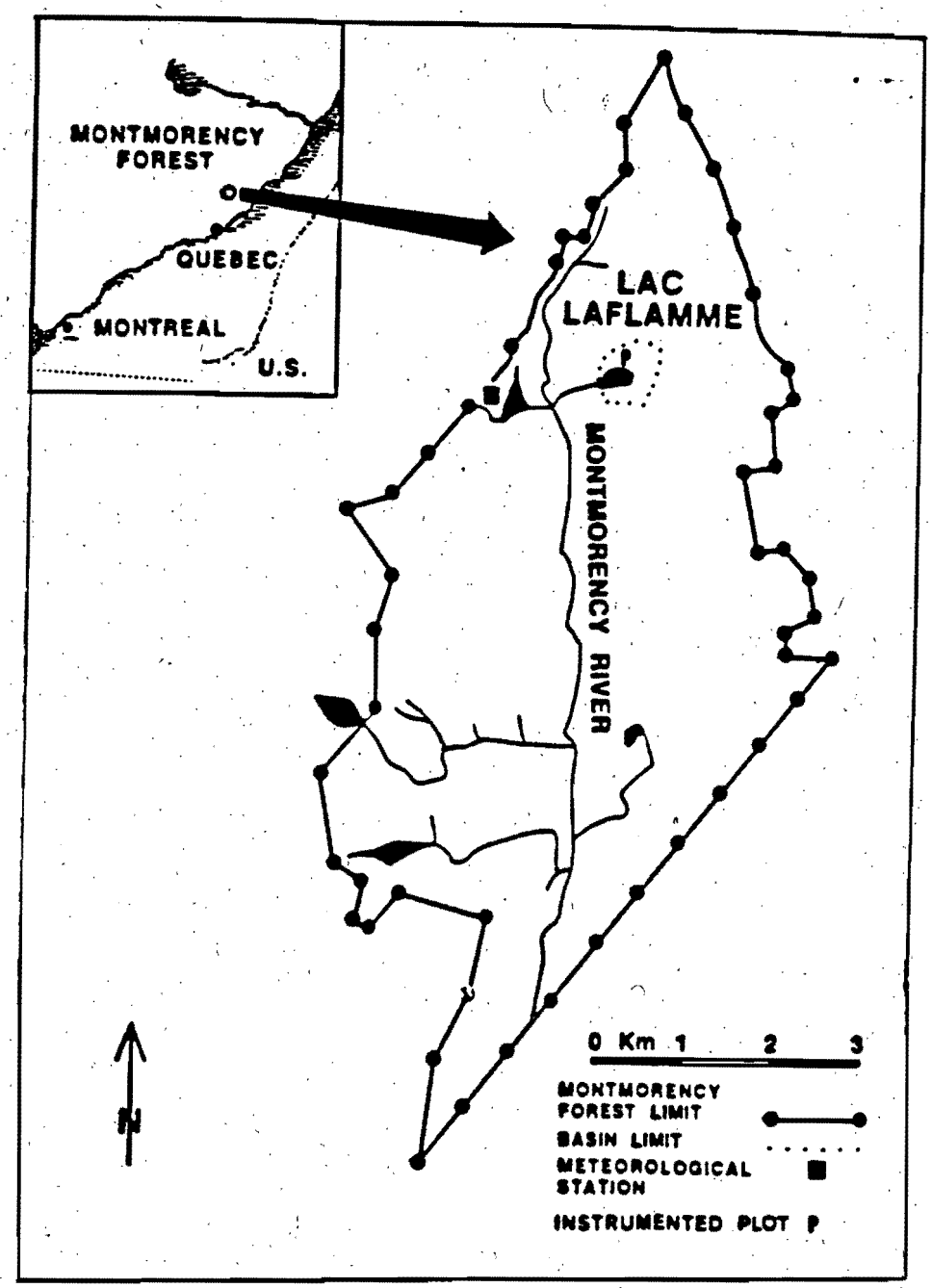

Fig.1: Location of the Lac Laflamme watershed

5 000 stems per hectare (Plamondon et al., 1984). The mineral soil is covered by an organic layer of about 10 cm (Martel, 1983) mainly composed of mosses (Hylocomium sp., Shagnum sp.). The oldest stands (50-70 years old) cover 60% of the terrestrial part of the basin and are mainly located within a 200 m band around the lake. The young stands (10-30 years) established on chablis are situated at altitudes above 800 m(above sea level) and represent 40% of the stands area. The percentage of defoliation reached 20 to 70% of the total foliage depending on the stands (Plamondon et al., 1984) during the peak of the spruce budworm (Choristoneura fumiferana Clem.) epidemic between 1975 and 1984. Since then, the trees have kept their foliage. The impervious charnockitic gneiss bedrock is overlain by a sandy till rich in cobbles and boulders with a depth varying from 0.5 m on the ridge to over 15 m under the lake (Jurdant and Bernier, 1965; Robitaille and Wilhemy, 1981). The soil hydrologic properties (saturated hydraulic conductivity, porosity, bulk density) of different soil layers are given in Prévost et al., 1990). The average permeability of the deep deposits has been estimated to be between 5 cm hr^{-1} (Barry et al., 1988) and 15cm hr^{-1} (Bernier et al,, 1983) and the mean residence time for the lake water is around two months. The instantaneous discharge from the lake varied from 0.003 to 0.794 $m^3 s^{-1}$, for the 1985 to 1987 period (Prévost et al., 1990)).

MATERIALS AND METHODS

Measurements

The watershed was subdivided into 9 sub-basins (Figure 2), in each of which two or three snow sampling stations were placed at different altitudes. The data (snow water equivalent and depth) were collected with a "Western Snow Conference" snow core

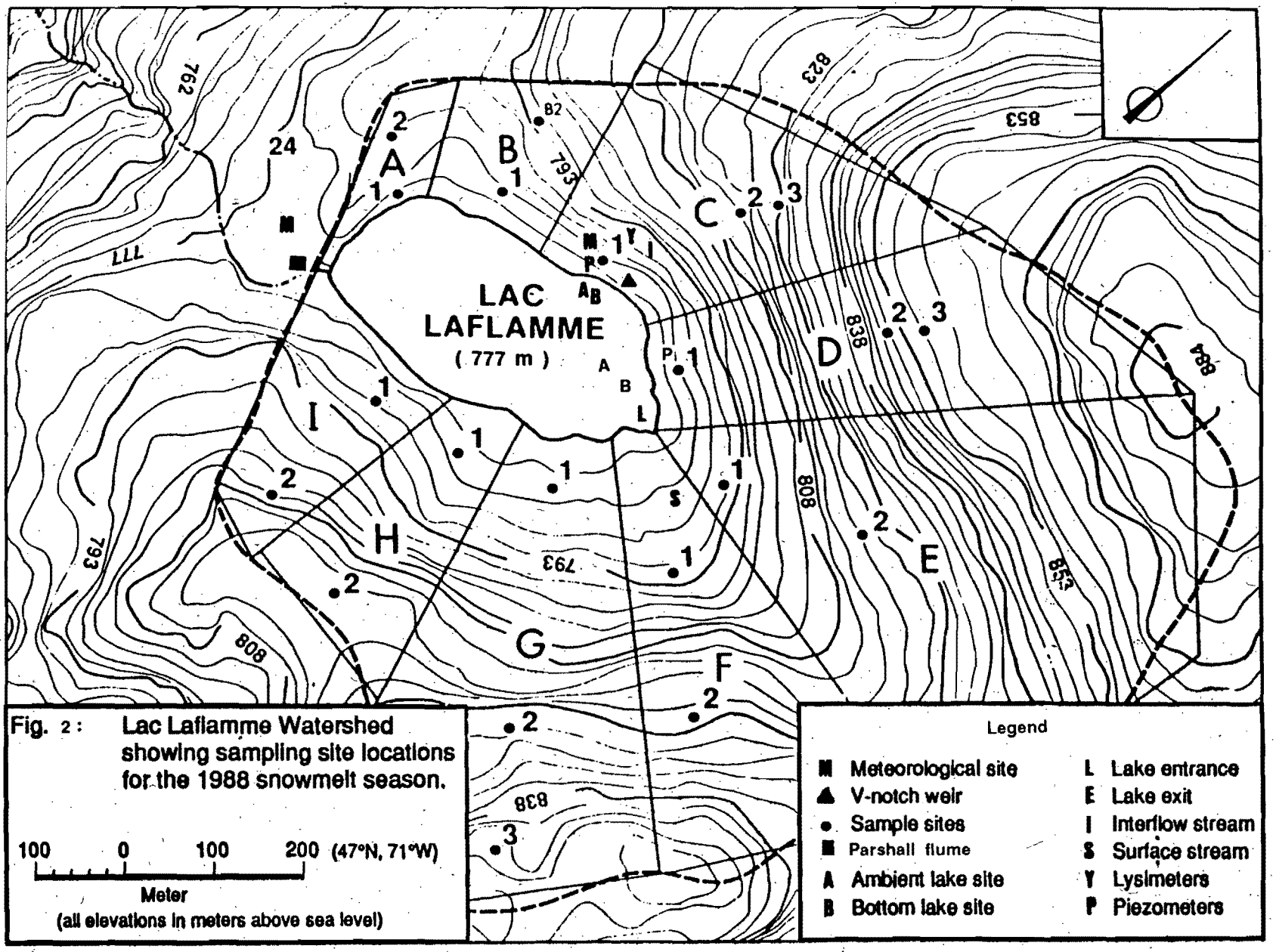

Fig. 2 : Lac Laflamme Watershed showing sampling site locations for the 1988 snowmelt season.

sampler. In each station, the volumetric soil liquid-water content was also measured at 10, 20, 40 and 80 cm depth with the time domain reflectometry (tdr) technique (Stein and Kane, 1983, Prévost et al., 1989). Two 33 cm length stainless steel rods, 5 cm apart, were inserted horizontally in the soil and connected to a coaxial cable. In rocky situations, to minimize site perturbation, the soil removed to insert the rods was put back in such a way to reconstitute the original profile. The dielectric constant of the soil was obtained with a reflectometer (Tektronic, model 1502) and related to its moisture content. Snow and soil moisture data were collected every two to seven days in March, April and May 1988. Nitrogen bubble systems were used to measure water yield at a Parshall flume located at the lake discharge, and to monitor lake water level changes. Precipitation data were obtained with a tipping bucket raingage at station 24, situated in a clearing of 150 m in diameter.

At about 50 meters from the lake shore in station C1, a small intermittent stream was gauged continuously with a V-notch weir and water quality samples were taken. Two tributaries located in sub-basin E were also added to gather water quality data. The interstitial water and the water 20 cm above the lake bottom were also collected at two spawning grounds.

Sub-basin C was chosen as the intensive site. The instrumentation was installed along a transect from station C1 to a spawning site about 10 m from the lake shore (Figure 3). Precipitation chemistry was collected with a Sangamo near the small snow lysimeters. Air temperature was monitored with thermistors connected to a data acquisition system (Campbell Scientific, CR-21) at station C1, located under the forest canopy. The snow water equivalent was estimated from 9 sampling points. The water quality data of the snowpack were also taken from three sites near station C1. Water outflow at the bottom of

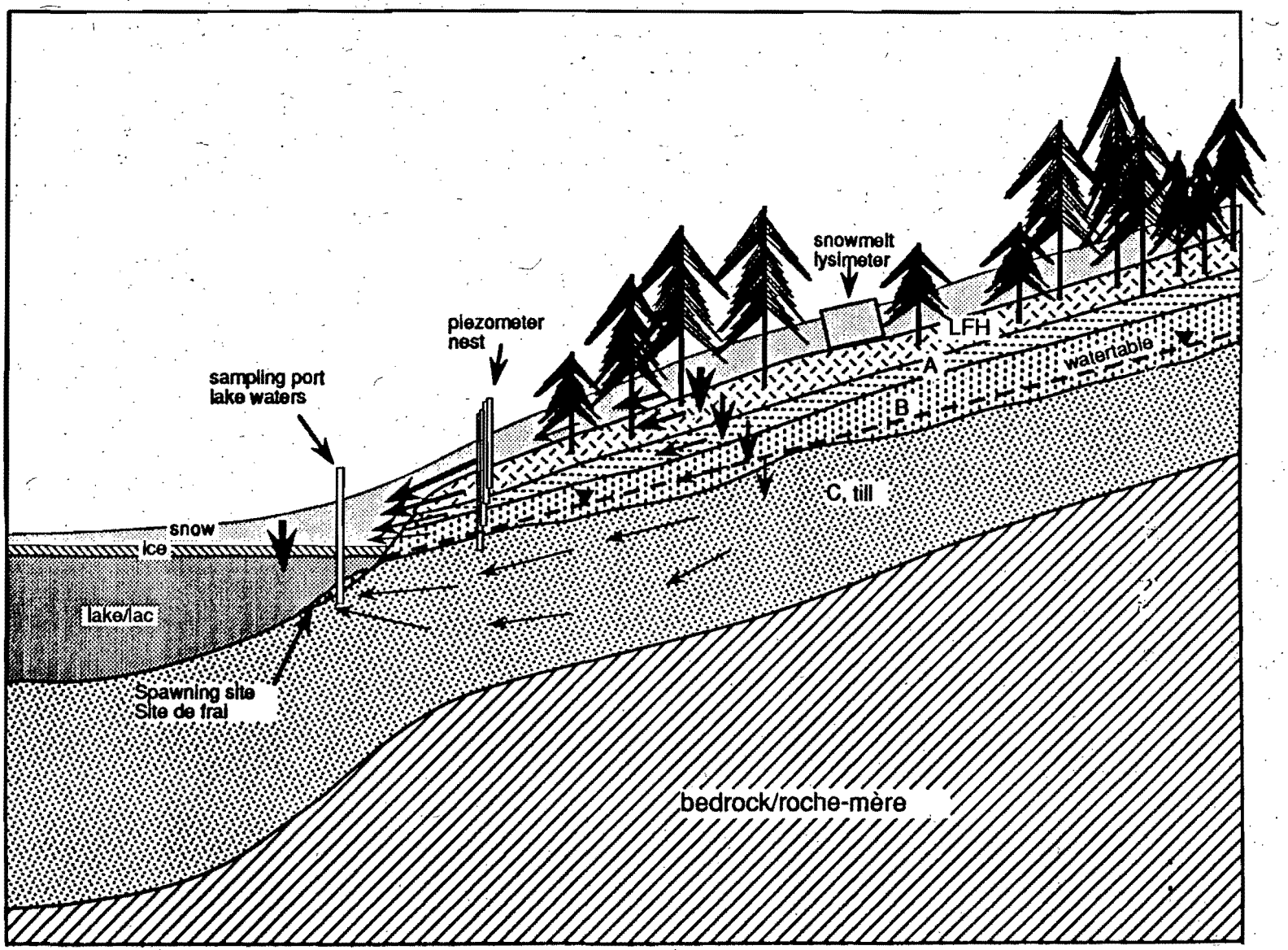

Fig.3: Transect from the snow lysimeter to the spawning site in segment C

the snow cover was collected at station C1 with a 20 m^2 lysimeter. Four squared shape small lysimeters (1m^2) were installed to collect water quality data. Two of these small lysimeters were installed in the open, while the third one was in a semi-open area and the fourth in a closed area. Meltwater samples representing the integrated sample of all meltwater discharges over 24 hours were taken at midday every day. Groundwater levels were measured along a transect perpendicular to the lake shore, in sub-basin C. Near the shore, about 5 m inland, four piezometers were installed during the fall of 1987 to gather water quality data and water levels. They were installed at the same depths as the tdr probes, i.e at 10, 20, 40 and 80 cm depths. Four piezometers were also installed about 15 m inland at the bottom of sub-basin D and at the same depths.

For all the water samples, the following chemical and physical parameters were measured: pH, conductivity, total monomeric Al, Al complexes, Ca^{2+}, Cl^-, EC, F^-, H^+, K^+, Mg^{2+}, Na^+, NH_4^+, NO_3^-, SO_4^{2-}. All samples were kept at 0°C during transport to the laboratory, pH and conductivity measurements were taken on arrival and the samples filtered and conserved for further chemical analysis (Jones, 1987)

METHODOLOGY

Description of the different modules

Presently, there are four modules which form the integrated model (Figure 4). SNOQUAL is the snow quality and quantity module which simulates the melting of the snow and the leaching of the different chemical constituents from the snow. VSAS2, a watershed model, constitutes the core of the model. It routes the water from the soil surface into the different soil horizons and down to the water table to finally end up in the lake. SOILEQ the soil chemistry module calculates the water chemistry changes during its

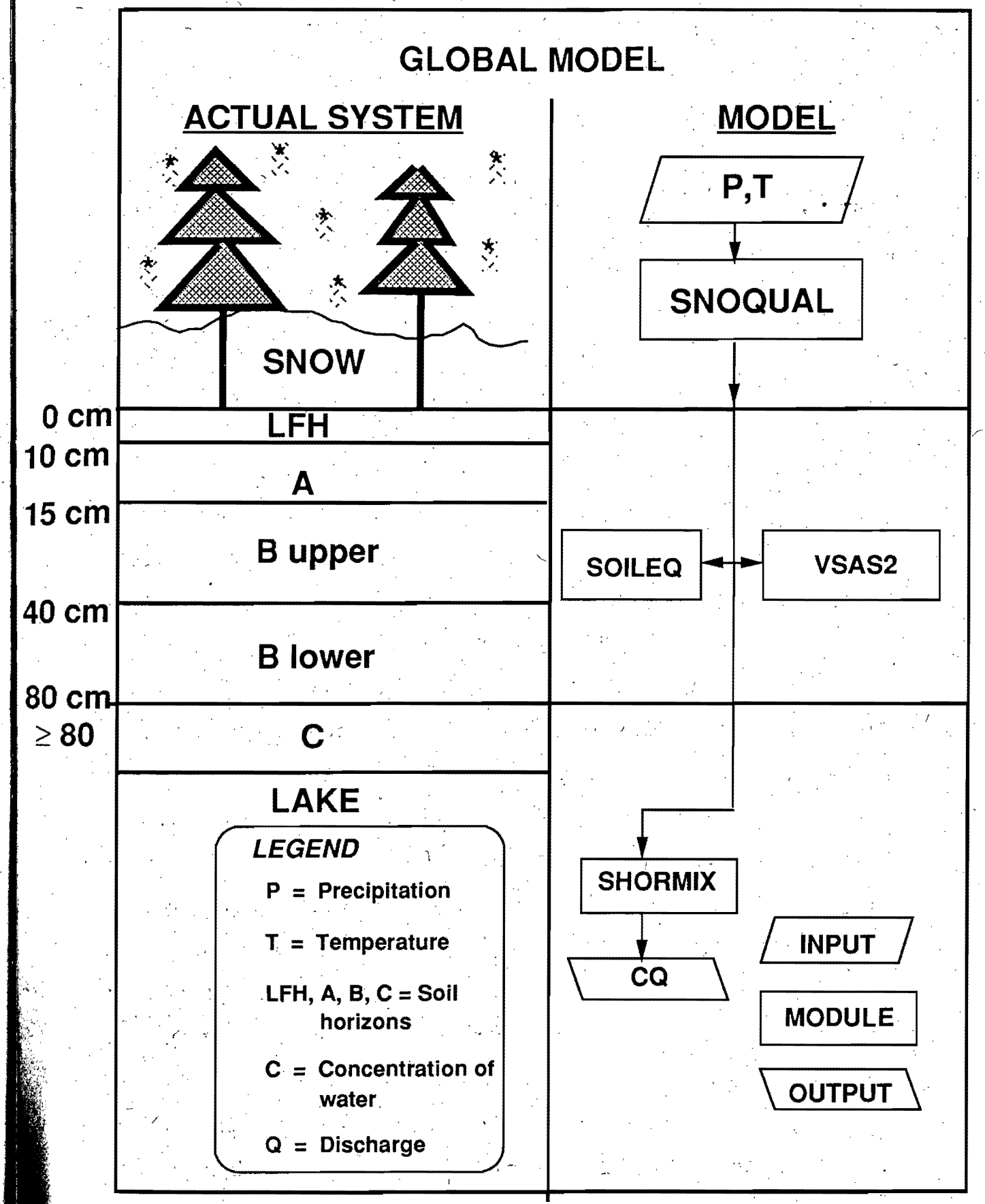

Fig.4: Flowchart of the integrated model along with the modeled system

travel from the bottom of the snowpack down to the lake or streams. The output of these two modules serve as the input for SHORMIX. SHORMIX calculates the water quality changes occurring in the lake or streams as a result of water coming from different sources and mixing with the water already present. Because the two verification sites for SOILEQ and SHORMIX were either in or near segment C, the simulation of the integrated model was run for segment C only.

SNOQUAL

SNOQUAL is a conceptual module that relates the quantity of meltwater released from the snowpack to the chemical composition of the meltwater discharge. The structure of the module consists of two components. The first, SNOW-17 (Anderson, 1973), simulates the rate of meltwater discharge from the estimation of energy exchange across the snow-air interface. It has been validated quite intensively with lysimeter data (Roberge et al., 1988). The values attributed to the major and minor parameters of the module are based on the work of Roberge et al., 1988, and Prevost et al. 1990. Since snowmelt water release at the bottom of the snowpack varies according to aspect and elevation on the Lac Laflamme basin (Prevost et al. 1989), SNOW-17 gives snowmelt rates for the four different topographic zones (Prevost et al. 1990). The basin is divided in two aspects, North and South, which are further divided in upper and lower parts of the slopes. For the lake portion, the melt rate factors for the lower parts are utilized. The second component takes the output from SNOW-17 and calculates the concentration of ions in each discrete discharge by a routine which is derived from a, or two, first order leaching expression (s) for the soluble species from the snowpack. It is based on the physical concept of the leaching of solubles from the pack matrix by a diminishing reserve of ice meltwaters. The parameter for the rate of leaching is a leaching coefficient "k" (Foster, 1978). A flowchart

of the model is presented in Figure 5. For more details the reader is referred to Jones, 1987, Jones et al., 1986, Stein et al. 1986 and Jones et al., 1990.

A variant of the chemical module (SNOQUALR) has been used in the integrated model. The value of the leaching coefficient represents the net leaching effect of solubles from the pack; the snow and organic matter being lumped together. However, in this particular module the material to be removed from the snowpack is segregated into two components. The first component consists of concentrated solutions of ionic species on the surfaces of snow grains. The segregation and concentration of ionic solutions on the surfaces of the grains is known to occur during the metamorphism of snow crystals to grains prior to the melt season (Tranter et al., 1986). This process, however, leaves some of the ions as a residual component of the original composition of the snow crystals within the ice lattice structure of the snow grains.

Presently, the qualitative algorithm of the SNOQUAL module cannot take into account the effect of new precipitation (rain or snow) once the simulation has started because it does not allow the stratification to occur. Therefore we have joined a component that can add to the snowpack, the chemistry of the new precipitation. SNOQUALR, in its present state can be regarded as a development tool to simulate satisfactorily the accumulation of precipitation between snowmelt periods.

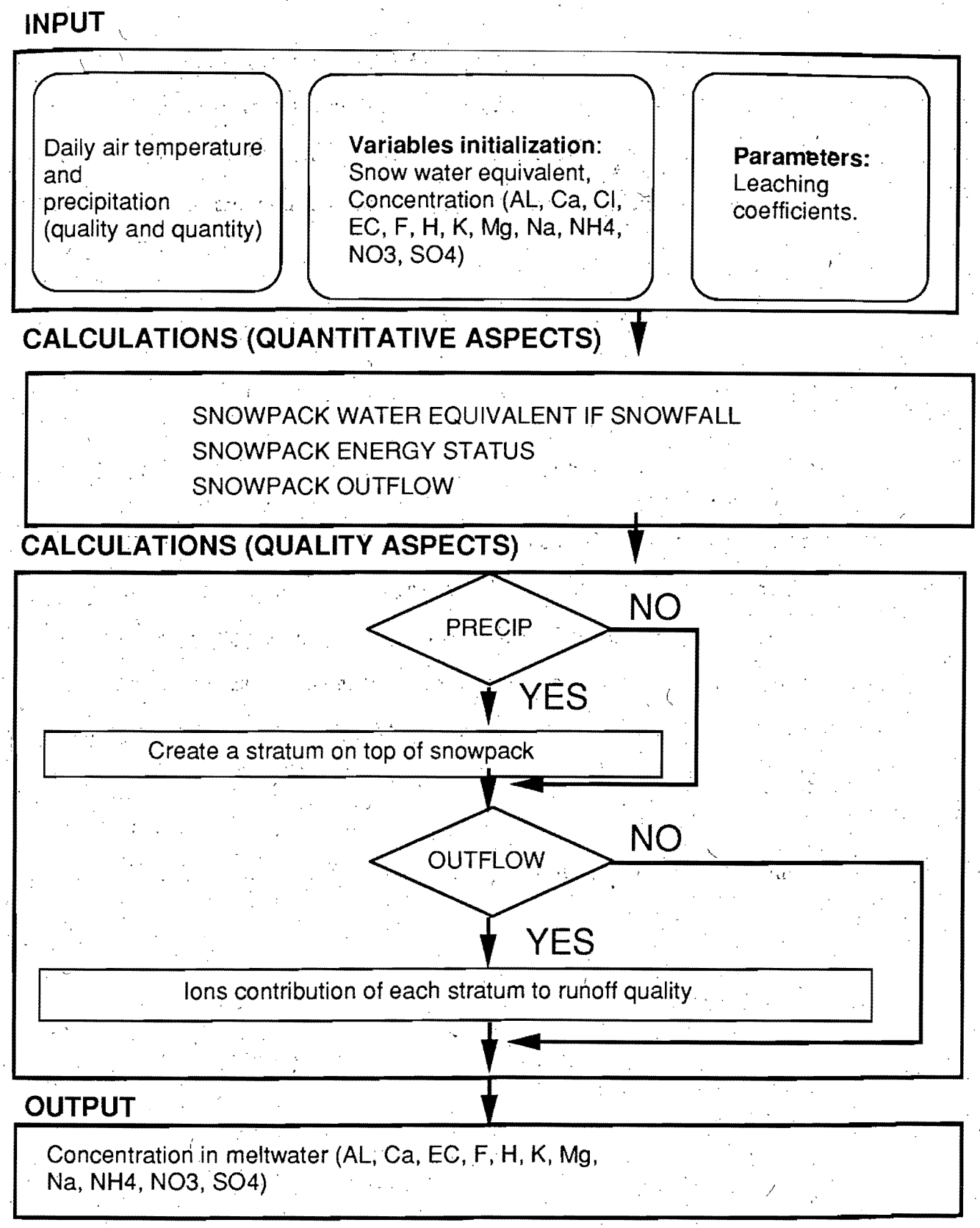

Fig. 5: Flowchart of SNOQUAL: snowmelt quality-quantity model

The values of k and R for the following ions: Cl^-, F^-, Mg^{2+}, K^+, Ca^{2+}, Na^+ and Al^{3+} have been set to the average of the k and R for the ions H^+, NO_3^-, SO_4^{2-} and NH_4^+ because the snow does not have chromatographic properties(Hewitt et al, 1989). The electric conductivity was determined following an empirical relationship using the 1988 data:

$$EC = 0.09\,[H^+] + 0.34\,[NO_3^-] + 0.24\,[SO_4^{2-}] \qquad (1)$$

where [ ] concentration in $\mu mol\ l^{-1}$
EC electrical conductivity in $\mu mho \cdot cm^{-1}$

The r^2 is equal to 0.994 and the data points are plotted in Figure 6.

The simulated cumulative discharges are calculated from the daily melt obtained from station C1. The snow water equivalent of the snowpack at the start of the simulation is the average of station A1, B1, C1 and D1 (Figure 2). The initial pollutant concentrations present in the snowpack are calculated from the measurements taken at three sites near C1. The observed cumulative discharges are calculated from the average of the daily melts from 4 lysimeters installed under different forest openings and normalized using the total cumulative simulated melt. The average observed daily concentration is calculated by dividing the total load of pollutants by the total volume of daily melt from the four lysimeters.

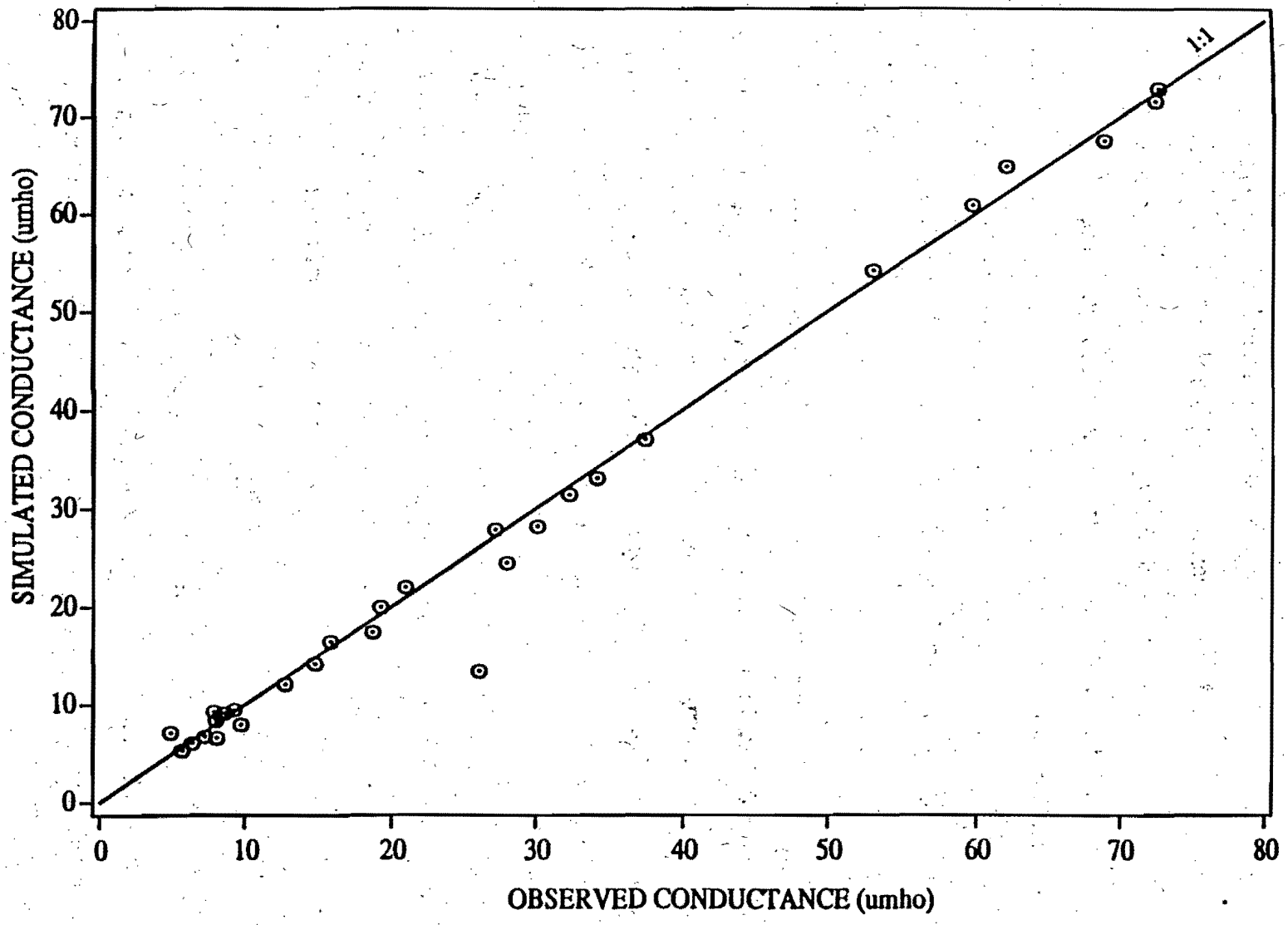

Fig.6: Simulated versus observed conductance

VSAS2

The hydrological simulator VSAS2 is based on the physical processes governing water movement in a basin. The input data necessary to use VSAS2 are surficial topography, geometry of deposit, soil hydrodynamic properties (saturated hydraulic conductivity, water retention curve, unsaturated conductivity curve, total porosity) and water input to the soil surface. There are no adjustment parameters included in VSAS2 since it is totally based on basin and soil physical properties. The model predicts water outflow and soil water content, layer by layer for all sub-basins and a hydrograph for the entire basin.

The basin must be subdivided into sub-basins (segments) according to the topography and soil types (Figure 2); these segments are submitted independently to the simulator: it is assumed that there is no water flow between segments. VSAS2 represents each segment tridimensionally and subdivides it into characteristic soil layers and increments paralleling the stream to form volumetric units called elements, for which horizontal and vertical components of water flow are computed. Each soil element occupies the total width of a segment. The key components of VSAS2 are the geometric representation of the basin, the variable slope incrementation and the maintenance of mathematical accuracy in hydrologically sensitive source areas (Bernier, 1985). There is no provision in the model to calculate the effect of soil freezing on soil hydrologic properties.

The maximum soil freezing depth for three winter years(1985,86,87) does not exceed about 40-60 cm in the Lac Laflamme basin (Prevost et al., 1989) and the lowest ground temperature recorded is -1.3°C. Knowing that the saturated hydraulic conductivity of the soil layer 0-60 cm deep at room temperature being greater than 267 mm h^{-1}; it was felt that the snowmelt arriving on the soil at a maximum rate of 5 mm hr^{-1} (melt + rain)

observed during the 1982 to 1986 Springs should not have any problem to infiltrate in the ground. We also knew from water levels measurements (Roberge and Plamondon, 1987) that the snowmelt did not seem to have any problem to infiltrate. It was believed that even though concrete frost existed in the watershed it was not a widespread phenomenon (Roberge and Plamondon, 1987, Prevost et al., 1990). Prevost et al., 1990 showed after a first simulation effort with VSAS2, that peak flows were underestimated. Because VSAS2 does not take into account soil freezing effects on soil hydrologic properties, they hypothesized that as the snowmelt proceeds, concrete frost develops locally at the soil surface due to subfreezing night temperatures, lowers the soil hydraulic conductivity and induces surface flow. The fraction of bare ground was used as an index (snow cover areal extent factor) to the decrease of infiltration capacity on the basin. The proportion of bare areas generated by SNOW-17 were treated as impervious areas. When the proportion reached 85% it was assumed that the soil had thawed. The inclusion of this index strongly improved the simulation of peak flows (Prevost et al. 1990). The same index was used in VSASQ1.

More details about the model are given in Bernier (1985) and Prévost et al. (1990). A simplified flowchart along with the input, parameters and output is presented in Figure 7.

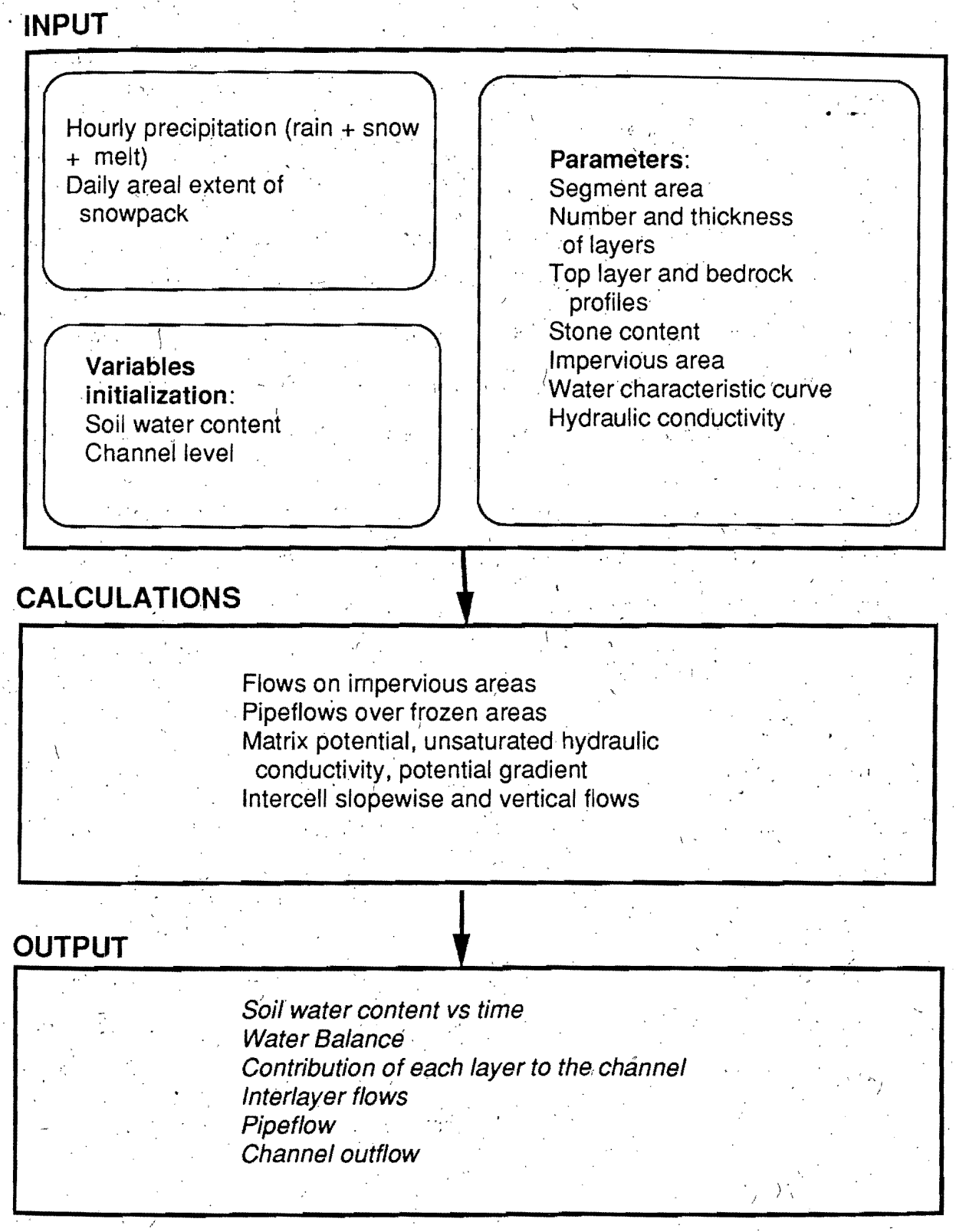

Fig. 7: Flowchart of VSAS2: watershed module

SOILEQ

When water enters the soil horizon under consideration there is a mixing of old pore water, already in equilibrium with the soil, and the new water. This new mixture is normally out of equilibrium in terms of Al^{3+} activity with respect to the soil solution pH and in terms of base cation and Al^{3+} activities with respect to the exchange complex. The model allows $Al(OH)_3$ to precipitate, releasing H^+ and decreasing Al^{3+} in solution. The model then allows an adjustment in CEC to correspond to the new soil solution pH which also either consumes or releases H^+ to the soil solution. As pH changes, the speciation of Al changes; the reactions of Al with OH^- will also have a direct effect on H^+ activity.

Finally the equilibria between the activities of base cations and Al^{3+} in solution and absorbed on the exchange complex are calculated. Since each of these steps affects each of the others, the mathematical solution is determined by recalculating the steps iteratively until the equilibrium condition has been found.

The soil profile was divided into 4 layers based on chemical and hydrological characteristics (hydraulic conductivity and porosity): the organic surface layer 5 to 10 cm thick, and three mineral layers, 30, 40, and greater than 40 cm thick corresponding to Ae, Bhf and Bfh, Bf and BC and C horizons, respectively (Soil Survey Staff, 1975). Water entering the surface layer was assumed to reach equilibrium within one time step (24 h) and this calculated water chemistry became the input chemistry for the next lower layer at the start of the next time step. The surface runoff generated by the snow cover areal extent factor was given the chemistry of waters flowing through the organic surface layer. A simplified flowchart of this module is presented in Figure 8.

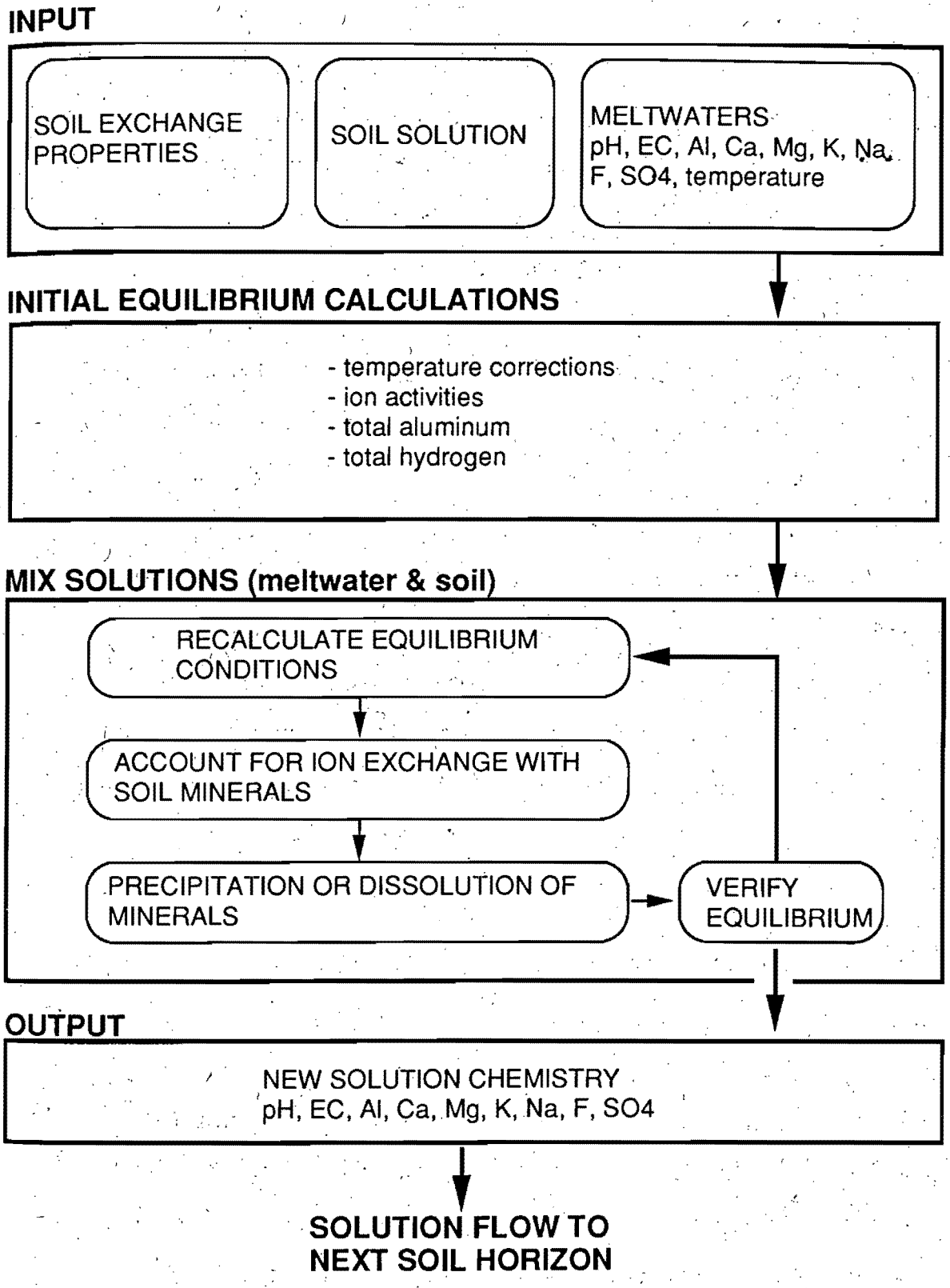

Fig. 8: Flowchart of SOILEQ: soil solution mixing and exchange module

SHORMIX

The model (Figure 9) is a relatively simple chemical equilibrium model for Al aqueous complexes of -OH, F, and SO_4^{2-}. Aluminum speciation with these complexes is calculated using the stability constants given by Nordstrom et al. (1984) (Table 1). Thermodynamic calculations are corrected for the effects of temperature using the van't Hoff equation and activity coefficients using the Debye-Huckel approximation (Lindsay 1979) with ion strength estimated from electrical conductivity (millimhos cm^{-2}) using a multiplier factor of 0.018 (Lindsay 1979). Input parameters are water temperature, pH, partial pressure of CO_2 in water, inorganic monomeric aluminum, total fluoride, sulphate, electrical conductivity, and volumes of the water to be mixed. The model equilibrates each water source separately, in terms of H activity, by using gibbsite thermodynamic values to calculate total amount of dissolved Al present in the water. The water sources and the total ion concentrations of the various Al species are then mixed according to the relative volumes, the aluminum species and H recalculated iteratively until minimal change occurs. As the pH changes the speciation of Al changes and the resulting reactions of Al with OH, F, and SO_4^{2-} ligands change, which in turn have a direct effect upon the H^+ activity. The mathematical solution is then determined by an iterative process.

SHORMIX utilizes 6 inputs provided by the integration of SOILEQ and VSAS2. The first one is the water released from the snowpack on the ice itself, the chemistry is the same as the chemistry of snowmelt. The second one is the snowmelt water which runs at the soil surface having the chemistry of soil layer one and is calculated using the snow cover areal extent factor. The third, fourth, fifth and sixth one are waters that are flowing in soil layer 1, 2, 3 and 4 as calculated by VSAS2 and have the chemistry as calculated by SOILEQ. We consider the sediments of the lake do not to alter the chemistry of layer 4.

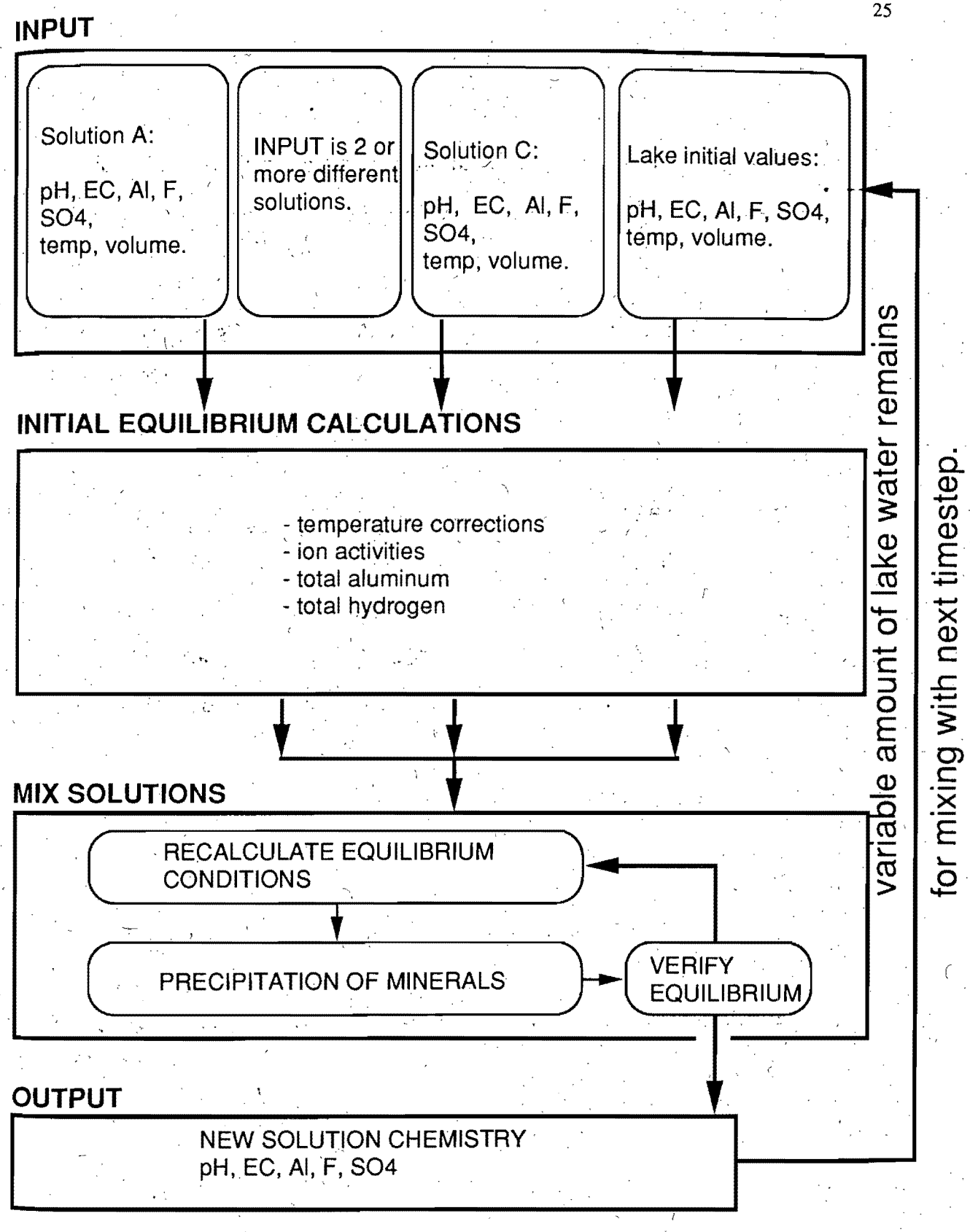

Fig. 9: Flowchart of SHORMIX: lake shore waters mixing module

Table 1. Thermodynamic data used in the SHORMIX model equilibrium calculations.

	Reaction			log K**
1.	$Al^{3+} + H_2O$	=	$Al(OH)^{2+} + H^+$	-4.987
2.	$Al^{3+} + 2H_2O$	=	$Al(OH)_2^+ + 2H^+$	-10.13
3.	$Al^{3+} + 3H_2O$	=	$Al(OH)_3^0 + 3H^+$	-16.76
4.	$Al^{3+} + 4H_2O$	=	$Al(OH)_4^- + 4H^+$	-22.16
5.	$Al^{3+} + F^-$	=	AlF^{2+}	6.98
6.	$Al^{3+} + 2F^-$	=	AlF_2^+	12.60
7.	$Al^{3+} + 3F^-$	=	AlF_3^0	16.55
8.	$Al^{3+} + 4F^-$	=	AlF_4^-	19.03
9.	$Al^{3+} + SO_4^{2-}$	=	$AlSO_4^+$	3.01
10.	$Al^{3+} + 2SO_4^{2-}$	=	$Al(SO_4)_2^-$	4.98
	$Al(OH)_3$ (S)	=	$Al^{3+} + 3OH^-$	natural gibbsite
	dissociation constant for gibbsite = 8.5			
	H_2CO3	=	$H^+ + HCO_3^-$, pK = 7.81	

**K= Stability constant

The program uses the free ion activities of the Al-complexes to calculate the saturation state of the solution with respect to gibbsite. If the solution is super saturated then Al is allowed to precipitate thus releasing H^+ and decreasing Al^{3+} in solution. It is assumed that no solid phase Al is available for dissolving if the solution is undersaturated. The model uses the following assumptions:

1. the stability constants and selectivity coefficients remain constant over time and the selectivity coefficients are independent of pH; and
2. the system attains equilibrium during each time step.

RESULTS AND DISCUSSION

For the first simulation exercise, the four modules were put together and the only exogenous variables necessary to run the model were the precipitation and air temperature. Naturally the initial conditions of the state variables, e.g. total concentration of different ions in the snowpack and the rate variables, (e.g. soil hydraulic conductivity) were provided when necessary. Finally the geometric features of the simulated system like segment area, number of soil layers, etc., were also given.

The output of each module is then compared with field measurements. It should be emphasized here that the integrated model was run once only and the results presented are from that first run .

SNOQUAL

The simulated snowmelt, along with the cumulative discharge of the lysimeter for season 1988 is presented in Figure 10. The 1988 melting season can be divided in two periods. The first one starts on the 22nd of March and ends on April the 15th releasing 145 mm of cumulative snowmelt + rain. It is followed by a cold period that lasts until April 22nd. During this period 50 mm of snow water equivalent falls on the snowpack. The second melt period starts slowly on April 23rd and is followed by a marked increase in snowmelt on May 2nd. It ends the 24th of May releasing 320 mm of cumulative snowmelt and rain. The variation in concentration of the different ions (Al, Ca^{2+}, Cl^-, F^-, H^+, K^+, Mg^{2+}, Na^+, NH_4^+, NO_3^-, SO_4^{2-}) and conductivity of the meltwaters during the springmelt are presented from Figure 11 to 22 respectively.

In general the simulations are quite good except for EC and F^-. The differences between the observed and simulated values of the cumulative discharge are sometimes divergent with time (Ca^{2+}, F^-, K^+, Na^+, SO_4^{2-}) or constant (Al, Cl^-, H^+, Mg^{2+}, NH_4^+, NO_3^-). The overestimation of the observed values (Na^+, Cl^-, F^-, Mg^{2+}, NH_4^+) are split evenly with the underestimation of the observed ones(Ca^{2+}, K^+, SO_4^{2-}, H^+, NO_3^-) . Except for Al, Cl^- and Na^+ all the simulated ions concentration are underestimated drastically when the observed cumulative discharge increased from 163 to 213 mm (April 23rd to May 3rd). The theoretical model used to model the leaching of pollutants from the snowpack does not take into consideration the seggregation effects occurring in the snowpack at the surface of snow crystals during cold periods once the melting period has started. Therefore, it can not simulate these events properly. The small increase in concentration is probably related to the melting of a new layer of snow (80 mm of SWE) that fell between April 15th and April 30th.

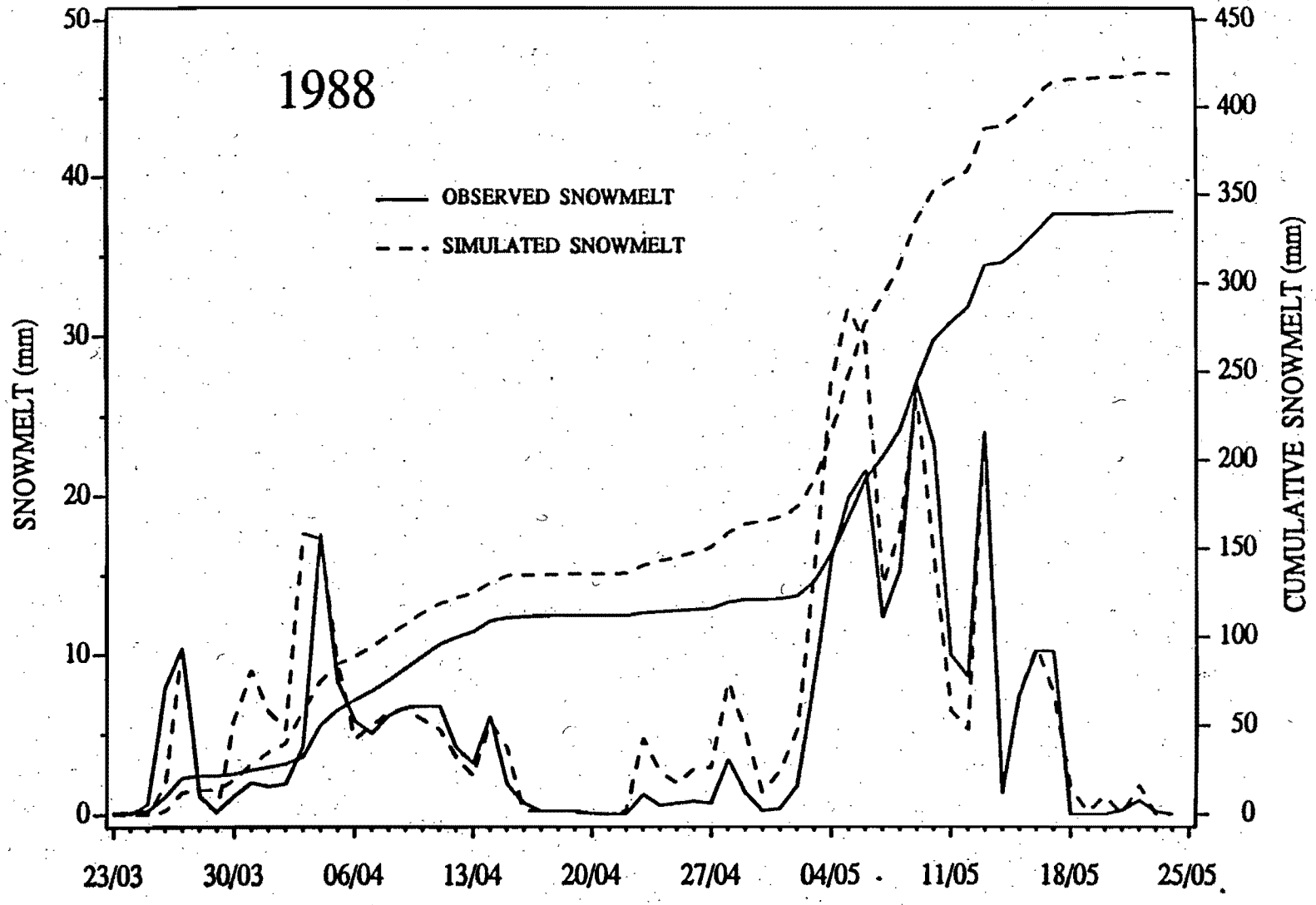

Fig.10: Daily and cumulative snowmelt observed and simulated for the 20 m^2 lysimeter for the 1988 season

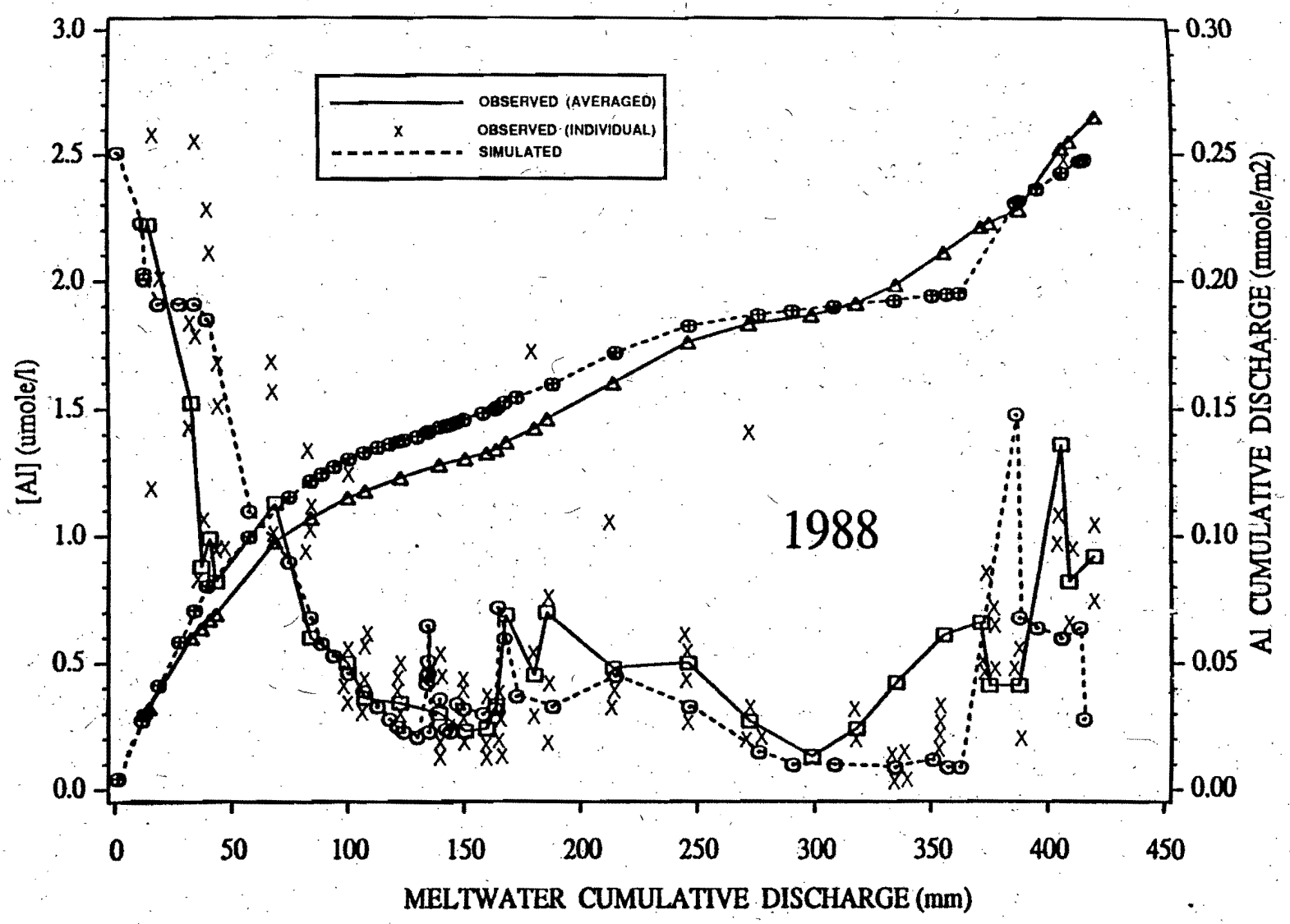

Fig.11: Daily aluminium(Al) concentration and cumulative discharge observed and simulated by VSASQ1 in segment C

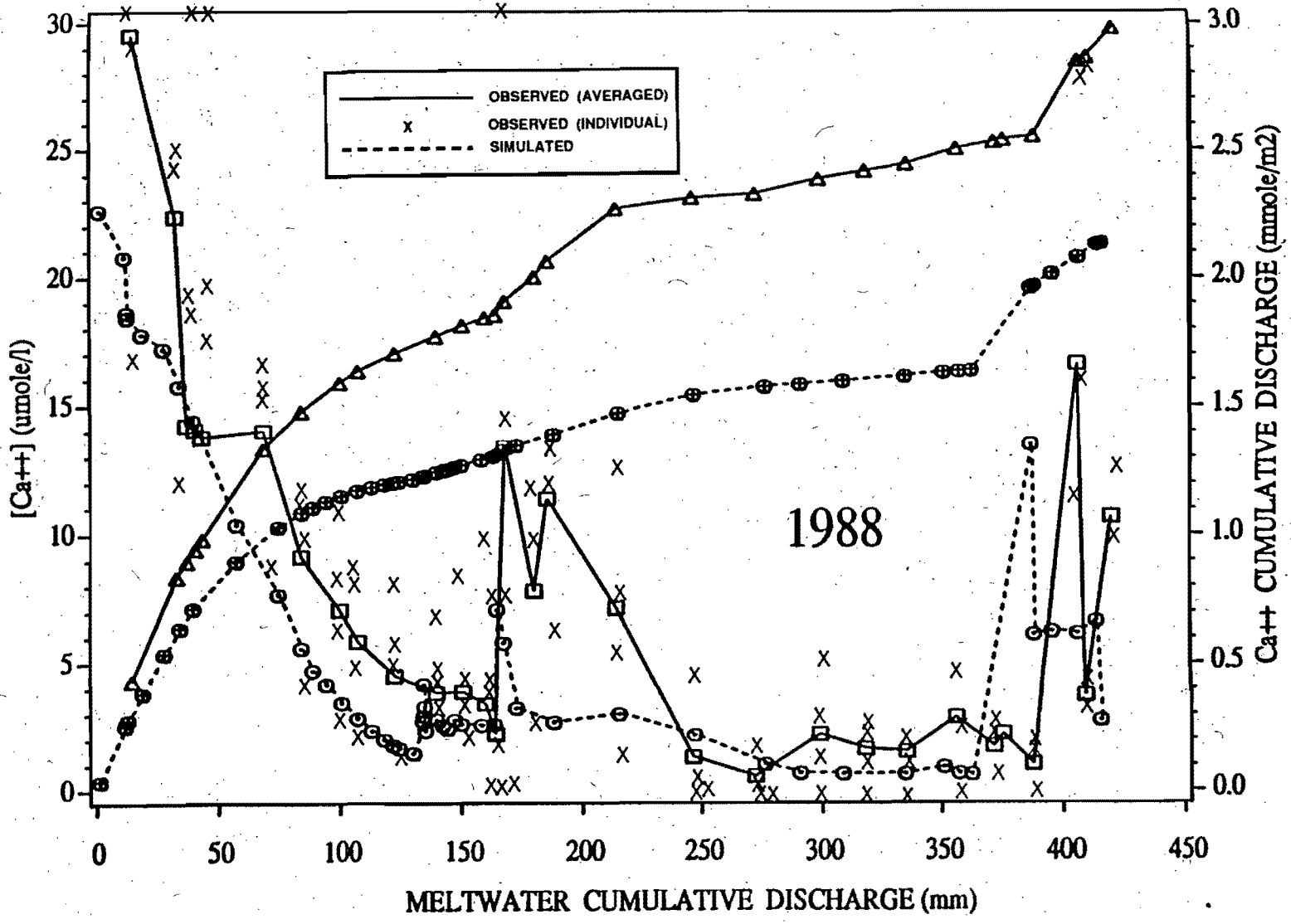

Fig.12: Daily calcium (Ca^{2+}) concentration and cumulative discharge observed and simulated by VSASQ1 in segment C

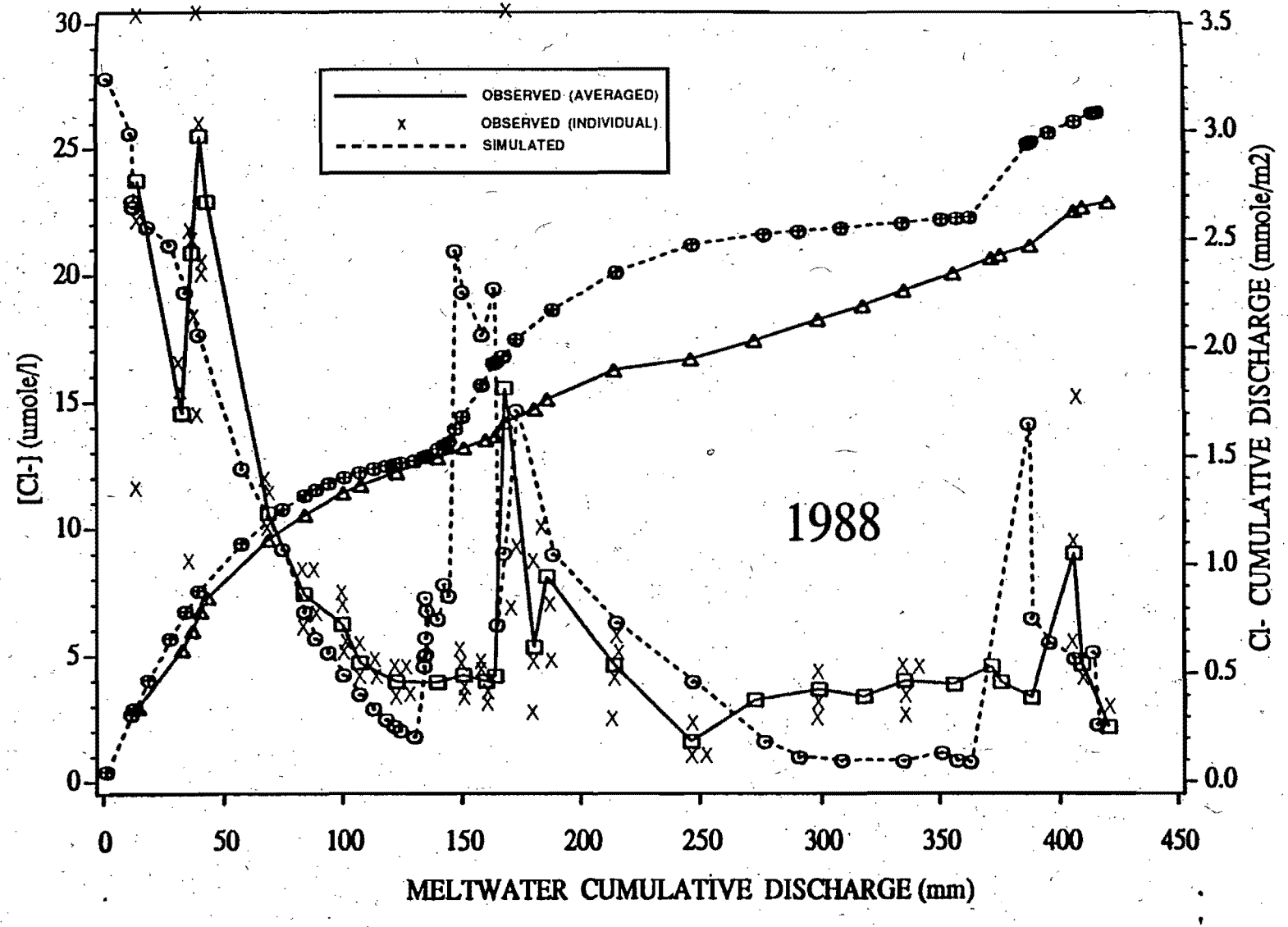

Fig.13: Daily chlorine (Cl^-) concentration and cumulative discharge observed and simulated by VSASQ1 in segment C

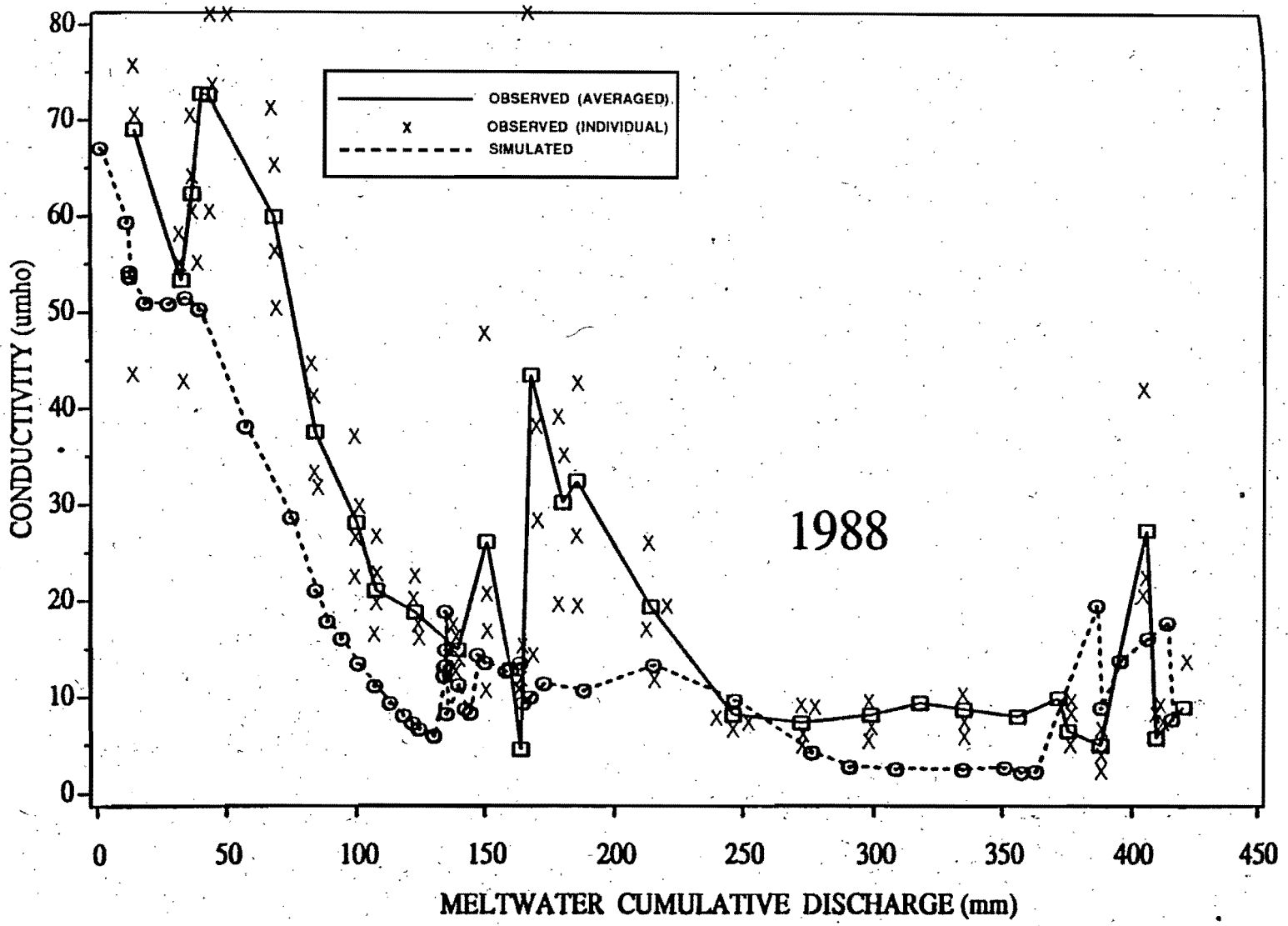

Fig.14: Daily electrical conductivity (EC)values observed and simulated as simulated by VSASQ1 in segment C

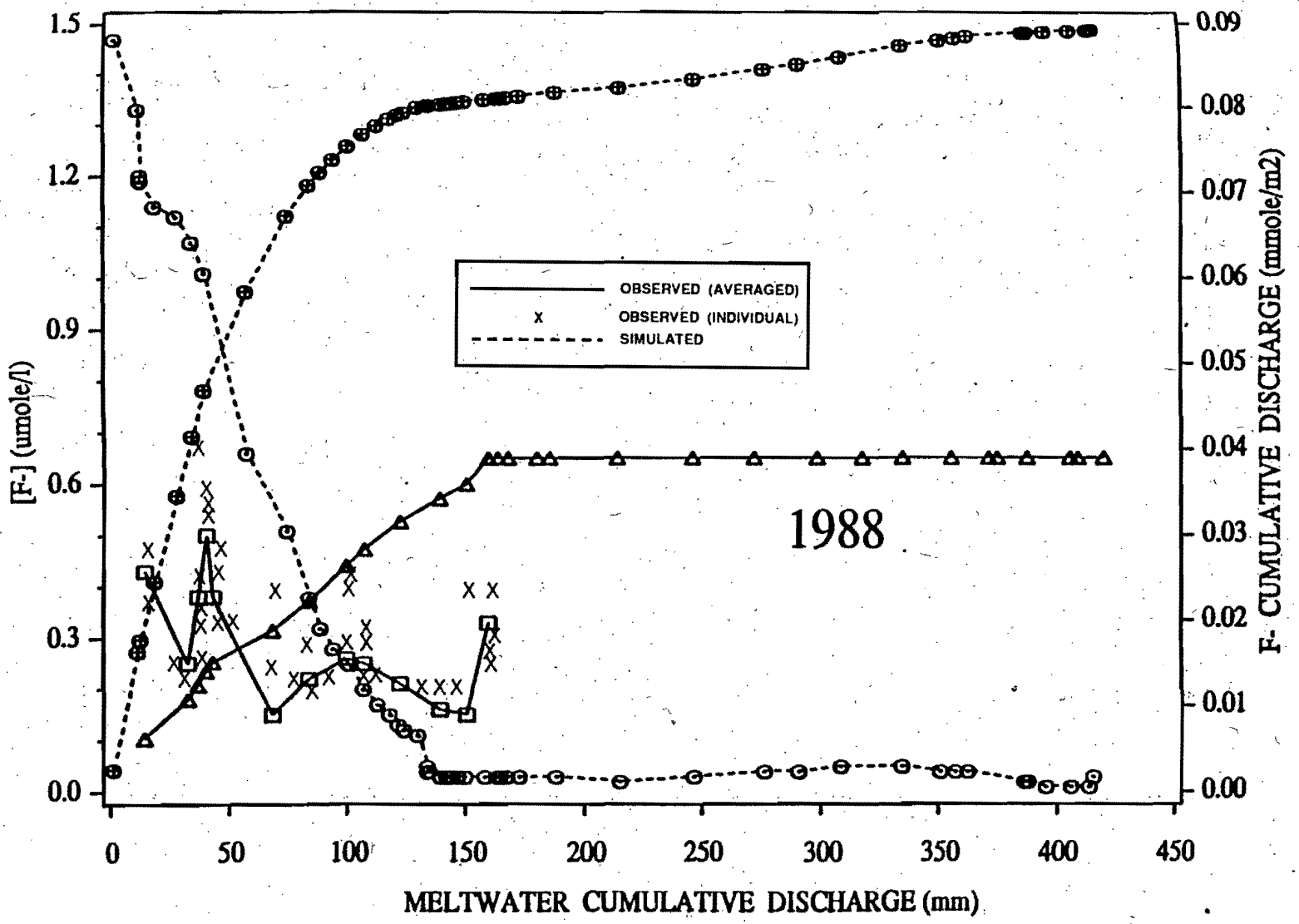

Fig.15: Daily fluoride (F^-)concentration and cumulative discharge observed and simulated by VSASQ1 in segment C

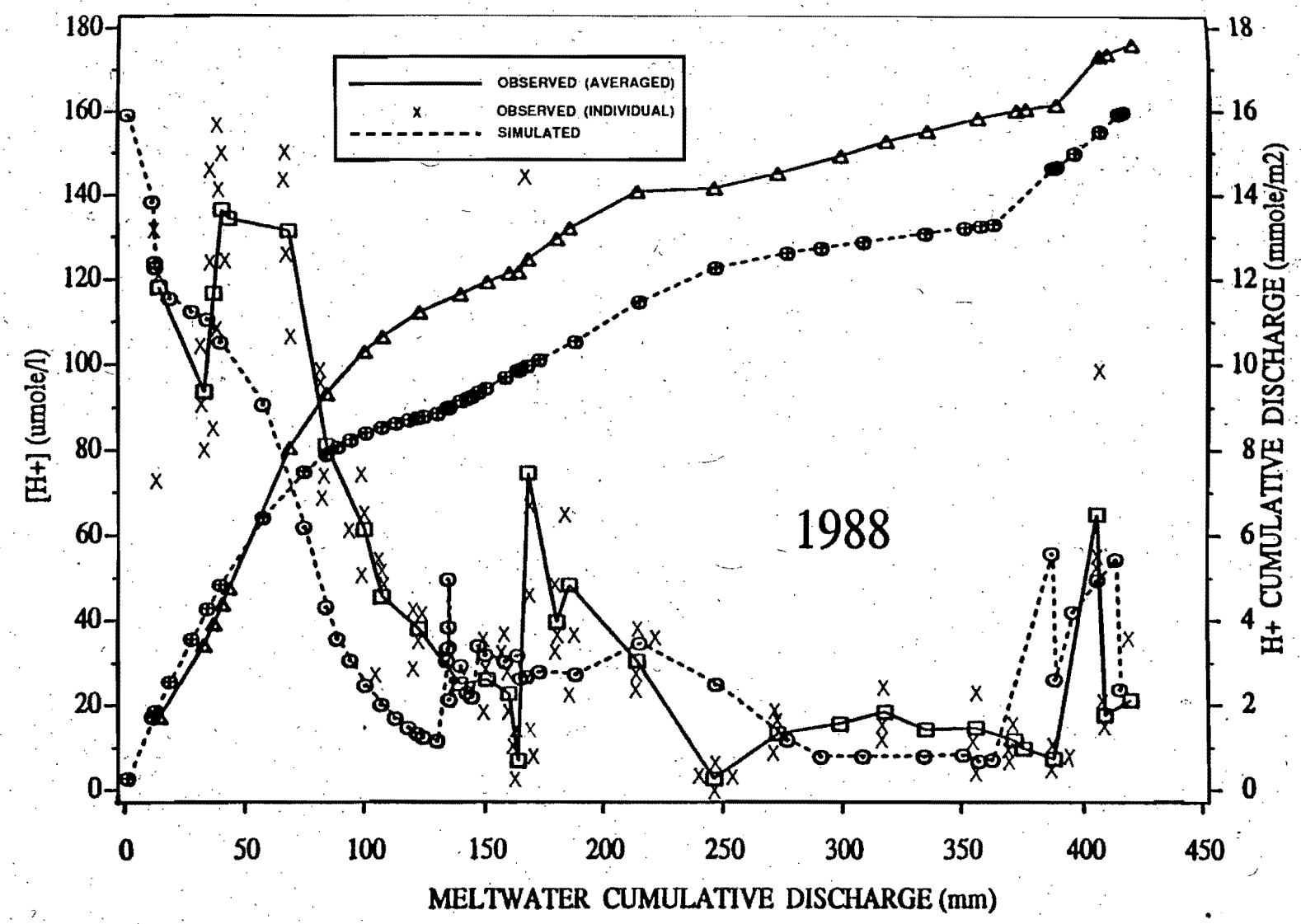

Fig.16: Daily hydrogen (H^+) concentration and cumulative discharge observed and simulated by VSASQ1 in segment C

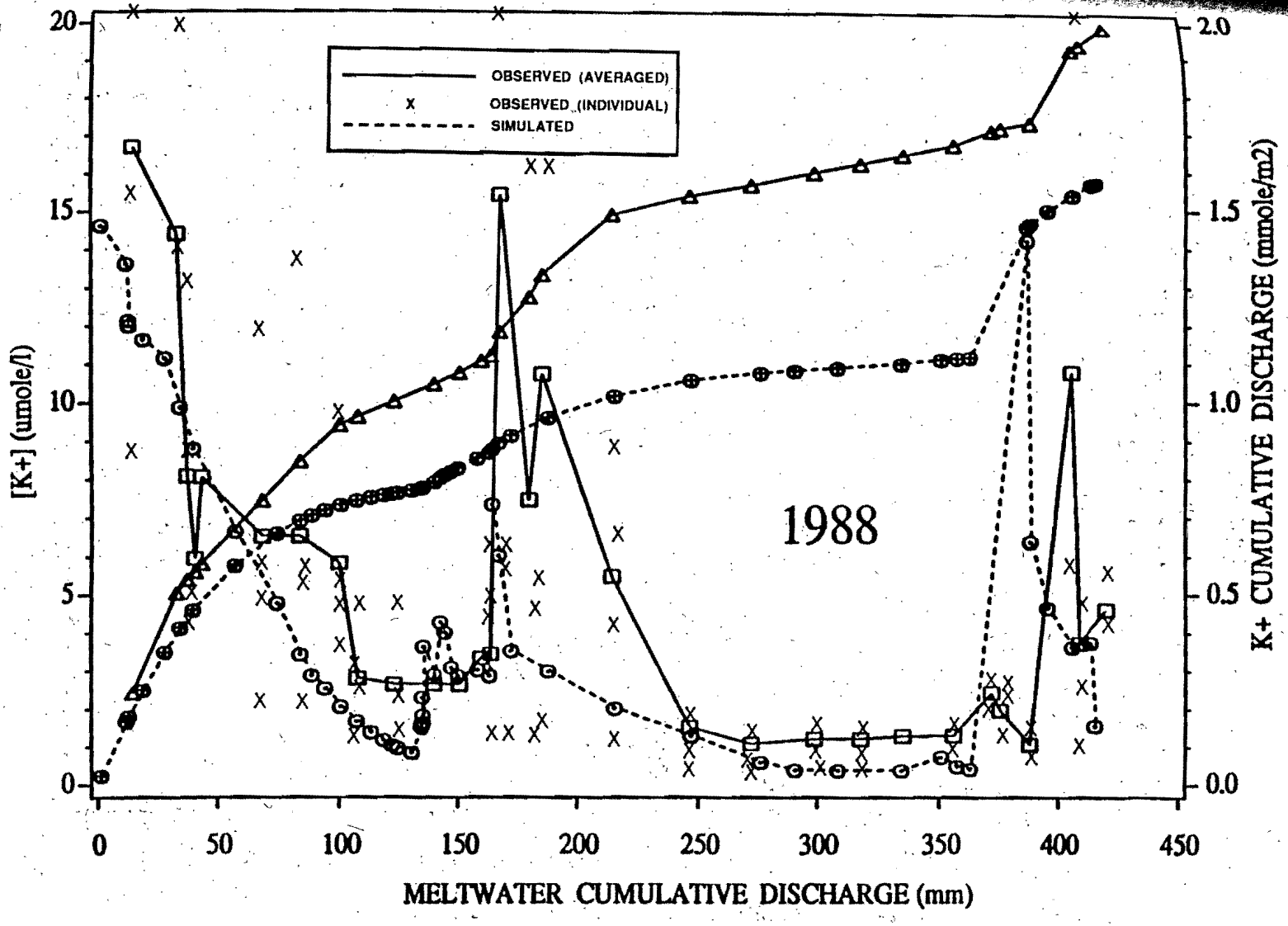

Fig.17: Daily potassium (K^+) concentration and cumulative discharge observed and simulated by VSASQ1 in segment C

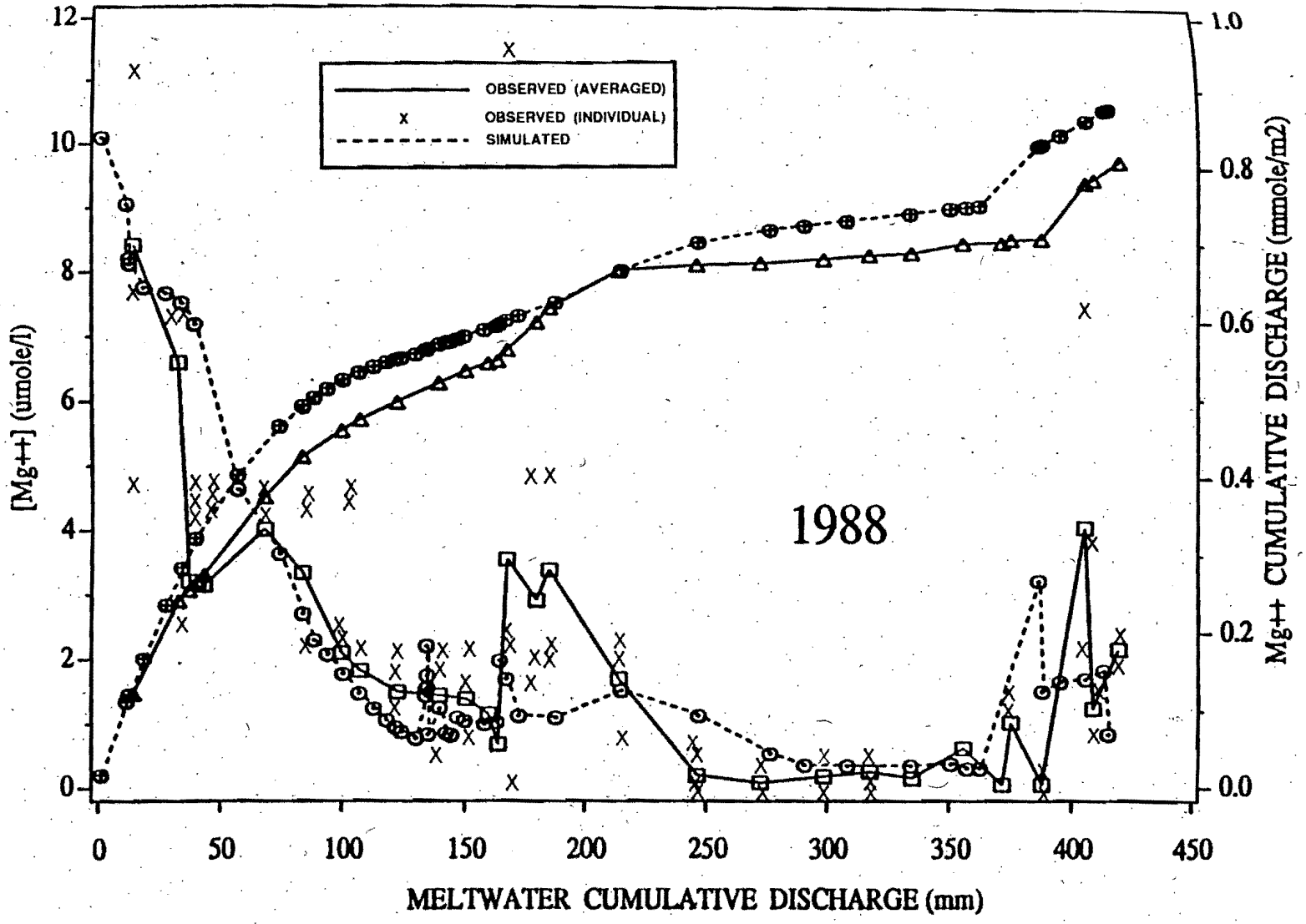

Fig.18: Daily magnesium (Mg^{2+}) concentration and cumulative discharge observed and simulated by VSASQ1in segment C

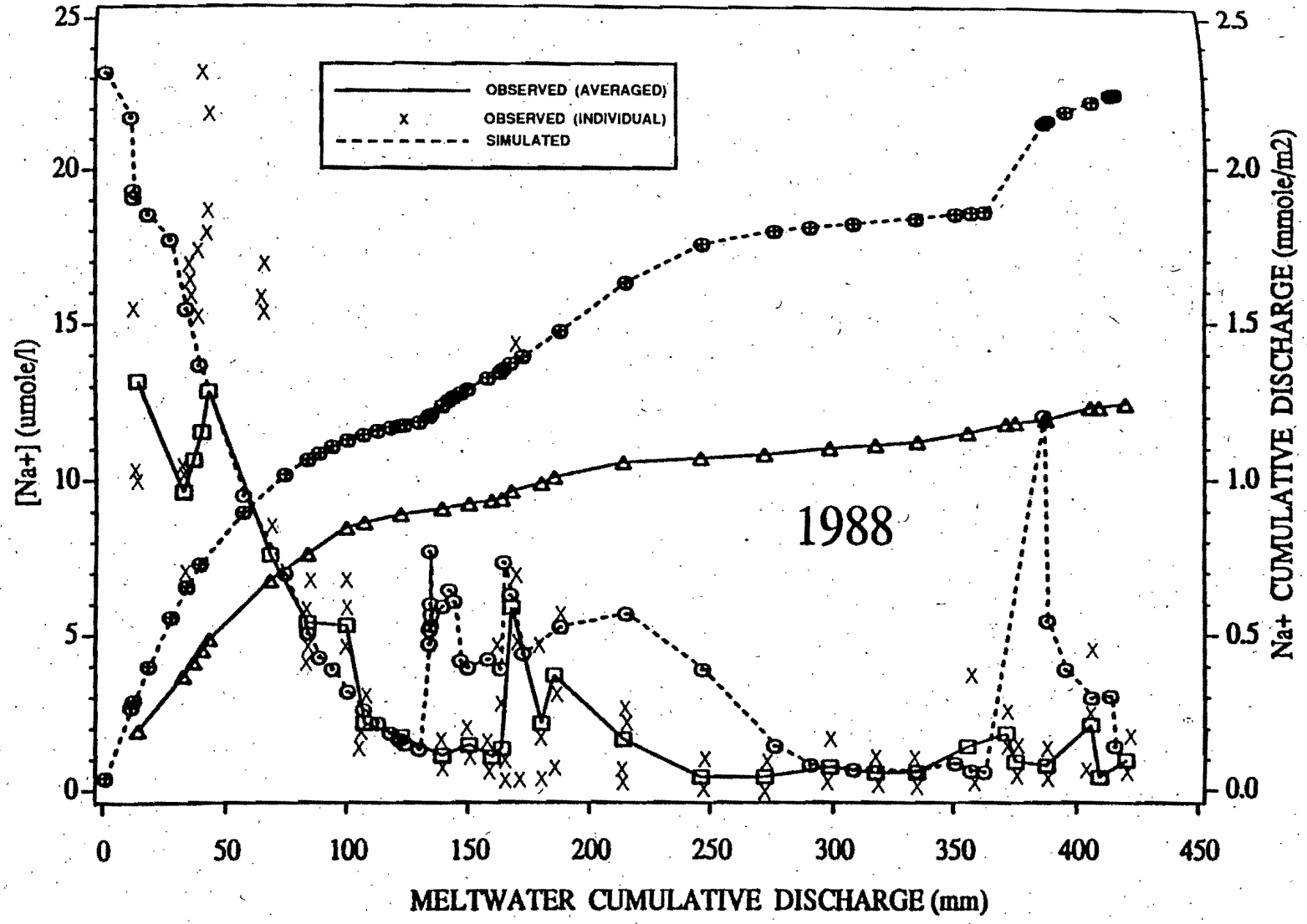

Fig.19: Daily sodium (Na^+) concentration and cumulative discharge observed and simulated by VSASQ1in segment C

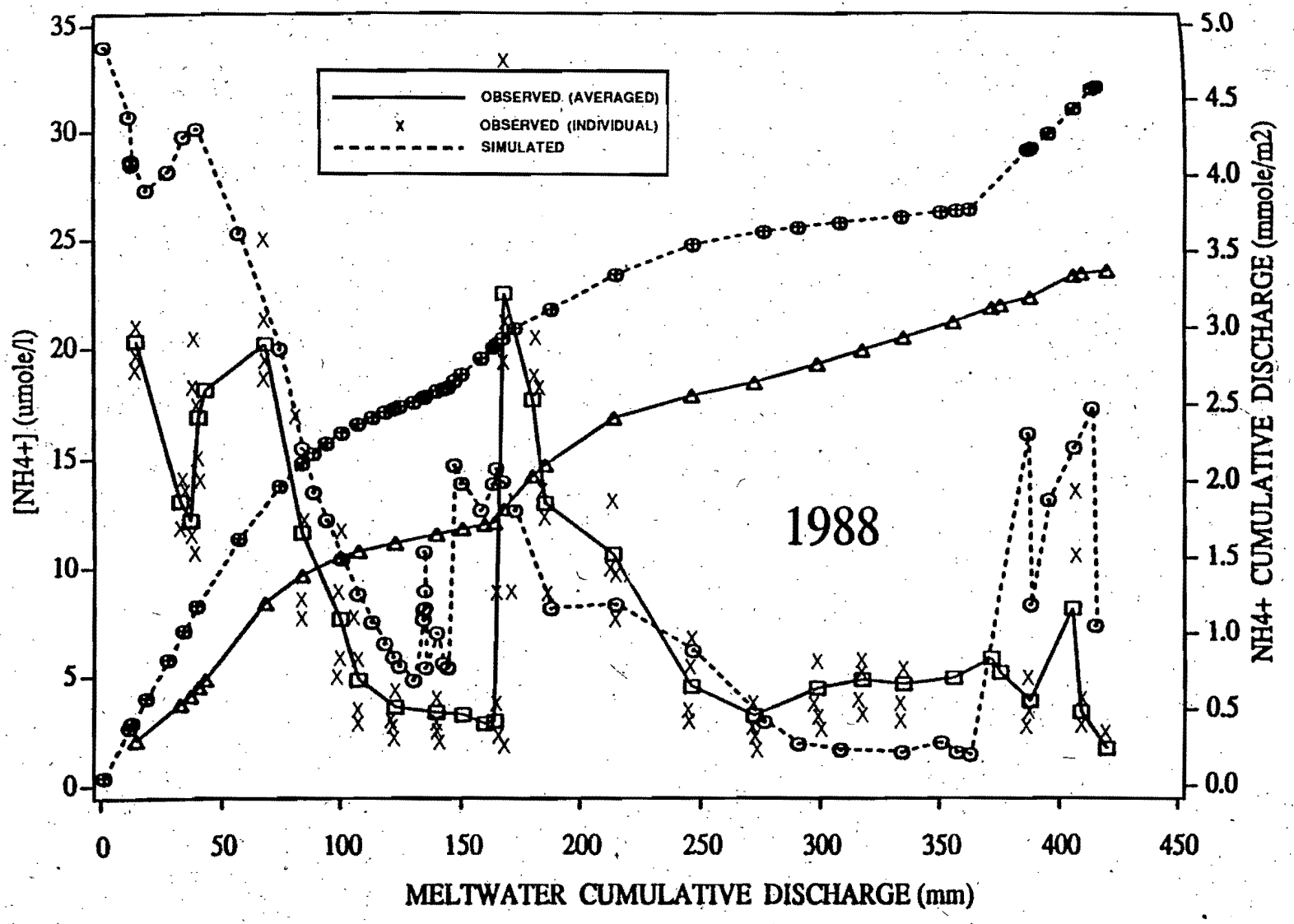

Fig.20: Daily ammonium(NH_4^+) concentration and cumulative discharge observed and simulated by VSASQ1in segment C

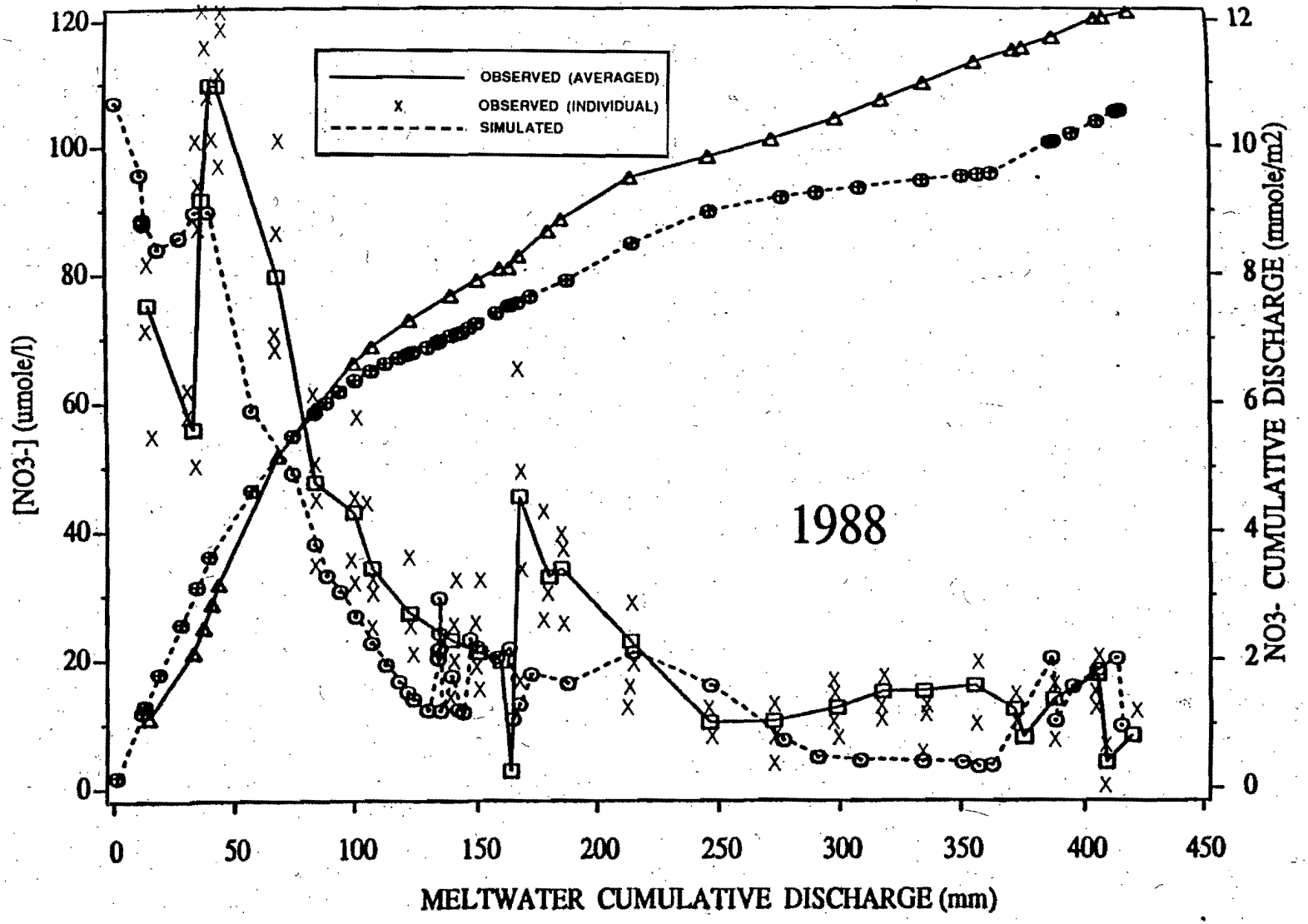

Fig.21: Daily nitrate (NO_3^-) concentration and cumulative discharge observed and simulated by VSASQ1 in segment C

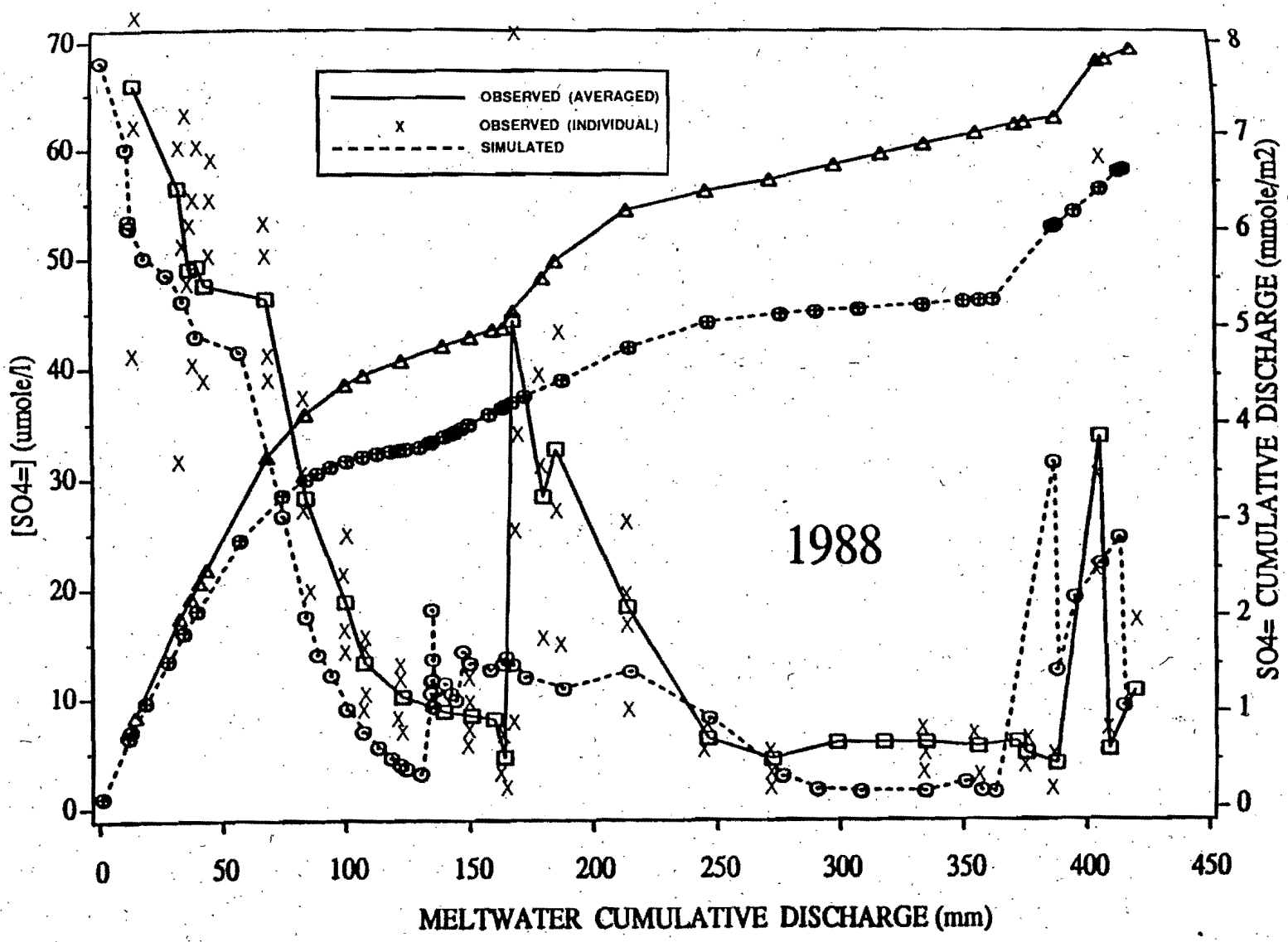

Fig.22: Daily sulphate (SO_4^{2-}) concentration and cumulative discharge observed and simulated by VSASQ1in segment C

Another discrepancy is observed for Al, Ca^{2+},Cl^{-}, EC, H^{+}, K^{+}, Mg^{2+} when the cumulative discharge reaches 382 mm. The simulated snowcower concentrations are much higher than the observed values. However from the response of meltwater during this period, it seems that the peak should have occurred when the cumulative discharge reached 406 mm instead. Had we used the dates for the abcissa instead of the cumulative discharge, the peaks would not have such an apparent lag. We believe that the lag is caused by cumulative errors between simulated and observed values of daily discharges. If we had used the dates, the whole simulated curve would shift to the right and the results would look better as a whole.

Considering the differences in concentration between the 4 lysimeters (due to spatial variablity) and the probable effect of segregation during cold periods, then the results of SNOQUALR are excellent.However, fundamental research is needed so that the leaching coefficients can be predicted instead of measured. Theoretical work is also needed to include into the model the segregation effects of ions resulting from refreezing once the melting period has started. For the quantitative aspects, melt factors will need to be found for the lake surface snowcover.

VSAS2

Sensitivity analysis

A sensitivity analysis was performed on the hydraulic conductivity and the depth of deposits. The analysis was done on segment C. The simulated snowmelt is presented for this segment and the expected discharge is obtained by multiplying the observed discharge at the lake exit by the percentage of the whole basin occupied by segment C. During this sensitivity analysis the snow cover areal extent factor was turned off. The hydraulic conductivity of layer 2 (Figure 23) was varied and as can be seen there is no change in the simulated discharge until the hydraulic conductivity was lowered to 0.08 $cm \cdot hr^{-1}$. As to the depth of deposits (Figure 24), as soon as you increase the deposit thickness by 50%, a reduction in peak flow is observed.

Water Balance

The water balance for the entire snowmelt season as calculated by the model is given by the following formula:

$$P = E + \Delta S + \Delta L + R \qquad (2)$$

where P = Precipitation (including rain, snow and snowmelt)

E = Evaporation

ΔS = Change of water volume in the soil

ΔL = Change of water volume in the lake

R = Runoff at the lake outlet

The values found in m^3 were

$$281864 = 0 + (688152 - 547655) + (21984 - 19806) + 140258$$

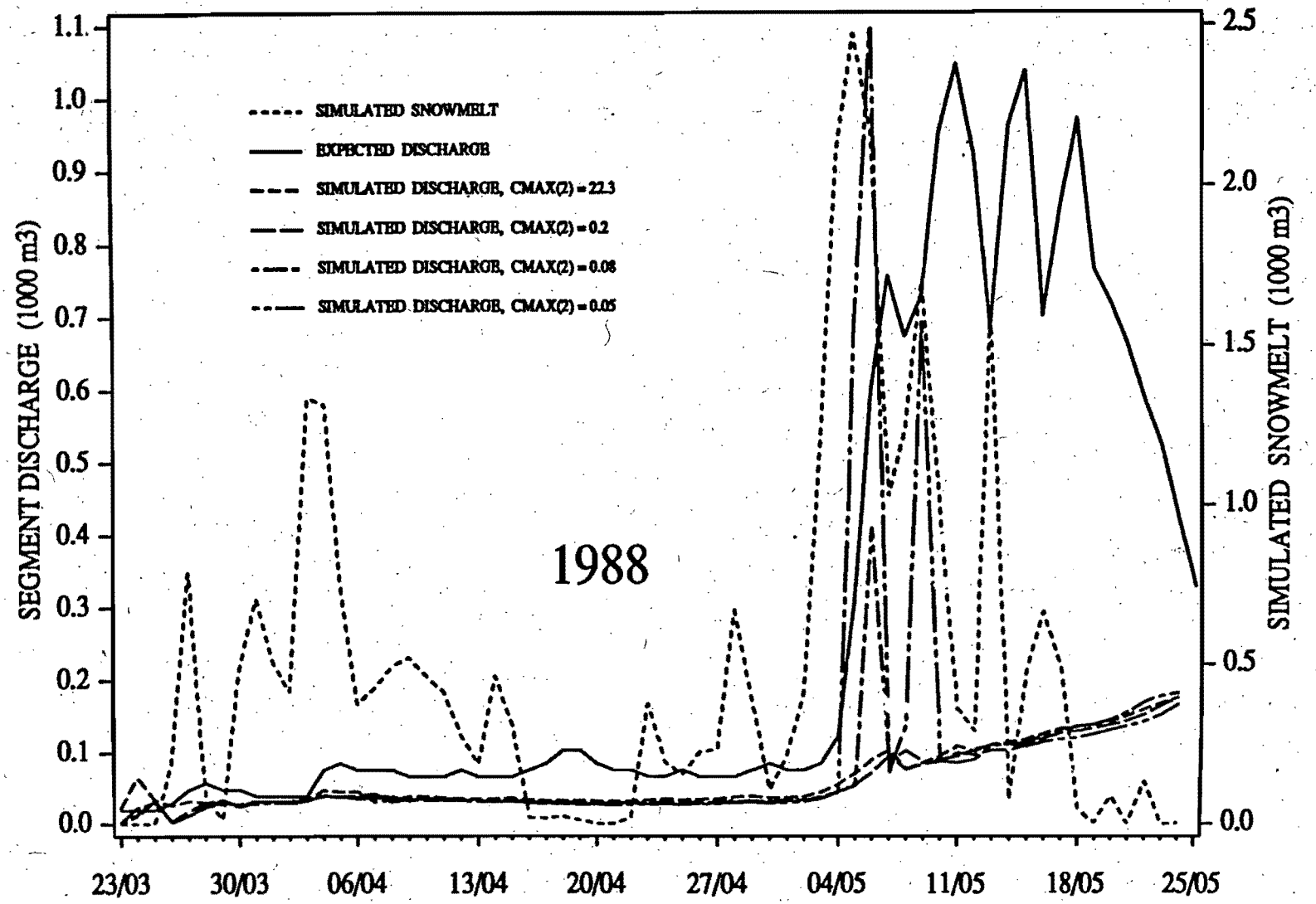

Fig.23: Effect of changes of hydraulic conductivity of layer 2 on the segment C discharge. The simulated discharge of the whole basin is multiplied by the fraction of segment C over the total area

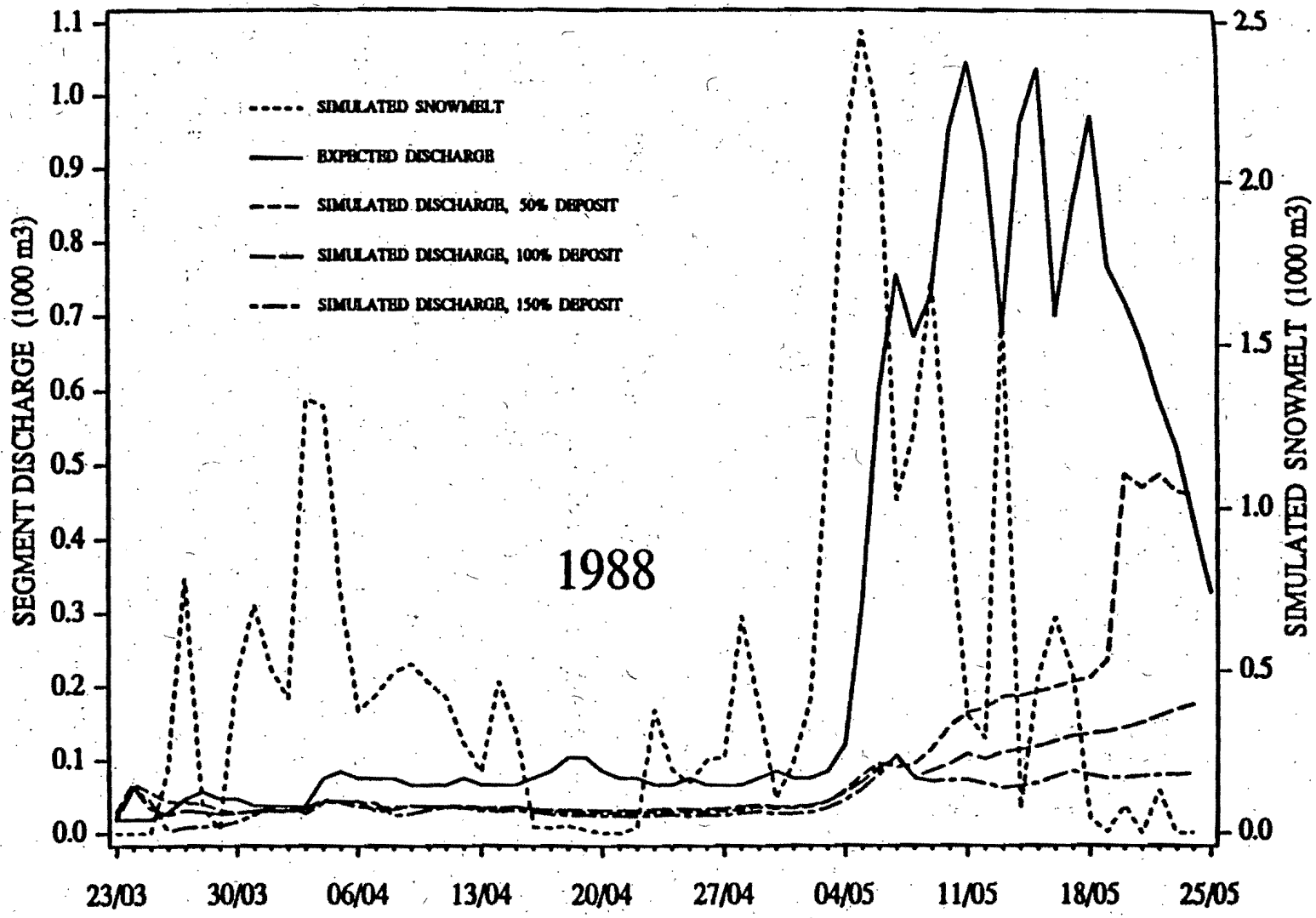

Fig.24: Effect of deposit thickness changes on the segment discharge. The simulated discharge of the whole basin is multiplied by the fraction of segment C over the total area

The evaporation was neglected and the error for the whole balance is 0.4%. The daily discharge of the whole watershed is presented in Figure 25. As can be seen, the simulated values are overestimated in the first part of the melt i.e. the first 170 mm of melt while it is underestimated the last 30 mm of the 410 mm input to the soil. With the inclusion of the snow cover areal extent factor (Prévost et al., 1990) to the model, the surface runoff, (i.e. snowmelt not entering the mineral matrix) was equal to 56% of total streamflow for the whole watershed. Maulé and Stein (1990) found for an interflow stream using two tracers methods, a surface runoff value of 47% for the same basin and snowmelt event. If the model is to be transportable, a module calculating the effect of soil freezing on soil hydrologic properties need to be added.

SOILEQ

The results for the following different ions (Al, Ca^{2+}, Cl^-, F^-, K^+, Mg^{2+}, Na^+, NH_4^+, NO_3^-, pH, SO_4^{2-}) are presented in Figure 26 through 36 respectively. Horizons 1, 2, 3 and 4 stand for the layers between 0-10, 10-40, 40-80 and > 80 cm respectively. The observed results presented are originating from two nests of piezometers near the shore; one in segment C and the other in segment D (Figure 2). From figure 26, the simulation of Al for the four layers are greatly underestimated, it is even zero for layer 1. For Ca^{2+}, K^+, Cl^-, Mg^{2+}, Na^+, SO_4^{2-} ions; generally it simulates a decrease of values for horizon 1, 2 and 3 from the beginning of melt to the end as the observed values. For horizon 4, it simulates an increase from the beginning to the end while the observed values stay more or less constant. In general, the simulations values are not far from the observed ones. In the case of F^- the results are good at the beginning of the season but at the end of the season an increase is observed while the predicted values show a decrease. For NO_3^- and pH, the results are good for horizon 3 and 4. For NH_4^+, the simulations are not better than Al and the link between the observed and simulated value is hard to find.

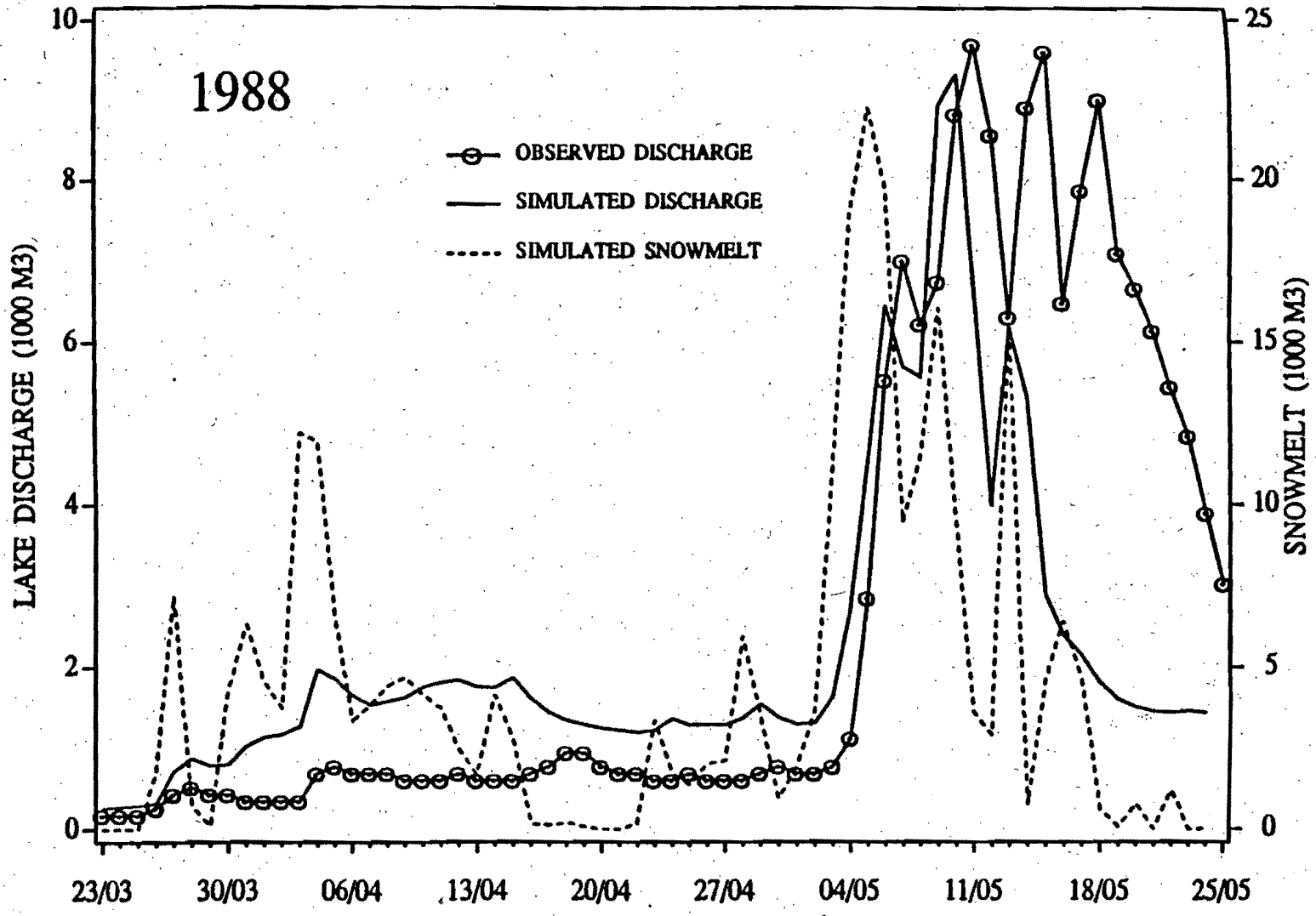

Fig.25: Snowmelt rates and discharges for the whole watershed

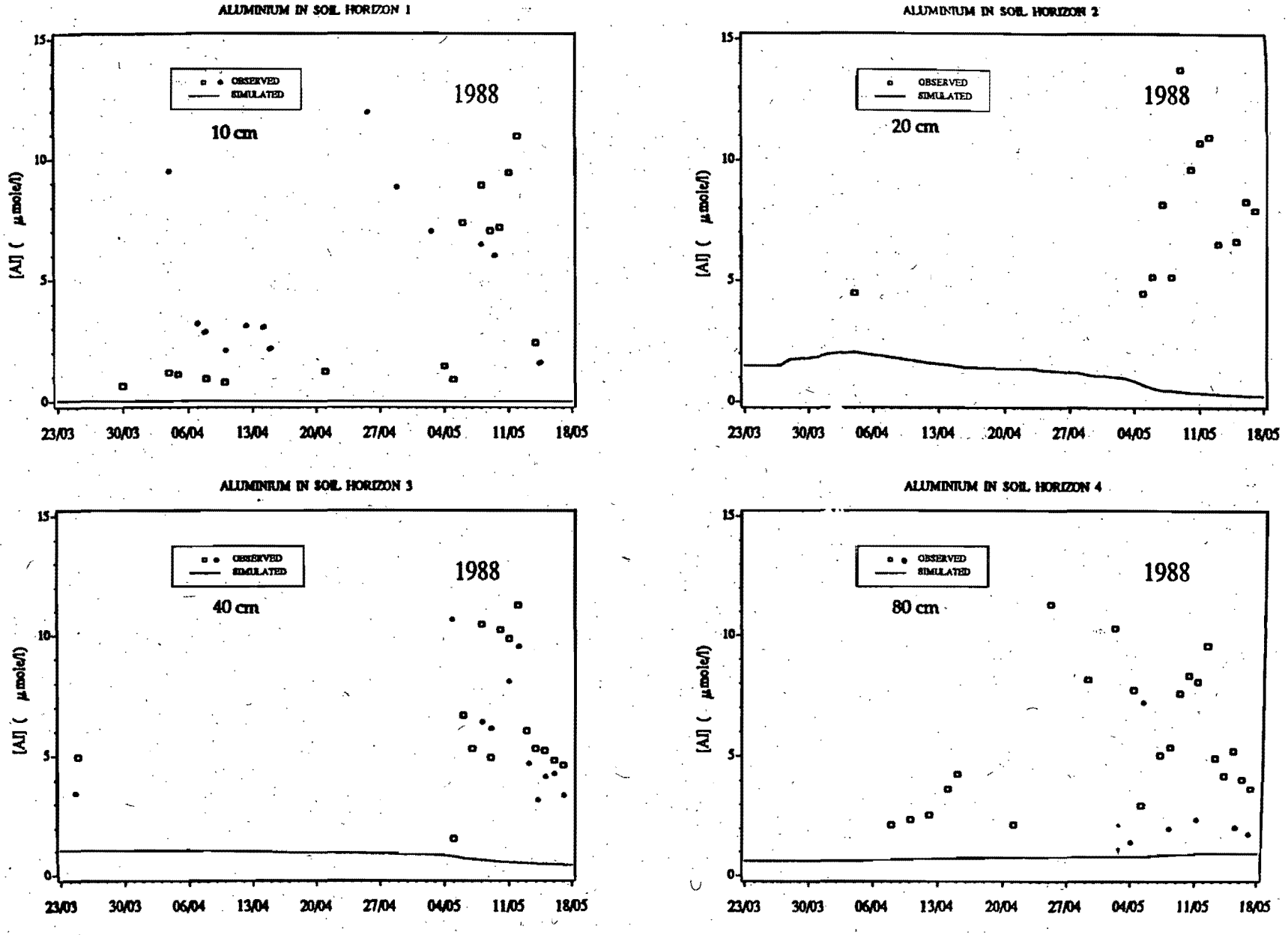

Fig.26: Concentration of Al^{-} in the soil horizons (1 = 0-10 cm, 2 = 10-40, 3 = 40-80, 4 = > 80 cm deep) as simulated by VSASQ1 along with the observed values in segments C (□) and D (●).

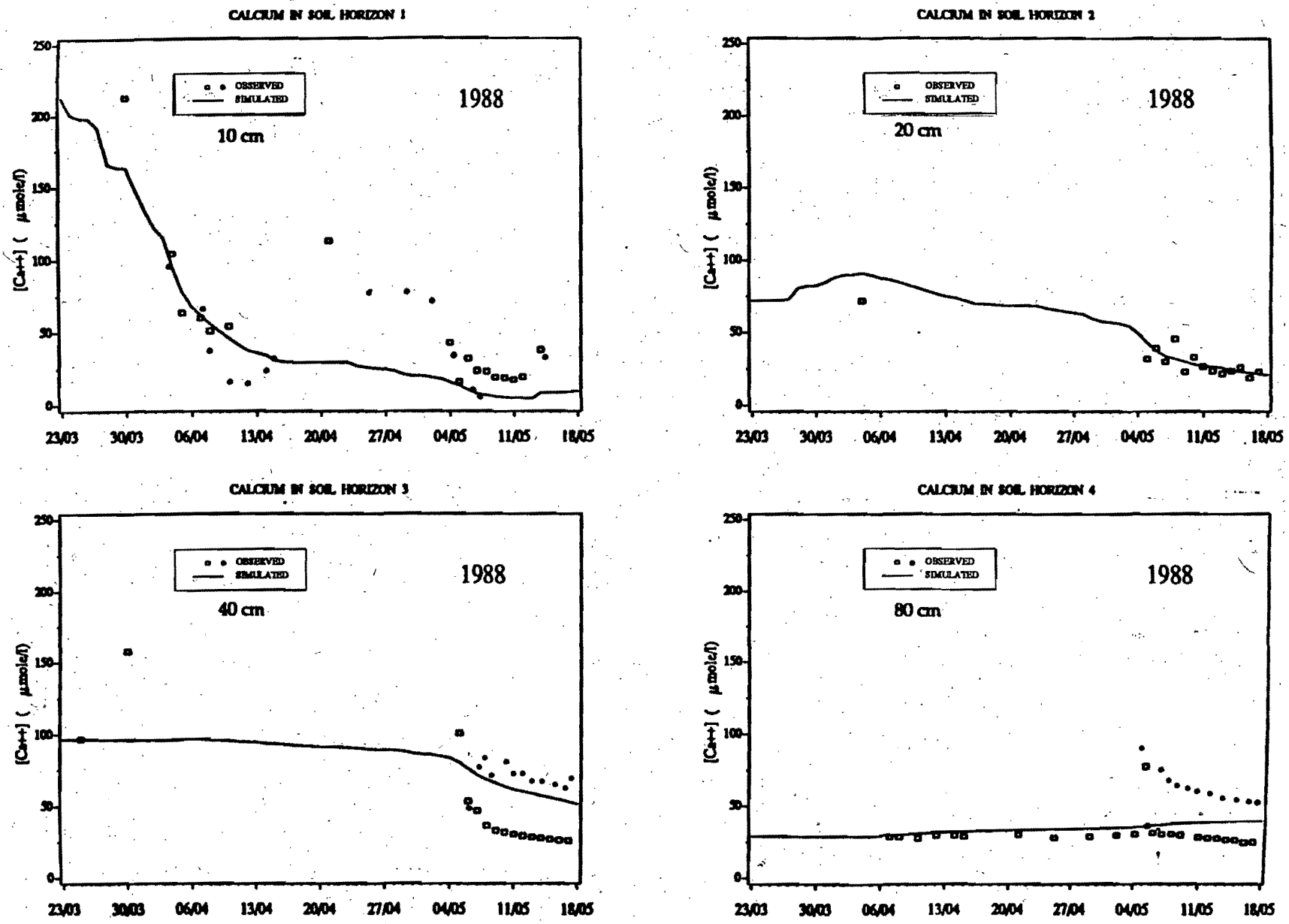

Fig.27: Concentration of Ca^{2+} in the soil horizons (1 = 0-10 cm, 2 = 10-40, 3 = 40-80, 4 = > 80 cm deep) as simulated by VSASQ1 along with the observed values in segments C (□) and D (●).

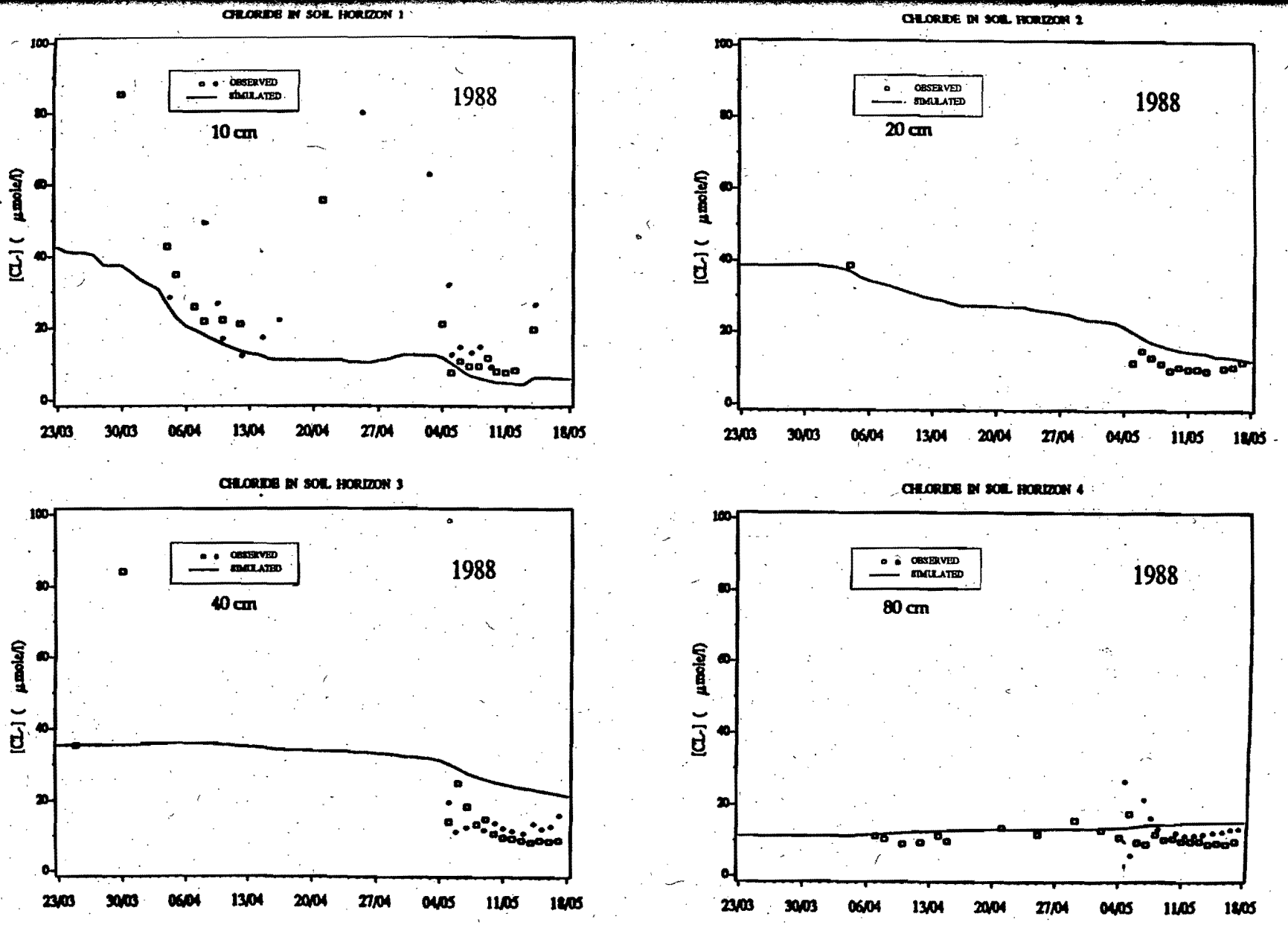

Fig.28: Concentration of Cl^- in the soil horizons (1 = 0-10 cm, 2 = 10-40, 3 = 40-80, 4 = > 80 cm deep) as simulated by VSASQ1 along with the observed values in segments C (□) and D (●).

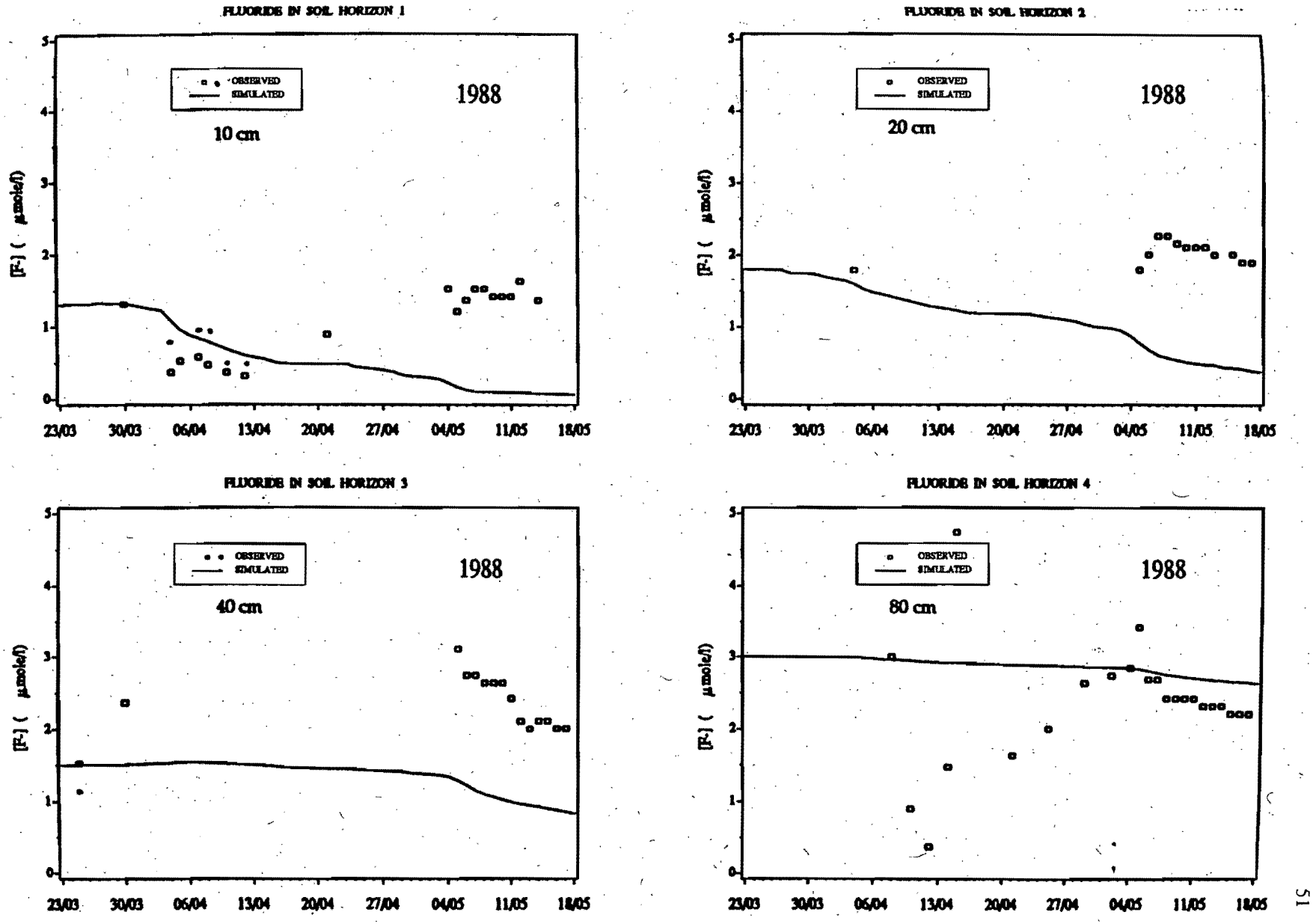

Fig.29: Concentration of F^- in the soil horizons (1 = 0-10 cm, 2 = 10-40, 3 = 40-80, 4 = > 80 cm deep) as simulated by VSASQ1 along with the observed values in segments C (□) and D (●).

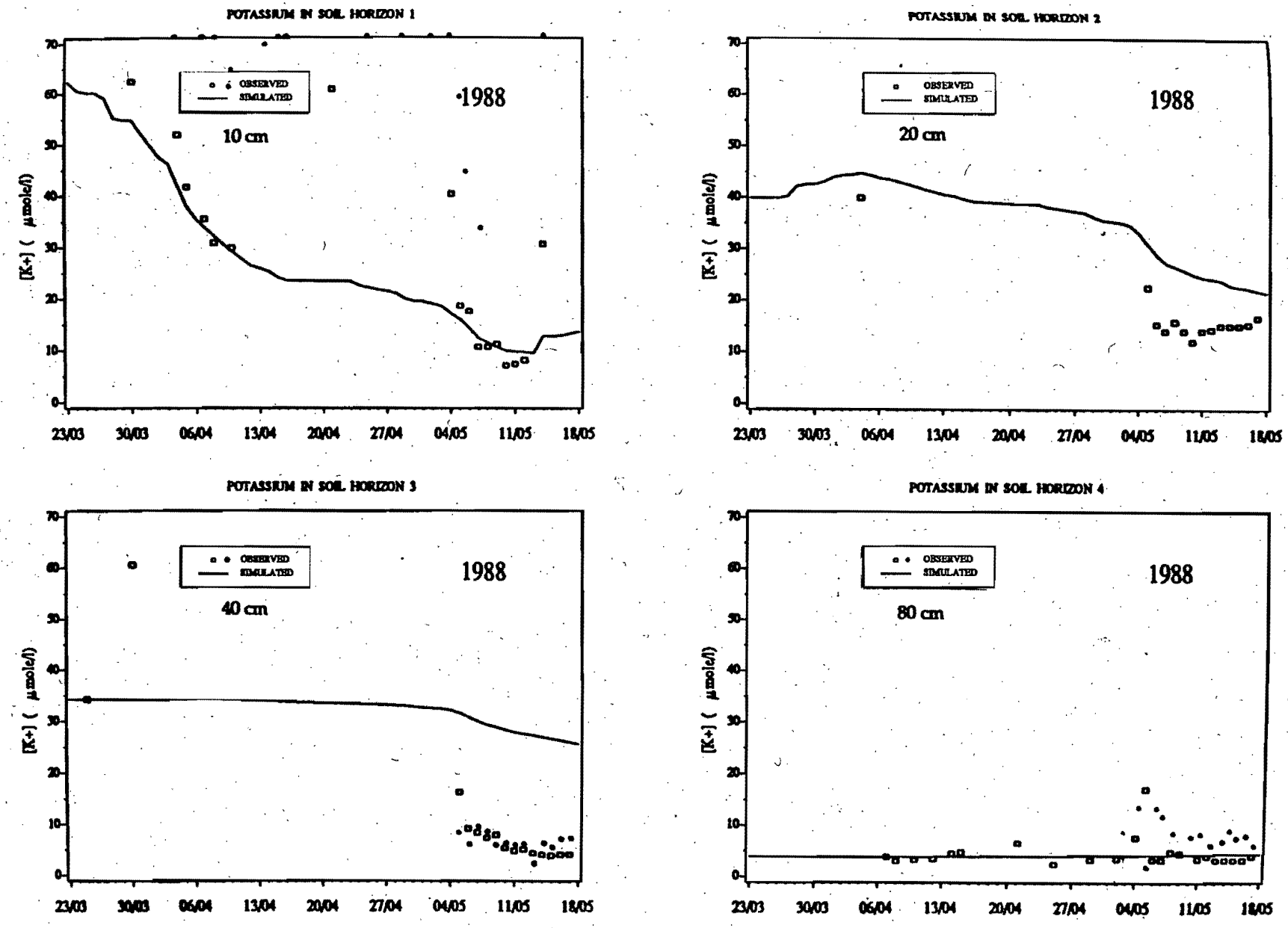

Fig.30: Concentration of K^+ in the soil horizons (1 = 0-10 cm, 2 = 10-40, 3 = 40-80, 4 = > 80 cm deep) as simulated by VSASQ1 along with the observed values in segments C (□) and D (●).

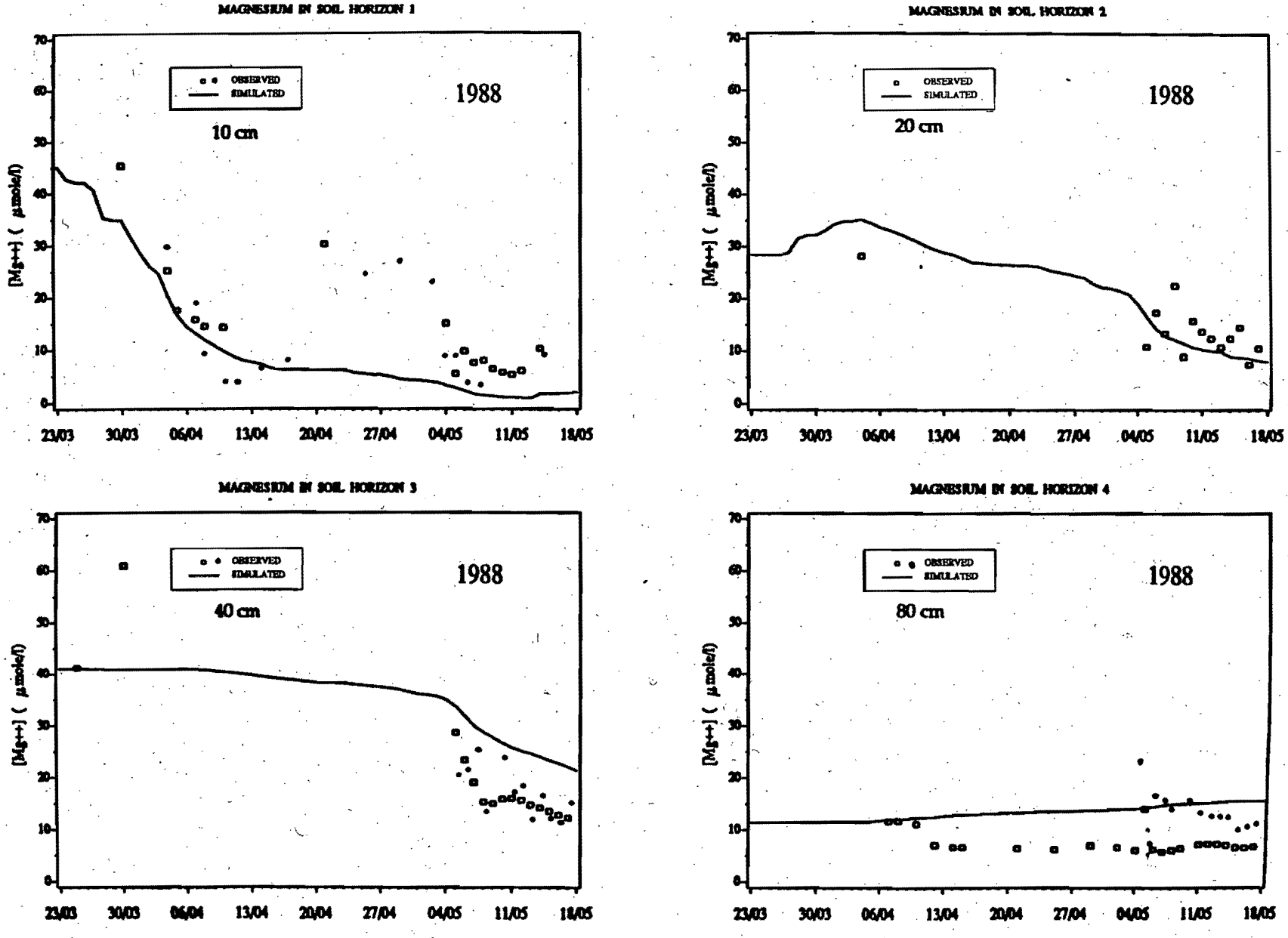

Fig.31: Concentration of Mg^{2+} in the soil horizons (1 = 0-10 cm, 2 = 10-40, 3 = 40-80, 4 = > 80 cm deep) as simulated by VSASQ1 along with the observed values in segments C (□) and D (●).

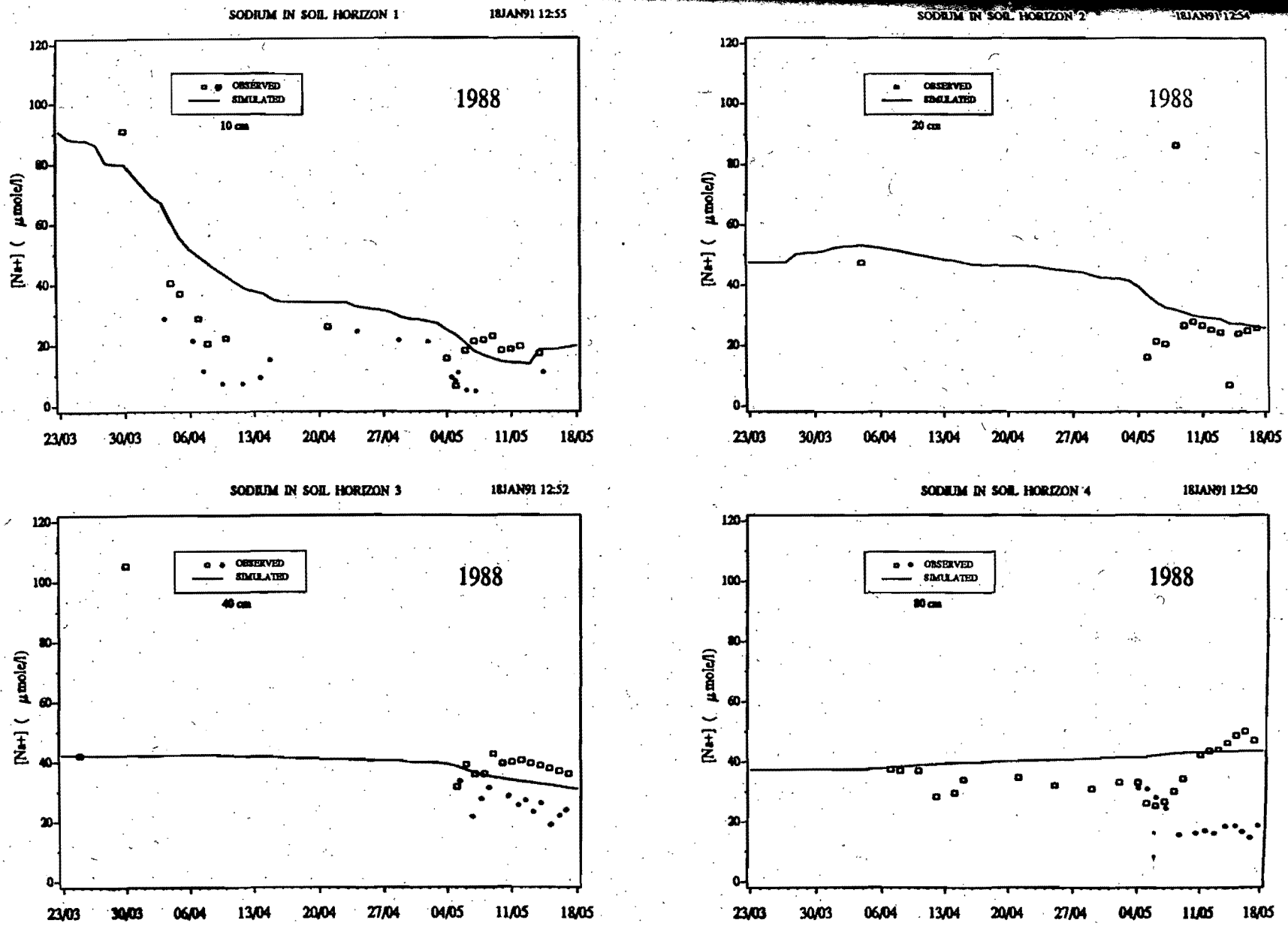

Fig.32: Concentration of Na^+ in the soil horizons (1 = 0-10 cm, 2 = 10-40, 3 = 40-80, 4 = > 80 cm deep) as simulated by VSASQ1 along with the observed values in segments C (□) and D (●).

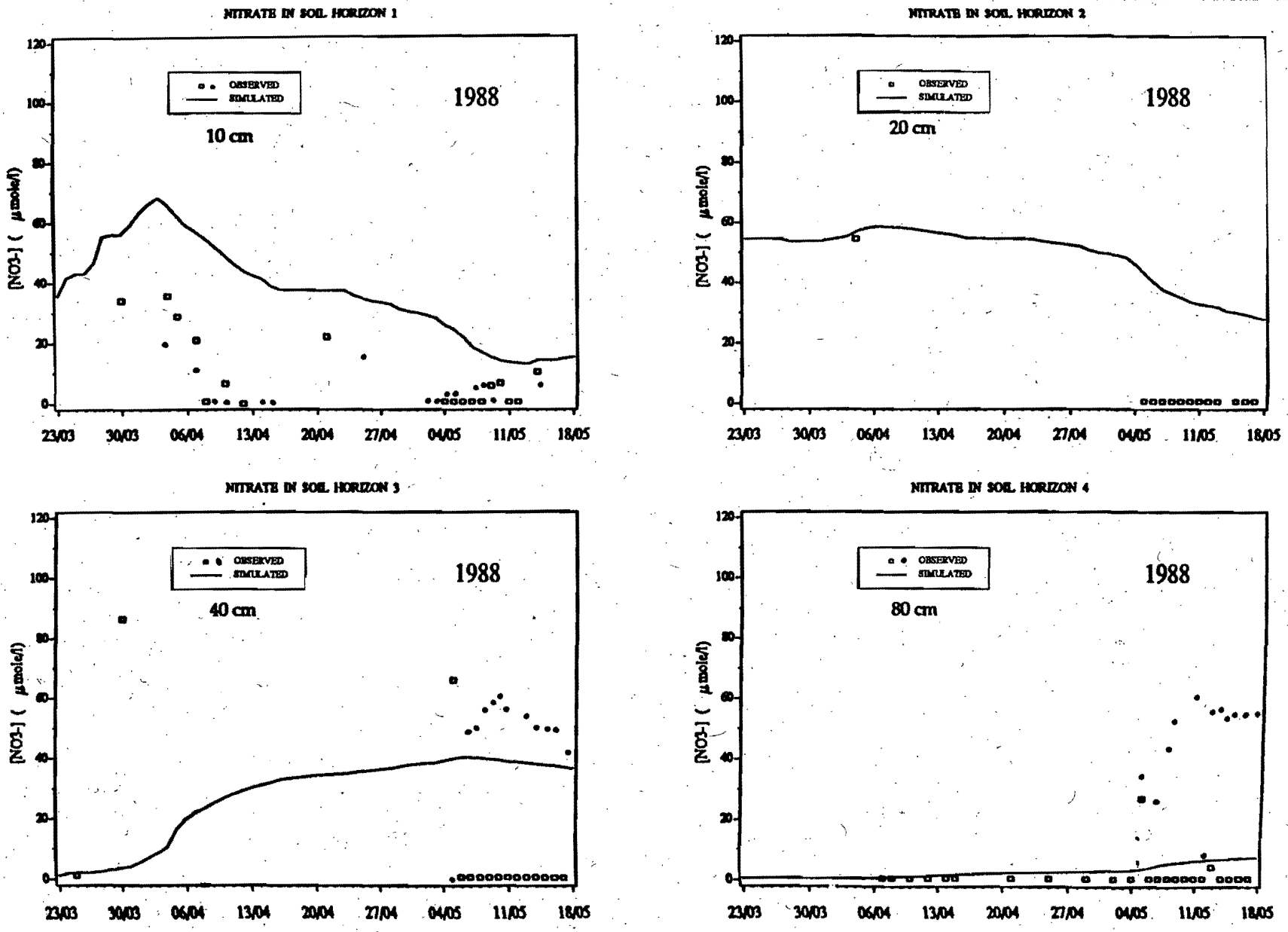

Fig.33: Concentration of NO_3^- in the soil horizons (1 = 0-10 cm, 2 = 10-40, 3 = 40-80, 4 = > 80 cm deep) as simulated by VSASQ1 along with the observed values in segments C (□) and D (●).

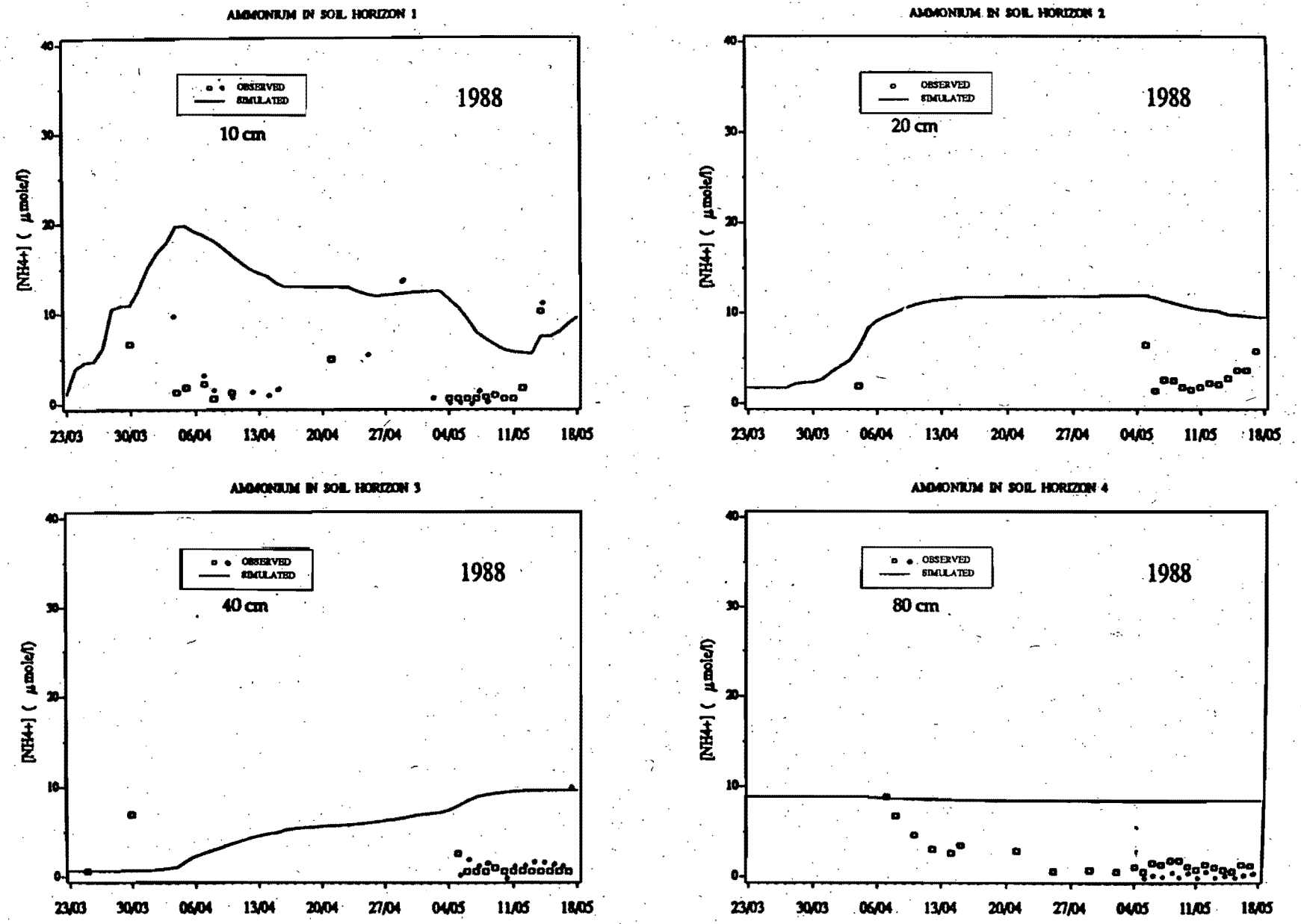

Fig.34: Concentration of NH_4^+ in the soil horizons (1 = 0-10 cm, 2 = 10-40, 3 = 40-80, 4 = > 80 cm deep) as simulated by VSASQ1 along with the observed values in segments C (□) and D (●).

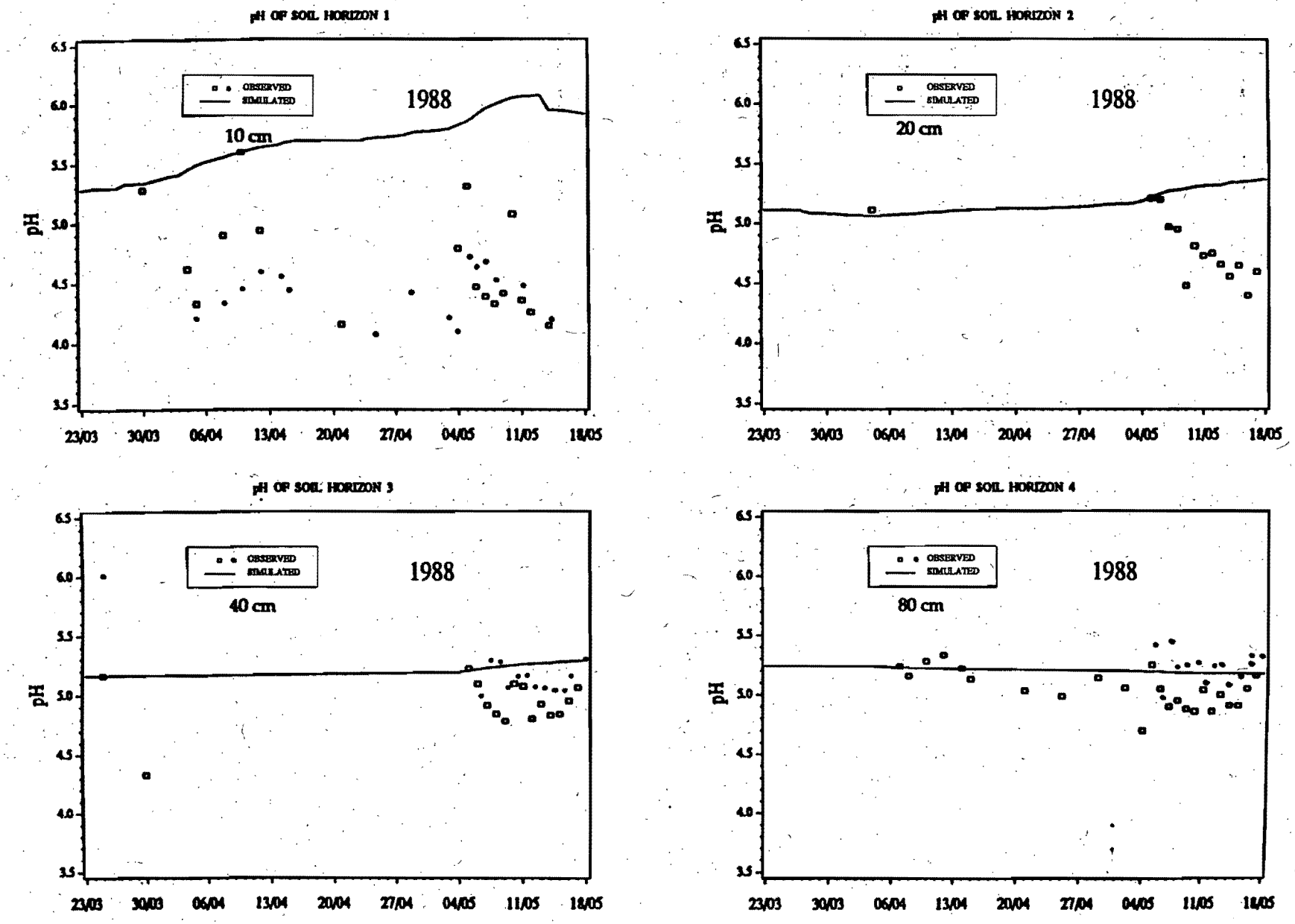

Fig.35: pH in the soil horizons (1 = 0-10 cm, 2 = 10-40, 3 = 40-80, 4 = > 80 cm deep) as simulated by VSASQ1 along with the observed values in segments C (□) and D (●).

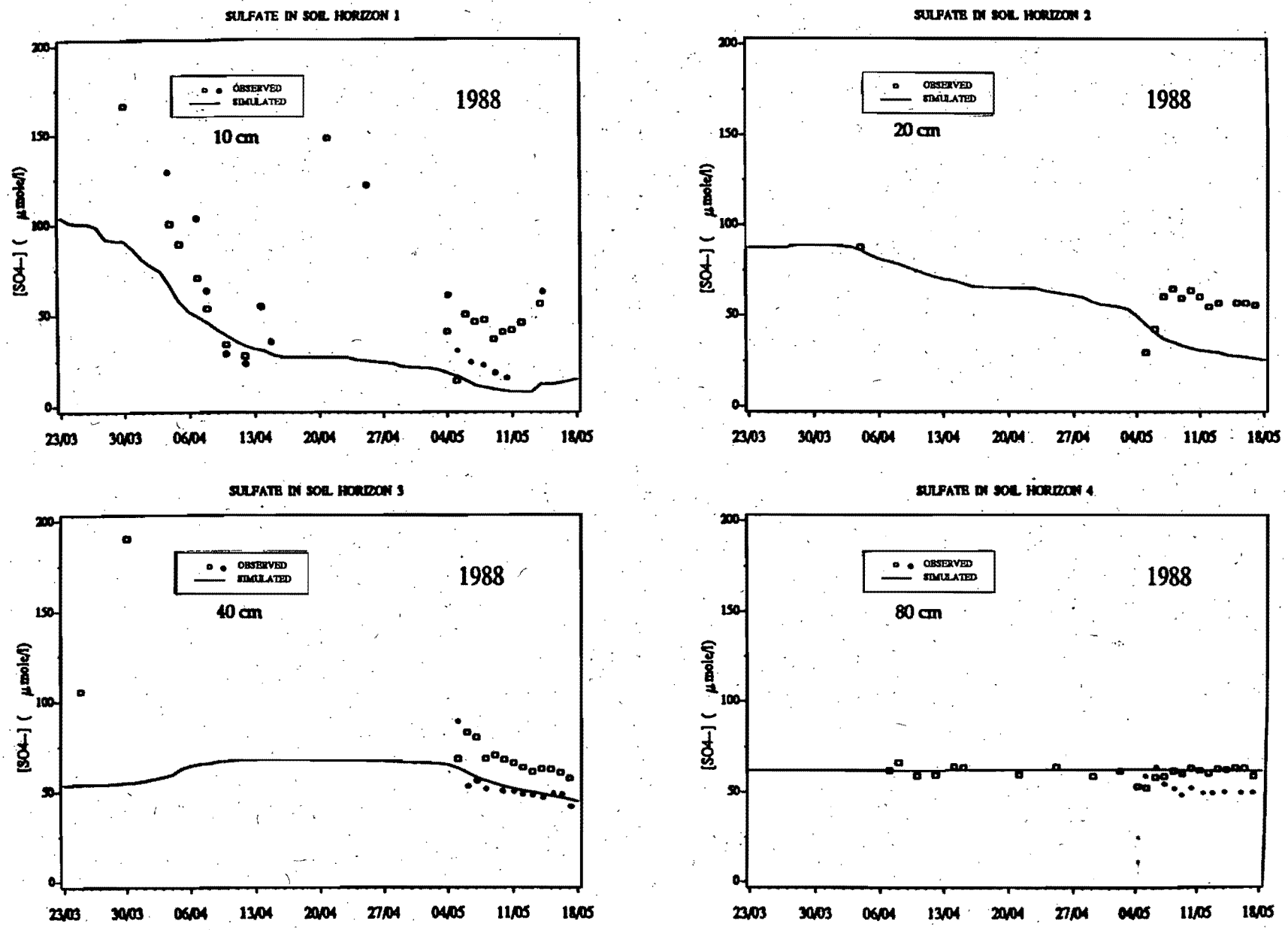

Fig.36: Concentration of SO_4^{2-} in the soil horizons (1 = 0-10 cm, 2 = 10-40, 3 = 40-80, 4 = > 80 cm deep) as simulated by VSASQ1 along with the observed values in segments C (□) and D (●).

The first version of SOILEQ that VSASQ1 is using, assumed that the water flow is only vertical. If the water flow is upward, it uses the snowmelt chemistry as the input to the lowest horizon instead of the chemistry of deep groundwater as it should have used. If the water flow as simulated by VSAS2 is lateral then SOILEQ can not take it into account in the simulation. During the initial days of the melt periods, the observed values of pH are quite low (4.2) at the 10 cm level, but the simulated values is much higher (5.3). It is partly caused by the prediction of SO_4 concentration. Some improvements are needed wherein adsorbed SO_4 is considered as a form of adsorbed acidity. If SO_4 desorbs as a result of decreasing concentration in the input waters, then this will result in an acidification of the soil solution. In general, the model does not look responsive to abrupt changes in water quality. Some of this does not originate solely from SOILEQ, but also from SNOQUALR. For example, when the second melt period starts on April 23rd, there is a major flux of ions out of the snowpack into the soil as observed for every measured ions. SOILEQ does not simulate this increase because SNOQUALR does not provide him with the right input. This is especially true for Ca^{2+}, H^+, K^+, Mg^{2+}, NH_4^+ NO_3^- and SO_4^{2-}. Another problem when comparing the simulations with the observed values is the representativeness of the field sampling point. For example, if your sampling station is placed where there is no upward vertical flow and you use it to compare simulation results with upward vertical flow, the results will not agree. This is clearly shown in part B of Tome IV (Hendershot, 1990). These simulations also show that up to a certain point it will be hard to improve the soil chemistry predictions if we can not model the hydrology adequately and if we do not have sufficient field data to compare the simulations.

SHORMIX

The simulation results for the following variables: Al^-, Ca^{2+}, Cl^-, EC, F^-, K^+, Na^+, Mg^{2+}, NH_4^+, NO_3^-, pH, SO_4^{2-} are presented in Figure 37 through 48 respectively. Observations of water quality of site C and D show that the two sites agree quite closely for some variables like Cl^-, EC, NH_4^+, F^-, pH, SO_4^{2-} or they do not like for Al^-, K^+ NO_3^-. For the other ions Ca^{2+}, Na^+, Mg^{2+} they agree closely until the 13th of April then, although they follow the same patterns the differences are larger. The model can simulate adequately the tendencies for the following variables: Ca^{2+}, Cl^-, EC, K^+, Na^+, Mg^{2+}, NH_4^+, NO_3^-. From May 2nd to may 11th which is the period where a massive pulse of melt occur, the simulation of SO_4^{2-} (Figure 48) and Al^- (Figure 37) reaches a minimum while the pH (Figure 47) reaches a maximum. Except for SO_4^{2-}, the observed values show the opposite trend for the same period.

The snowmelt rates of the first melt period decrease drastically from the 6th to the 13th of April (Figure 24). During this period, the snowmelt waters released are quite pure as shown by the observed values of all ions besides pH and Al^-. The simulations do not reproduce such minimum because of two unknowns. First, we do not know the volume of lake waters, input waters are mixing with. Secondly, we do not know the rate of replacement of initial lake waters and its quality near the sampling sites. For this first simulation, we used a volume of 826 m^3 and the rate of replacement of this volume was lowered to 100 m^3(Appendix 1) and 20 m^3 (Appendix 2) in the case of Cl^-, and it improved the simulations tremendously. A sensitivity analysis of SHORMIX model (Maulé, Hendershot and Stein, 1990) showed that the input variables which have the largest effect on the output pH are pH, ρCO^2, Al and volume of water, with pH and ρCO^2 having the largest effects. The problem with ρCO^2 is that it was not measured and a constant value was utilized. A decrease in ρCO^2 by an order of magnitude during lake ice-off in

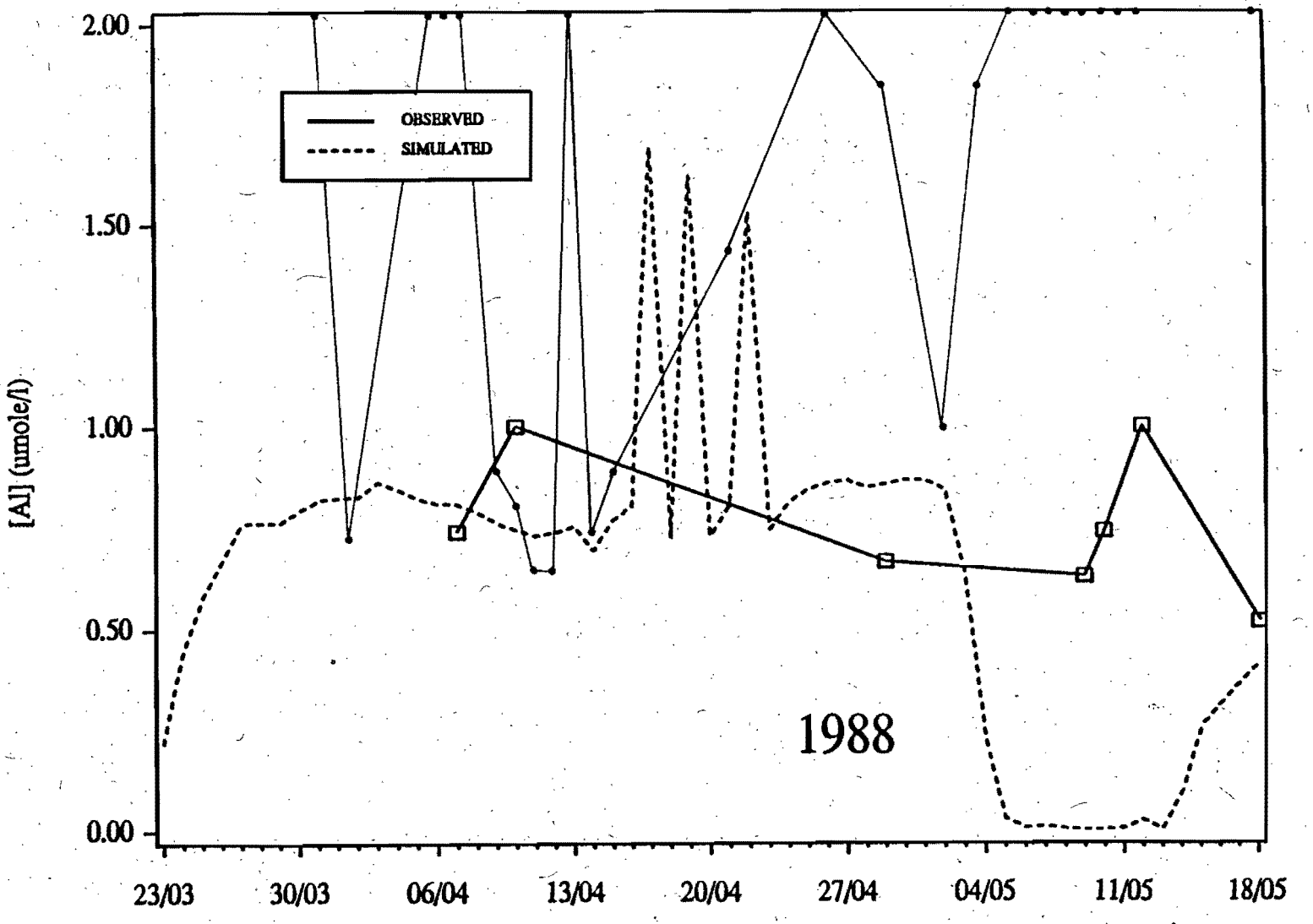

Fig.37: Concentration of Al in the ambiant waters above the spawning sites in segment C (□) and D (●) as simulated by VSASQ1

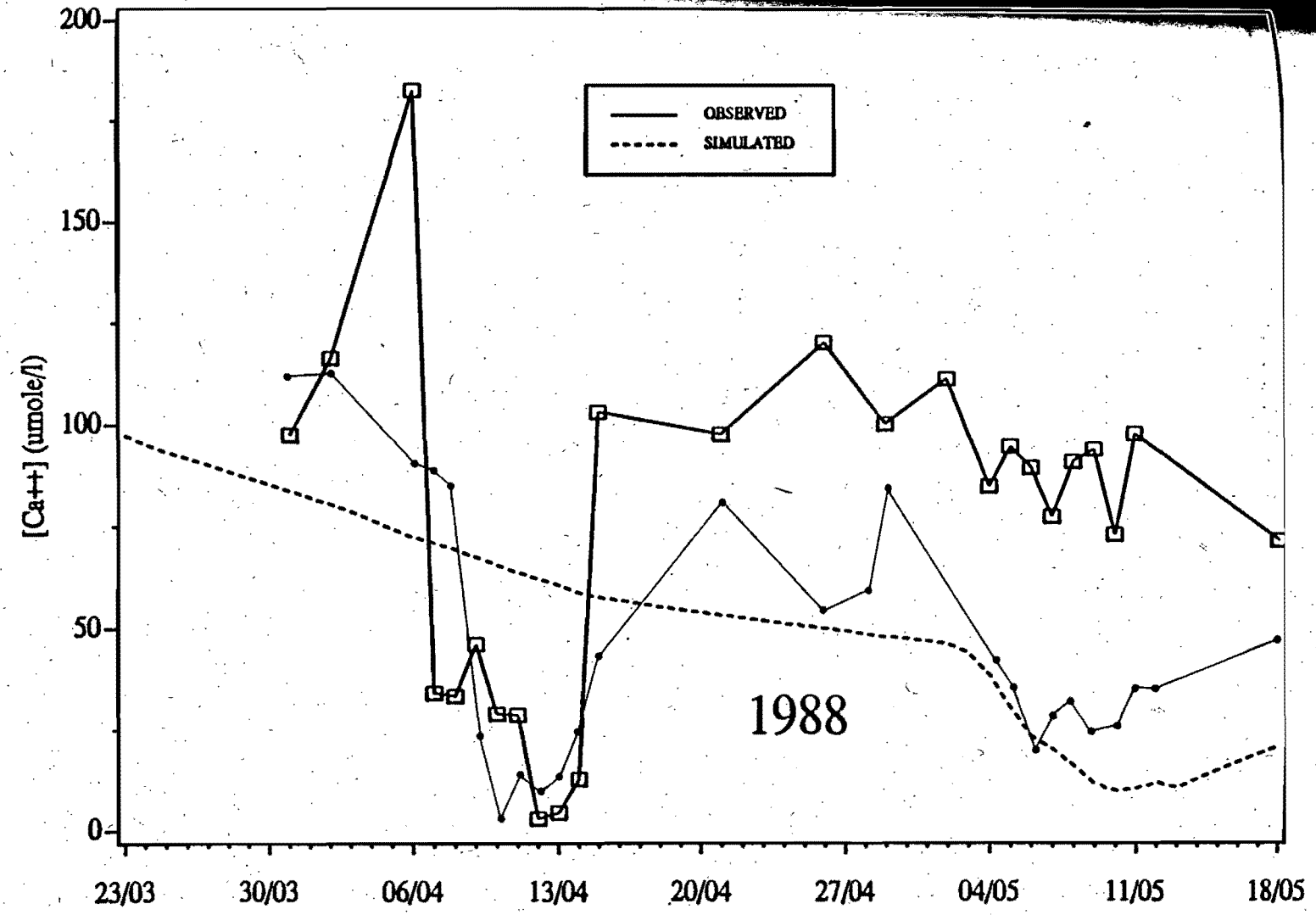

Fig.38: Concentration of Ca^{2+} in the ambiant waters above the spawning sites in segment C (□) and D (●) as simulated by VSASQ1

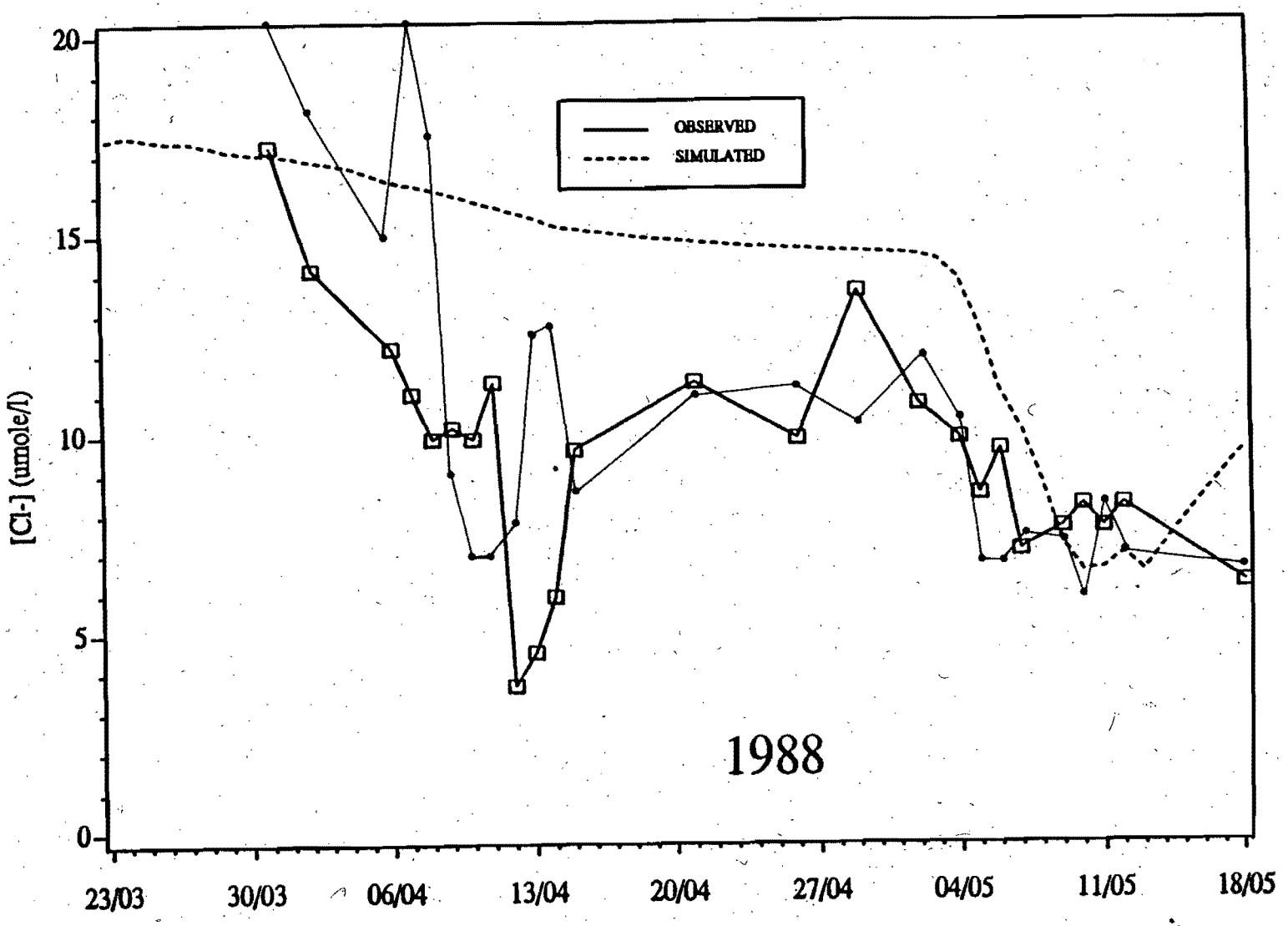

Fig.39: Concentration of Cl^- in the ambiant waters above the spawning sites in segment C (□) and D (●) as simulated by VSASQ1

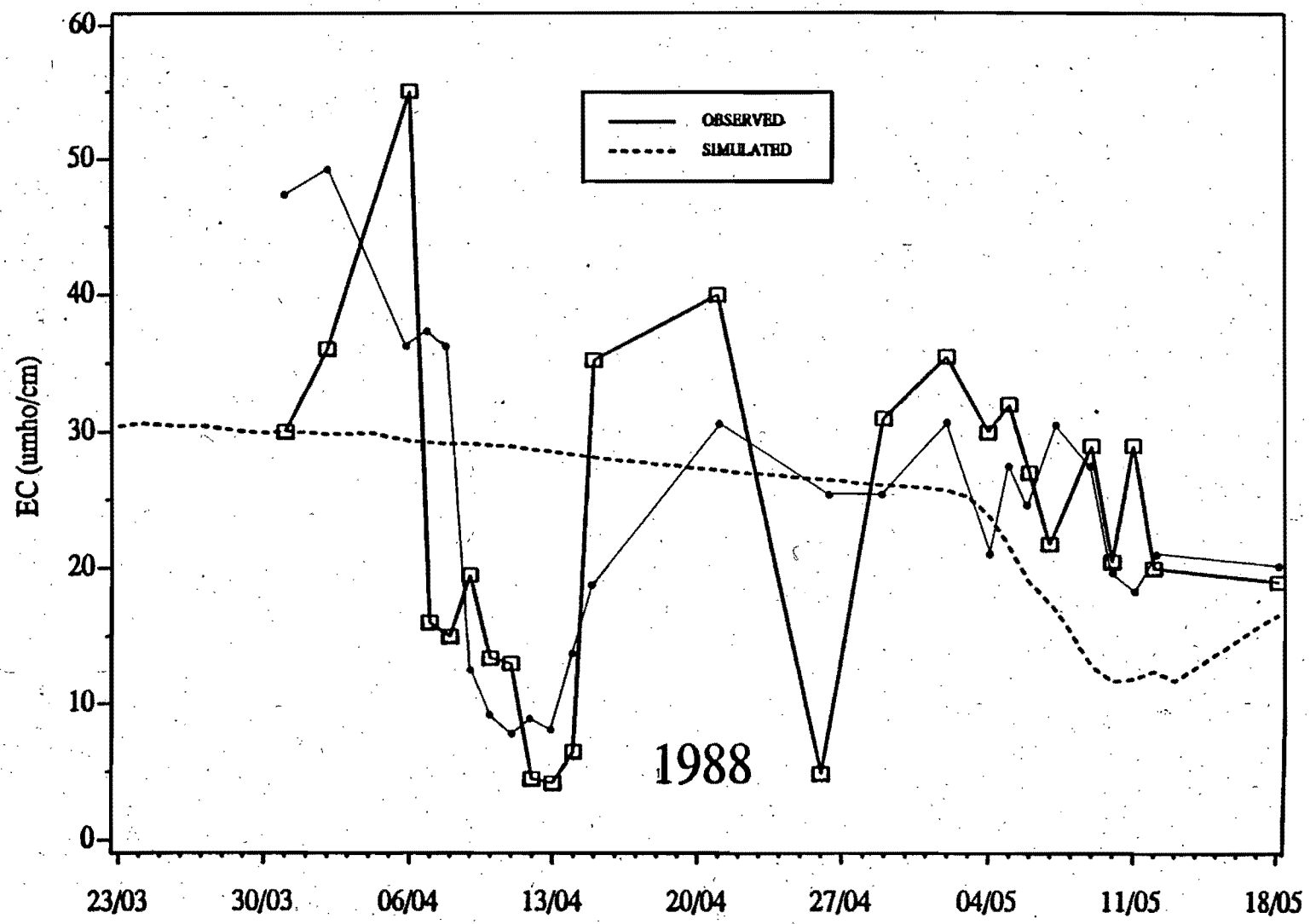

Fig.40: Values of EC in the ambiant waters above the spawning sites in segment C (□) and D (●) as simulated by VSASQ1

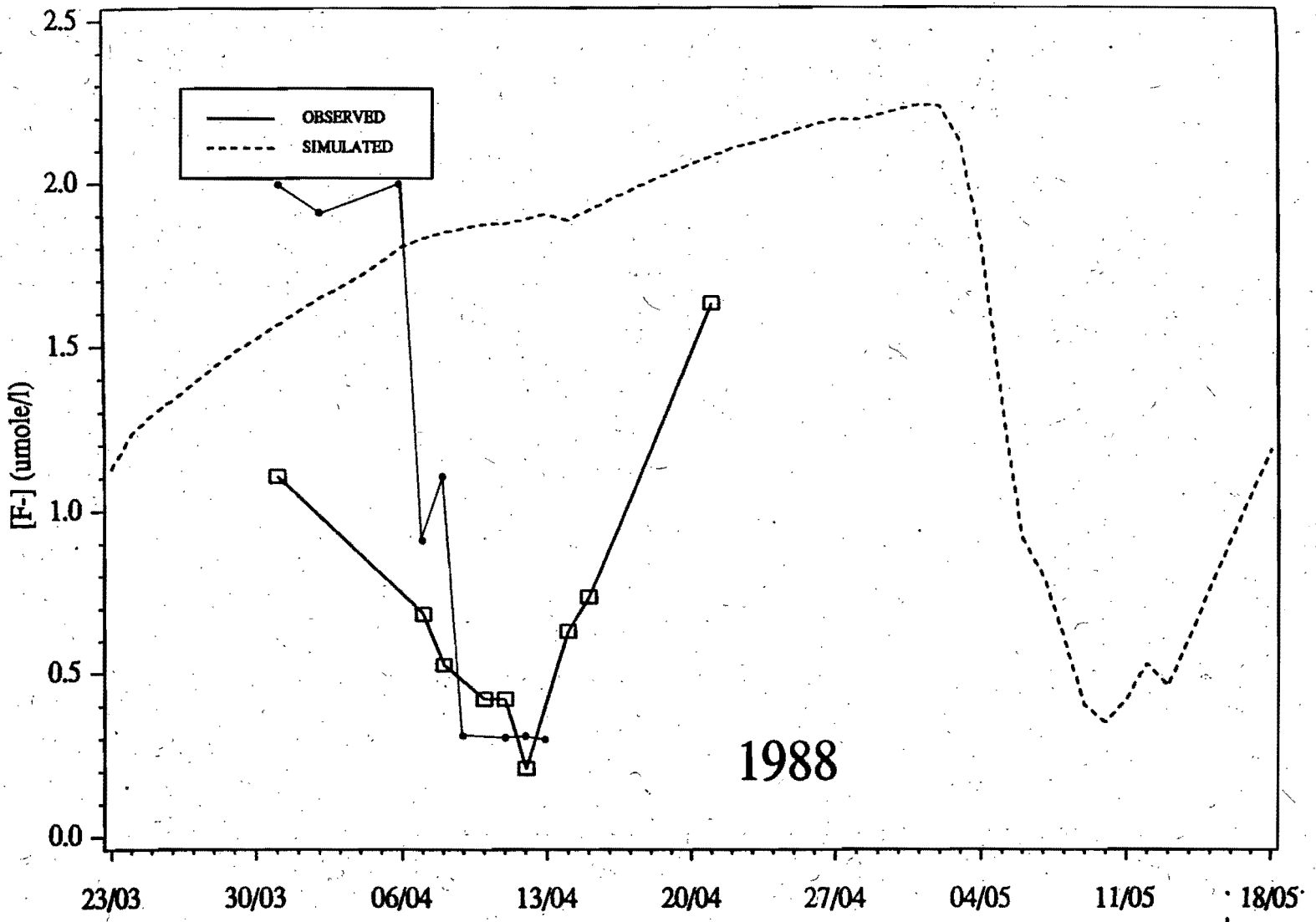

Fig.41: Concentration of F^- in the ambiant waters above the spawning sites in segment C (□) and D (●) as simulated by VSASQ1

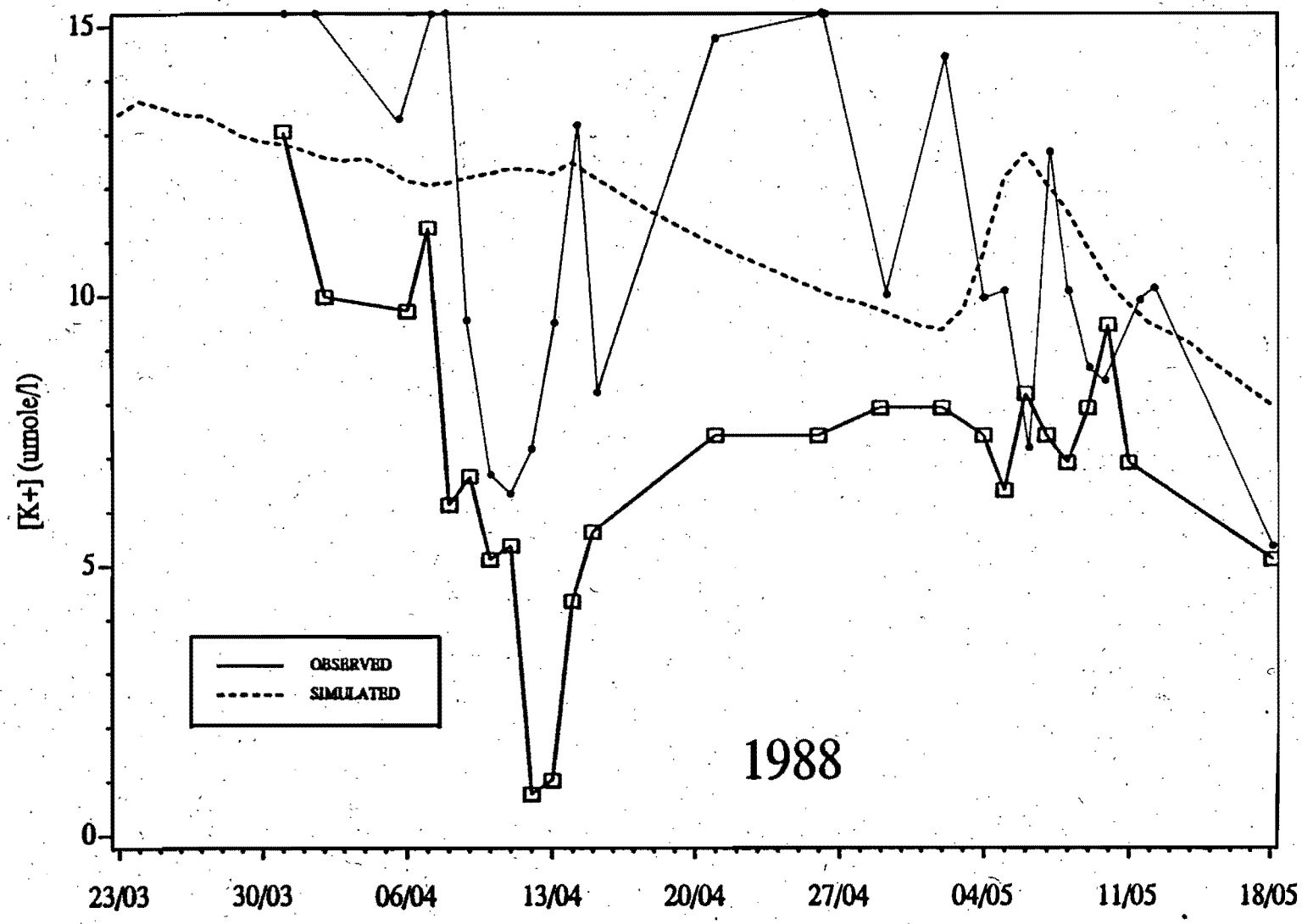

Fig.42: Concentration of K^+ in the ambiant waters above the spawning sites in segment C (□) and D (●) as simulated by VSASQ1

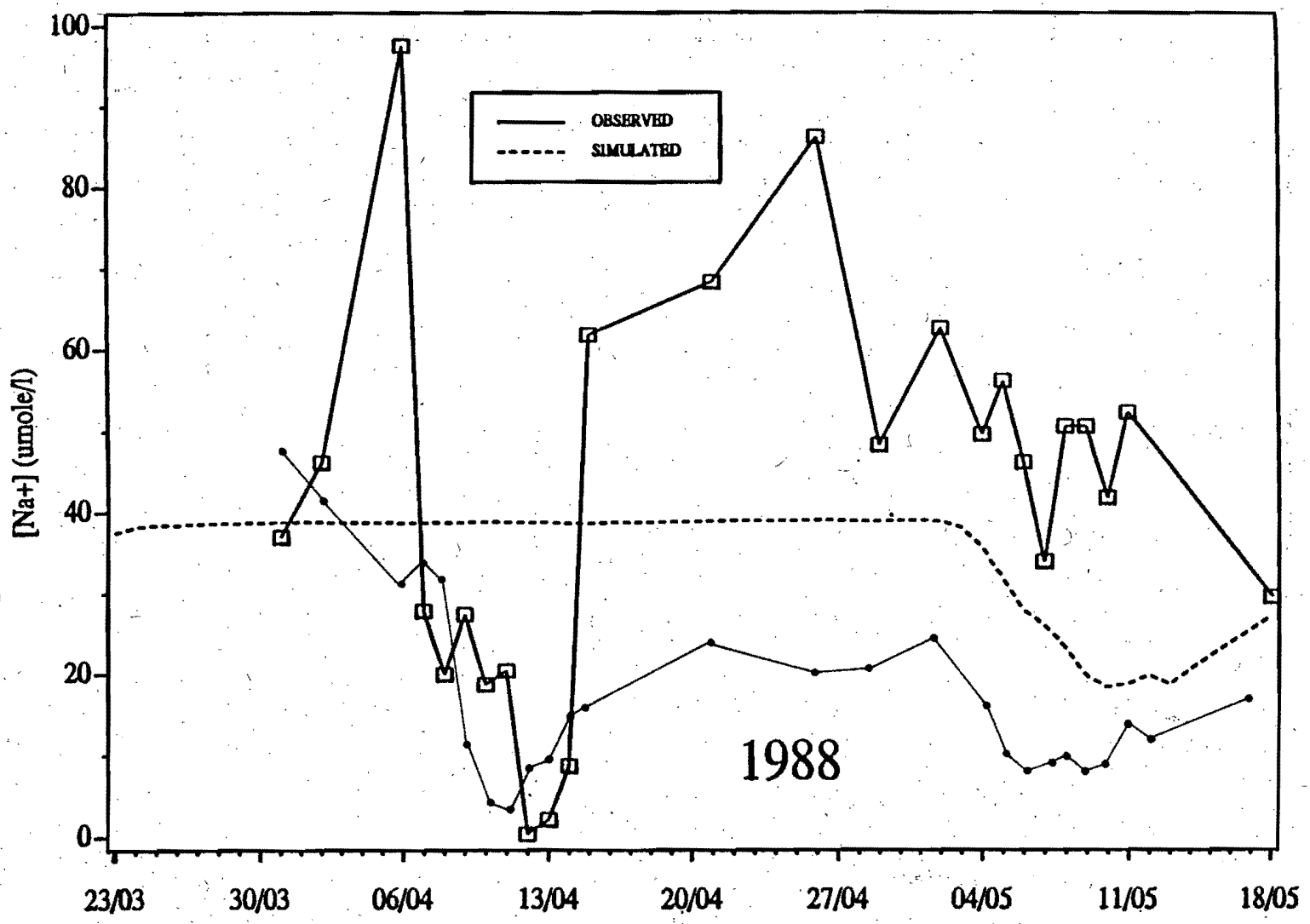

Fig.43: Concentration of Na^+ in the ambiant waters above the spawning sites in segment C (□) and D (●) as simulated by VSASQ1

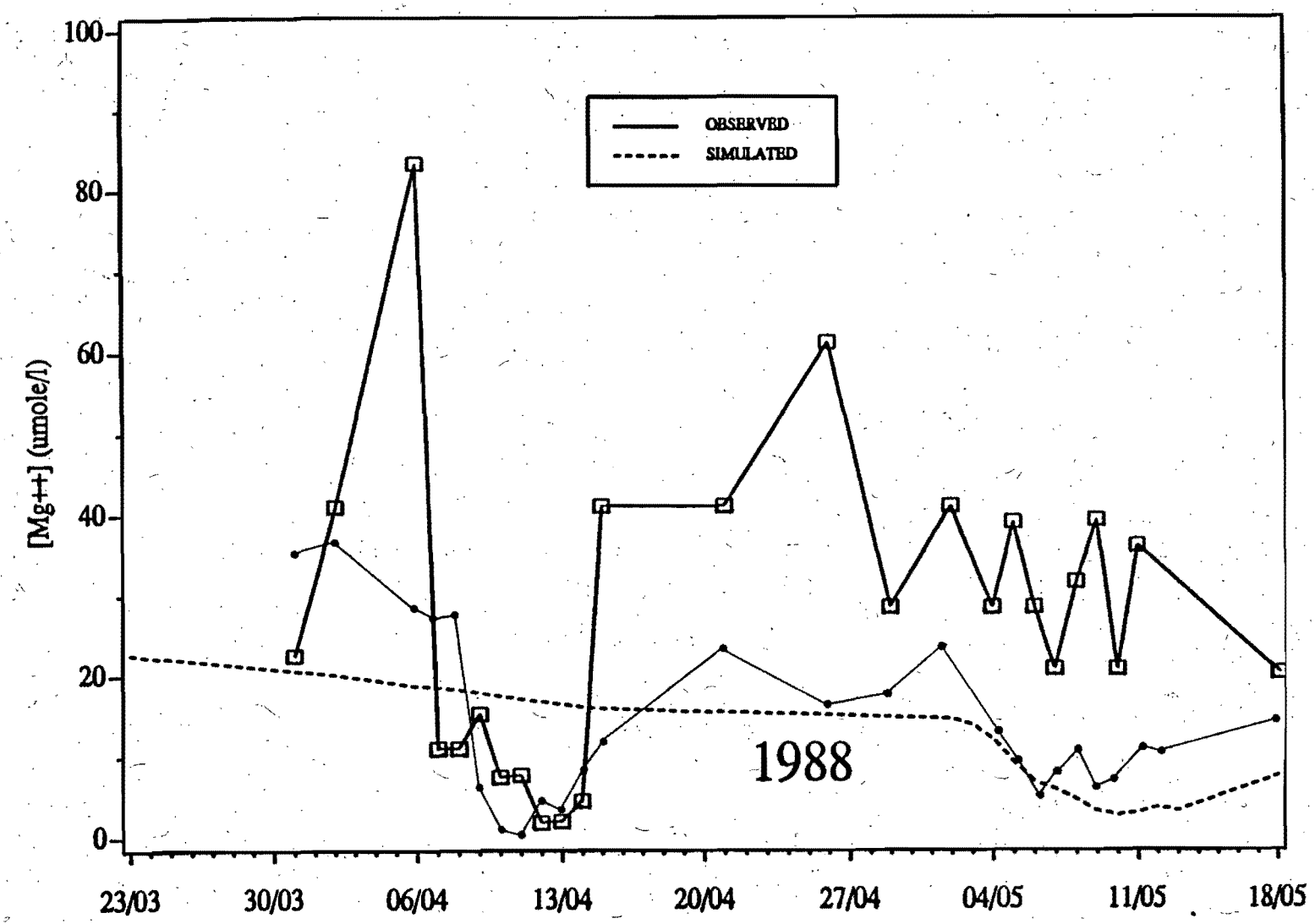

Fig.44: Concentration of Mg^{2+} in the ambiant waters above the spawning sites in segment C (□) and D (●) as simulated by VSASQ1

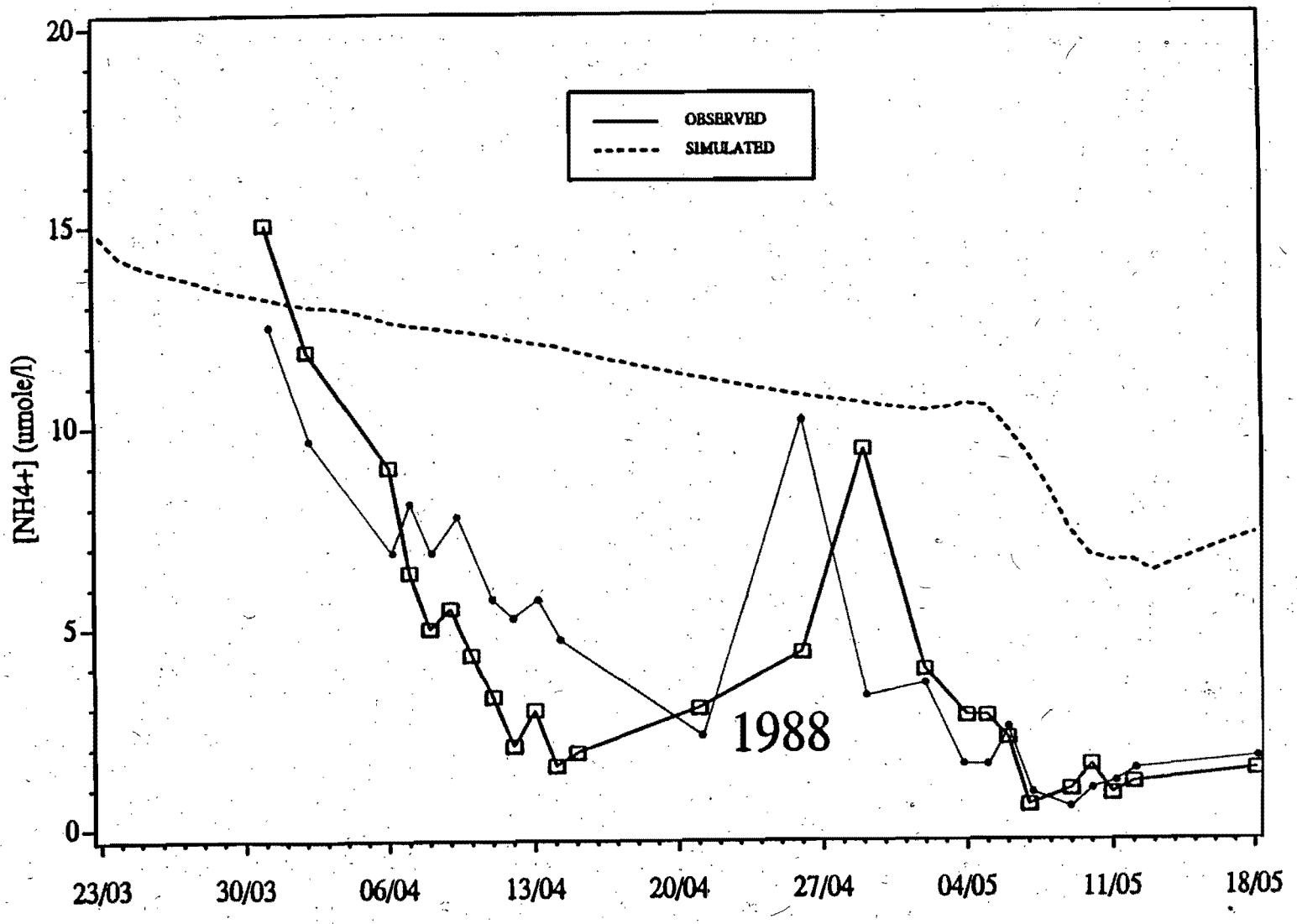

Fig.45: Concentration of NH_4^+ in the ambiant waters above the spawning sites in segment C (□) and D (●) as simulated by VSASQ1

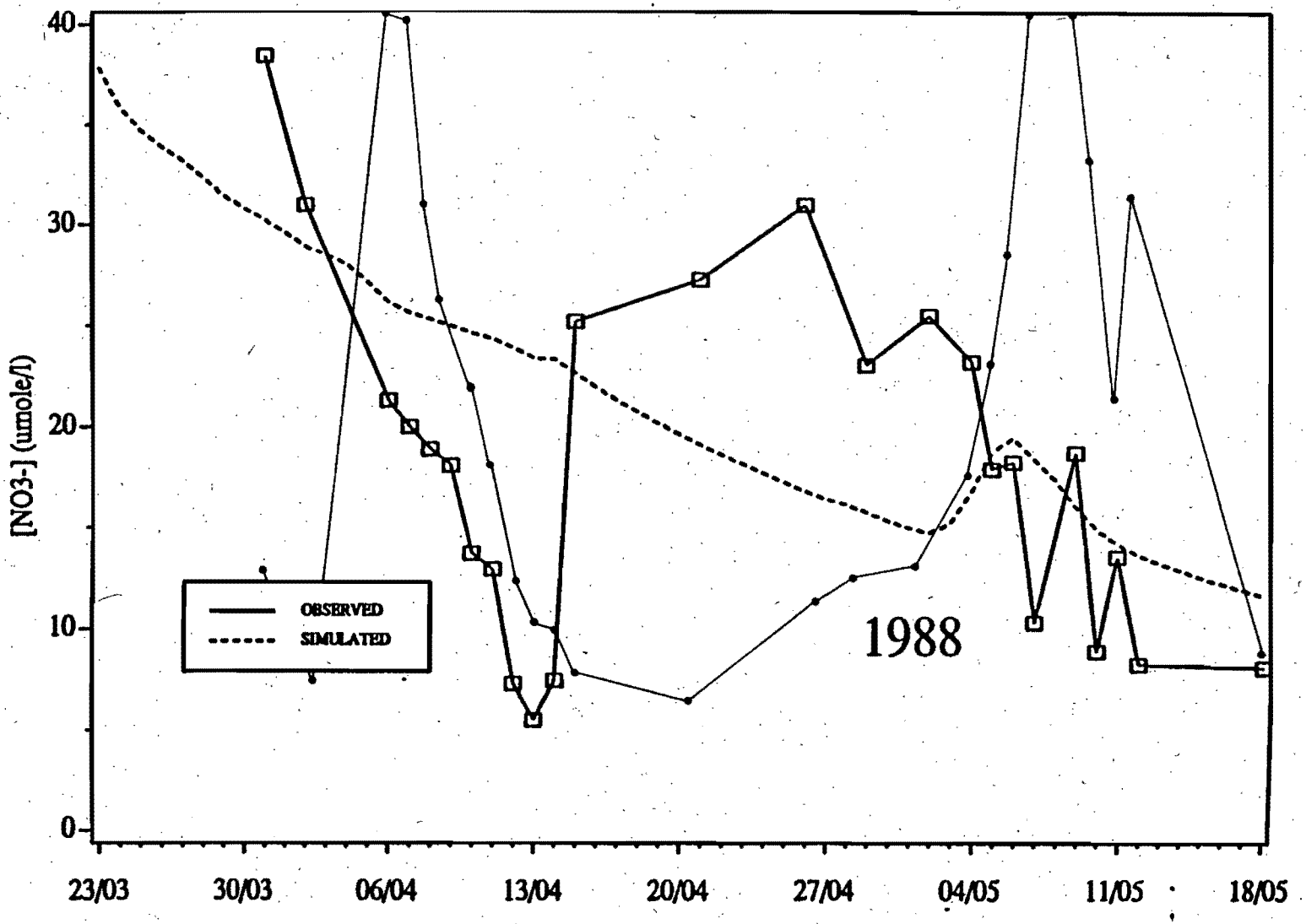

Fig.46: Concentration of NO_3^- in the ambiant waters above the spawning sites in segment C (□) and D (●) as simulated by VSASQ1

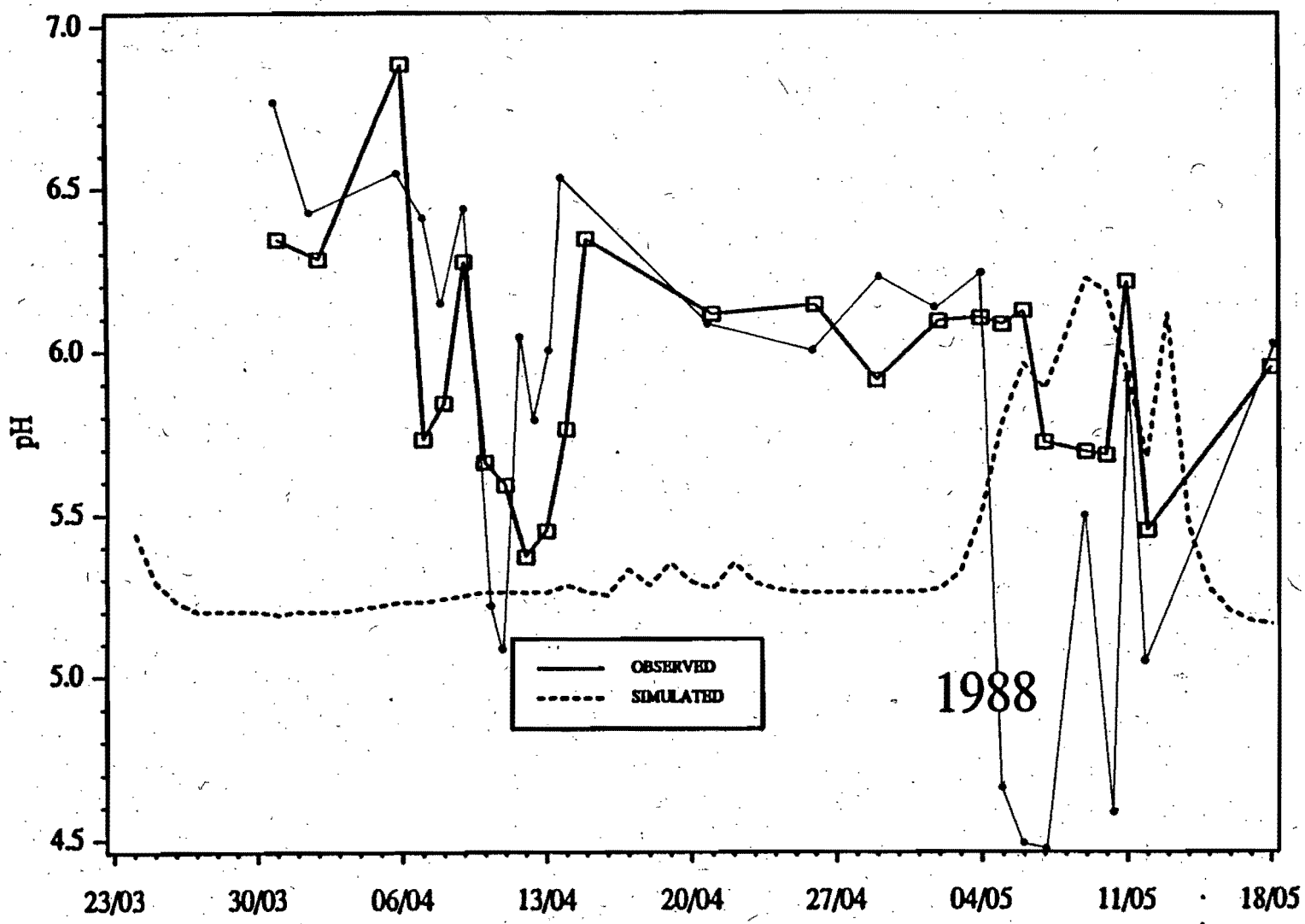

Fig.47: Values of pH in the ambiant waters above the spawning sites in segment C (□) and D (●) as simulated by VSASQ1

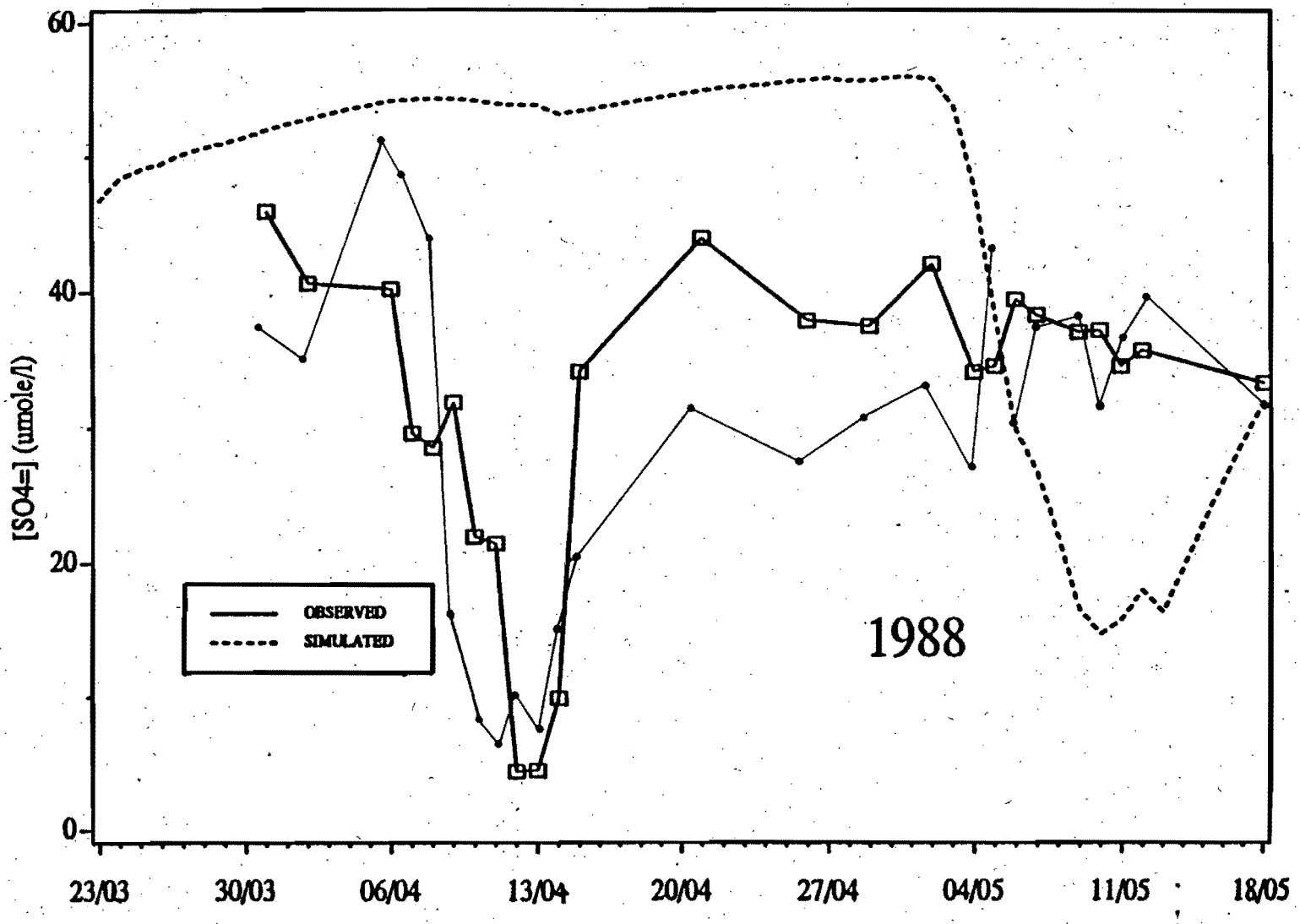

Fig.48: Concentration of SO_4^{2-} in the ambiant waters above the spawning sites in segment C ( ) and D (●) as simulated by VSASQ1

springmelt the ρCO^2 (Norton and Henriksen, 1983) or the alkalinity (Lac Laflamme - Papineau, 1987) can drop by about an order of magnitude within one week, due to degassing of supersaturated waters. Thus the use of a constant ρCO^2 value in the SHORMIX model likely poorly simulated the probable fluctuations that occurred with large amounts of snowmelt.

REFERENCES

Anderson, E., 1973. National Weather Service river forecast system. Snow accumulation and ablation model NOAA Tech. Mem. NWSH Hydro-17. U.S. Dept of Commerce, Silver Spring, Maryland.

Barry, R., A.P. Plamondon and J. Stein, 1988. Hydrologic soil properties and application of a soil moisture model in a balsam fir forest. Canadian Journal Forest Research, 18: 427-434.

Bernier, P., F. Padilla, M. Dessureault, P.S. Gélinas, L.M. Azzaria, and S. Goulet, 1983. Étude hydrogéologique et hydrogéographique du bassin versant du Lac Laflamme en 1982. Report prepared for Environment Canada. Dept of Geology, Laval University, Québec, 238 p.

Bernier, P.Y., 1985. Variable source areas and storm-flow generation: an update of the concept and a simulation effort, Journal Hydrology 79. 195-213

Cronan, C.S., W.A. Reiners, R.C. Reynolds, and G.E. Lang, 1978. Forest floor leaching; contributions from mineral, organic, and carbonic acids in New Hampshire subalpine forests. Science 200; 309-3.

Driscoll, C.T., J.P. Baker, J.J. Bisogne, and C.L. Schofield, 1980. Effect of aluminum speciation on fish in dilute acidified waters. Nature 284; 161-164.

Foster, P.M., 1978. The modelling of pollutant concentrations during snowmelt. CECB Report RDILIN 46178 Job No. VC 455.

Hewitt, A.D., J.H. Cragin and S.C. Colbeck, 1989. Does snow have ion chromatographic properties? Proceedings of the 1989 annual Eastern Snow Conference meeting.165-172.

Jeffries, D. S., D.C. Lam, and I. Wang, 1990. The predicted effects of SO2 emission controls on the water quality of eastern canadian lakes. Conference abstracts International Conference on Acidic deposition: its Nature and Impacts.Glasgow 16-21st sept.

Hendershot, W., 1990. A transportable geochemical model to predict the acidification of surface water during episodic events: Tome IV; Modeling soil solution chemistry. Report prepared for Environment Canada. 101 p.

Jones, H.G., 1987. Chemical dynamics of snowcover and snowmelt in a boreal forest. In: "Seasonal Snowcovers: Physics, Chemistry, Hydrology." D. Reidel Publishing Company, Dordrecht. Editors H.J. Jones and W.J. Orville-Thomas, 726 p., 531-574.

Jones, H.G., J. Stein, J. Roberge, W. Sochanska, J.Y. Charette, and A.P. Plamondon, 1986. Snowmelt in boreal forest site: an integrated model of meltwater quality (SNOQUAL1). Water, Air and Soil Pollution 31: 431-439.

Jones, H.G., J. Stein, and W. Sochanska, 1990. A transportable geochemical model to predict the acidification of surface water during episodic events: Tome II; SNOQUAL, a model for the simulation of meltwater quantity and quality in boreal forest catchments: a study of the model variants for the chemistry of snow meltwaters. Report prepared for Environment Canada. 37 p.

Jurdant, M. and B. Bernier, 1965. Carte écologique de la forêt Montmorency, Université Laval. In: Côté, M. (éditeur), 1968. Plan d'aménagement de la forêt Montmorency de l'Université Laval, P.U.L., Québec, 157 pp.

Likens, G.E., and T.J. Butler, 1981. Recent acidification of precipitation in North America. Atmospheric Environment. 15 (7), 1103-1109.

Lindsay, W.L., 1979. Chemical equilibrium in soils. John Wiley and Sons. New York, Chicago.

Martel, J.P., 1983. Caractéristiques physiques et hydrologiques, et bilan hydrique de la matière organique d'une sapinière laurentienne au Lac Laflamme, Forêt Montmorency, unpublished Ms thesis, Université Laval, Québec, Canada, 90 p.

Maulé, C. and J. Stein, 1990. Hydrologic flow path definition and partitioning of spring meltwater. Water Resources Research. 26 (12): 2959-2970.

Morrison, I.K., 1984. Acid Rain. A review of litterature on acid deposition effects in forest ecosystems. Review article 8. Forestry Abstracts. 45, 483-506.

Norton, S.A. and A. Henriksen, 1983. The importance of CO_2 in evaluation of acidic deposition, Vatten 39, 346-354.

Nordstrom, D.K., S.D. Valentine, J.W. Ball, L.N. Plummer, and P.F. Jones, 1984. Partial compilation and revision of basic data in the WATEQ program. U.S.G.S. Water Resources Investigation Report 84-4186.

Papineau, M., 1987. Effects of acid precipitation in a boreal forest ecosystem: Ion budgets and charges in water chemistry for the Laflamme Lake Watershed, Environment Canada, Conservation and Portection, Inland Water and Lands Branch, Quebec Region, 108 pp., 1987.

Plamondon, A.P., M. Prevost, and R.C. Naud, 1984. Accumulation et fonte de la neige en milieu boisé et déboisé. Géographie physique et quaternaire, XXXVIII (1), 27-35.

Prevost, M., R. Barry, J. Stein, and A.P. Plamondon, 1989. Evolution du couvert de neige et des profils hydrique et thermique du sol dans un bassin de la sapinière laurentidienne. Journal of Hydrology. 107;343-366.

Prevost, M., R. Barry, J. Stein, and A.P. Plamondon, 1990. Snowmelt runoff modelling in a balsam fir forest with a variable source area simulator (VSAS2). Water Resources Research. (26(5): 1067-1077

Robitaille, R. and J.F. Wilhemy, 1981. Étude sismique du bassin versant du lac Laflamme, Forêt Montmorency, Québec. Report prepared for Environment Canada, Département de géologie, Université Laval, 18 pp.

Rowe, J.S., 1972. Les régions forestières du Canada. Ministère de l'Environnement, Service Canada For., Publi. no 1300 F, 172 p.

Roberge, J. and A. P. Plamondon, 1987. Snowmelt runoff pathways in a boreal forest hillslope, the role of pipe throughflow. Journal of Hydrology, 95: 39-54.

Roberge, J., J. Stein, and A.P. Plamondon, 1988. Evaluation d'un modèle de fonte nivale dans la forêt boréale de l'est canadien. Journal of Hydrology, 97: 161-179.

Soil Survey Staff, 1975. Soil Taxonomy: A basic system of soil classification for making and interpreting soil surveys. USDA-SCS agric. Handb. 436. U.S. Gov. Print. Office, Washington, DC.

Stein, J., H.G. Jones, J. Roberge, and W. Sochanska, 1986. The prediction of both runoff quality and quantity by the use of an integrated snowmelt model. In: "Modelling snowmelt - induced processes". Editor E.M. Morris IAHS Publication No 155: 34-358.

Stein, J. and D.L. Kane, 1983. Monitoring the unfrozen water content of soil and snow using time domain reflectometry, Water Resources Research. 19 (6): 1572-1584.

Stroo, H.G. and M. Alexander, 1986. Available nitrogen and nitrogen cycling in forest soils exposed to simulated acid rain. Soil Sci. Am. J. 50, 110-114.

Tranter, M., P. Brimblecombe, T.D. Davies, C.E. Vincent, P.W. Abrahams, and I. Blackwood, 1986. The composition of snowfall, snowpack and meltwater in the Scottish Highlands - evidence for preferential elution. Atmospheric Environment, 20: 517-525.

APPENDIX

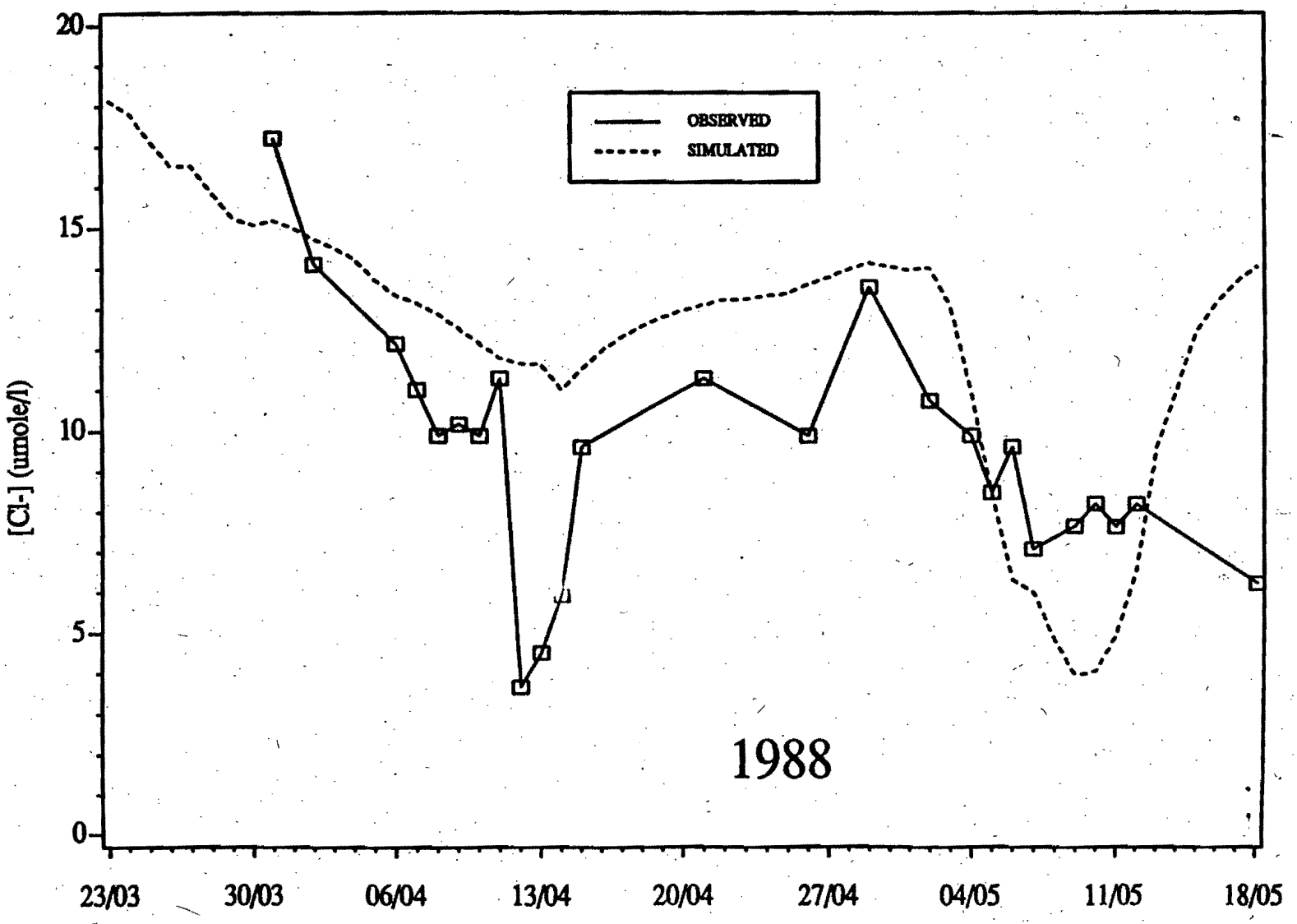

Appendix 1: Concentration of Cl^- in the ambiant waters above the spawning sites in segment C as simulated by VSASQ1 and using a lake volume of 100 m^3

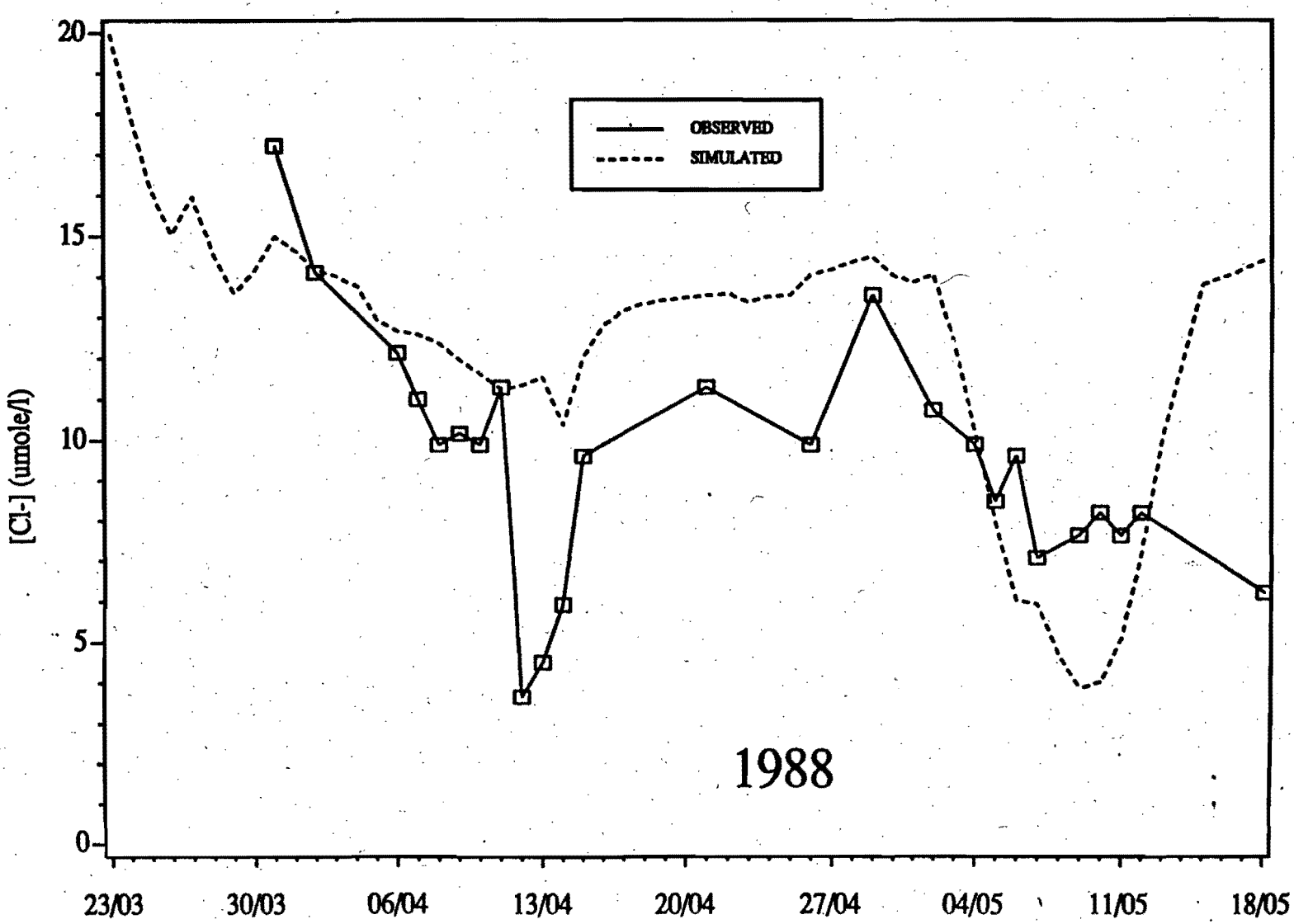

Appendix 2: Concentration of Cl^- in the ambiant waters above the spawning sites in segment C as simulated by VSASQ1 and using a lake volume of 20 m^3